ΟΙΚΟΝΟΜΙΚΟ ΠΑΝΕΠΙΣΤΗΜΙΟ ΑΘΗΝΩΝ

ATHENS UNIVERSITY OF ECONOMICS AND BUSINESS

ΣΧΟΛΗ ΕΠΙΣΤΗΜΩΝ & ΤΕΧΝΟΛΟΓΙΑΣ ΤΗΣ ΠΛΗΡΟΦΟΡΙΑΣ
SCHOOL OF INFORMATION SCIENCES & TECHNOLOGY

ΜΕΤΑΠΤΥΧΙΑΚΟ ΣΤΑΤΙΣΤΙΚΗ
MSc IN STATISTICS

Some recent developments on Profile Monitoring

By

Victoria E. Sipaki

A THESIS

Submitted to the Department of Statistics

of the Athens University of Economics and Business

in partial fulfilment of the requirements for

the degree of Master of Science in Statistics

Athens, Greece
February 2024

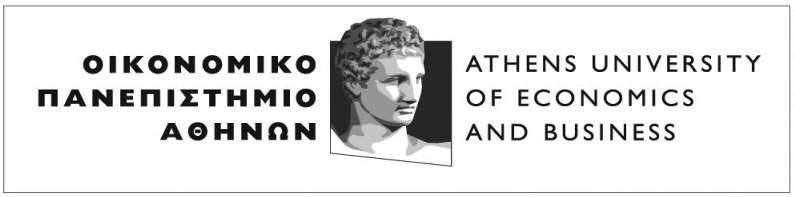

Μερικές πρόσφατες εξελίξεις σχετικά με την παρακολούθηση προφίλ

Βικτωρία Ε. Σηπάκη

ΔΙΑΤΡΙΒΗ

Που υποβλήθηκε στο Τμήμα Στατιστικής

του Οικονομικού Πανεπιστημίου Αθηνών

ως μέρος των απαιτήσεων για την απόκτηση

Διπλώματος Μεταπτυχιακών Σπουδών στη Στατιστική

Αθήνα

Φεβρουάριος 2024

DEDICATION

I would like to dedicate this thesis to my parents Anthi and Evangelo. You were my source of inspiration, support and guidance. You taught me to be decisive, bold, brave, strong and have faith in myself. Thank you for the encouragement, love and unique experience you gave me through this journey of knowledge. I feel immense gratitude to have you as my parents. I will love you forever and always.

ACKNOWLEDGEMENTS

Words cannot express my gratitude to my Supervisor Professor Stylianos Psarakis for his invaluable patience, guidance and feedback. I also could not have undertaken this journey without all my professors from the postgraduate program in Statistics, who through the courses and lectures generously provided me with knowledge, critical perception and competence. Lastly, I would be remiss in not mentioning my family, especially my parents and my brother George. Their belief in me has kept my motivation high during this process and all the emotional support they gave me made me go all the way.

VITA

Victoria E. Sipaki was born in Edessa, Greece, on August 28, 2000. Her undergraduate career began in 2018, the year she entered the Department of Mathematics of the University of Ioannina. In the fifth semester (third year) of her studies, in the process of choosing a direction, she turned to the direction of Statistics and Operations Research. In 2022 she successfully graduated from the above department and received the degree of Bachelor of Science in Mathematics. In the same year, in October, attended the postgraduate program in Statistics at Athens University of Economics and Business to obtain a Master of Science degree in Statistics the requirements of which are fulfilled with this thesis.

ABSTRACT

Victoria Sipaki

Some recent developments on Profile Monitoring

February 2024

Statistical profile monitoring can be considered as a subfield of statistical quality control that has attracted many researchers. This attractiveness is a result of the wide range of applications that can be identified for the concept of profiling in different service and manufacturing settings. More specifically, profiles appear when a quality – critical attribute is functionally dependent on one or more explanatory variables. Thus, at each sampling stage we observe a collection of data points that can be represented by a curve (profile). Checking over time the stability of such functional relationships using statistical methods is called “profile monitoring”. In some applications, the profile can be represented adequately by a simple linear regression model, while in some other more complicated models are needed. Fortunately, advances in technology have enabled researchers to collect many process or product measurements to reconstruct this functional relationship. Finally, because profiling is a relatively new area in statistical process monitoring, Woodall’s review paper (2007) is an important contribution and paved the way for the publication of an increasing number of papers in this area. This increasing trend is more noticeable during the period 2012 – 2017, while from 2018 onwards there is no document summarizing recent research in this area. In this thesis a discussion of recent studies and trends around profile monitoring especially in the period after 2018 be done.

ΠΕΡΙΛΗΨΗ

Βικτωρία Σηπάκη

Μερικές πρόσφατες εξελίξεις σχετικά με την παρακολούθηση προφίλ

Φεβρουάριος 2024

Η παρακολούθηση του στατιστικού προφίλ μπορεί να θεωρηθεί ως ένας τομέας του στατιστικού ποιοτικού ελέγχου που έχει προσελκύσει την προσοχή πολλών ερευνητών. Η ελκυστικότητα αυτή είναι απόρροια του ευρέως φάσματος εφαρμογών που μπορούν να προσδιοριστούν για την έννοια της δημιουργίας προφίλ σε διαφορετικά περιβάλλοντα υπηρεσιών. Πιο αναλυτικά, τα προφίλ εμφανίζονται όταν ένα χαρακτηριστικό κρίσιμο προς την ποιότητα εξαρτάται λειτουργικά από μία ή περισσότερες επεξηγηματικές μεταβλητές. Έτσι, σε κάθε στάδιο δειγματοληψίας παρατηρούμε μία συλλογή σημείων που μπορούν να αναπαρασταθούν από μία καμπύλη (προφίλ). Ο έλεγχος με την πάροδο του χρόνου της σταθερότητας τέτοιων λειτουργικών σχέσεων με την χρήση στατιστικών μεθόδων ονομάζεται «παρακολούθηση προφίλ». Σε ορισμένες εφαρμογές βαθμονόμησης, το προφίλ μπορεί να αναπαρασταθεί επαρκώς με ένα απλό μοντέλο γραμμικής παλινδρόμησης, ενώ σε άλλες εφαρμογές χρειάζονται πιο περίπλοκα μοντέλα. Ευτυχώς, η πρόοδος της τεχνολογίας έδωσε τη δυνατότητα στους ερευνητές να συλλέξουν μεγάλο αριθμό μετρήσεων διεργασιών ή προϊόντων για να ανασυνθέσουν αυτή τη λειτουργική σχέση. Επειδή η παρακολούθηση προφίλ είναι ένας σχετικά νέος τομέας στην παρακολούθηση της στατιστικής διαδικασίας, το έγγραφο ανασκόπησης του Woodall (2007) είναι μία σημαντική συμβολή και άνοιξε το δρόμο για τη δημοσίευση ενός αυξανόμενου αριθμού εργασιών. Η αυξητική αυτή τάση είναι πιο αισθητή κατά την περίοδο 2012 – 2017, ενώ από το 2018 και έπειτα δεν υπάρχει κανένα έγγραφο που να συνοψίζει πρόσφατες έρευνες στον τομέα αυτό. Στην παρούσα διπλωματική εργασία θα γίνει μία συζήτηση πρόσφατων μελετών και τάσεων γύρω από την παρακολούθηση του προφίλ, ειδικά κατά την περίοδο μετά το 2018.

TABLE OF CONTENTS

CHAPTER 1 Introduction to Profile Monitoring **1**

Introduction **1**

1.1 Functional relationships qualified as profiles **2**

1.1.1 Profiles of exosomal biomarkers **2**

1.1.2 Profiles of gut microbiota in Sardinian centenarians **3**

1.1.3 Profiles of extracellular vesicles **4**

1.1.4 Profiles of cyclic voltammetry **4**

1.2 Structure of this thesis **5**

CHAPTER 2 Basic principles **7**

Introduction **7**

2.1 Structure of the control chart **8**

2.2 Evaluation criterion **9**

2.3 Basic control charts **11**

CHAPTER 3 Simple linear profiles **13**

Introduction **13**

3.1 Methods for simultaneous shifts in the profile parameters **19**

3.1.1 A memory type structure based on progressive mean **20**

3.1.2 MEWMA control chart with innovative run – rules **22**

3.2 Robust estimation methods for simple linear parameters **25**

3.2.1 Robust two – stage process control chart **25**

3.2.2 A robust economic – statistical design **31**

3.2.3 Simple linear profiles in the presence of outliers **33**

3.3 Other techniques for monitoring simple linear profiles **36**

3.3.1 Influence of estimation on simple linear profile monitoring in non – normal conditions **36**

3.3.2 A Bayesian approach with random variables **39**

3.3.3 A novel approach to financial market monitoring **45**

CHAPTER 4 Generalized linear and generalized linear mixed profiles **49**

Introduction **49**

4.1 Robust estimation methods for generalized linear and generalized linear mixed profiles **53**
4.1.1 Robust estimators for logistic and Poisson profiles **53**
4.1.2 A semiparametric technique for Phase II analysis via residuals **55**
4.1.3 Robust profile monitoring for Phase I Analysis **58**
4.1.3.1 A nonparametric method for Phase I **58**
4.1.3.2 A semiparametric method for Phase I **60**
4.1.3.3 A comparison of methods **62**
4.2 Other techniques for monitoring generalized linear and generalized linear mixed profiles **64**
4.2.1 Adapting to variable sampling intervals: A VSI approach **64**
4.2.2 Residuals control chart profiling in gamma regression models **67**
4.2.3 Real-time monitoring of surgical outcomes **69**
CHAPTER 5 Geometric and Polynomial profiles **73**
Introduction **73**
5.1 Correlation in profile monitoring methods **76**
5.1.1 Monitoring circular profiles under spatial correlations **76**
5.1.2 Monitoring cylindrical profiles under spatial correlations **78**
5.1.3 Monitoring polynomial profiles based on attribute data **79**
5.2 Methods for simultaneous shifts in the profile parameters **81**
5.2.1 Development of a Phase II control chart using the weighted likelihood ratio test **82**
5.2.2 A method for enhancing sensitivity to minor changes **85**
5.3 Methods regarding the effects on the Phase II performance **87**
5.3.1 The impact of estimation methods on Phase II performance **88**
5.3.2 The effect of measurement errors on Phase II performance **91**
5.3.3 The impact of a practical application on the profile monitoring **95**
CHAPTER 6 Nonparametric profiles **99**
Introduction **99**
6.1 Change point detection approaches **101**
6.1.1 Advanced nonlinear profiling using support vector regression **101**
6.1.2 Nonlinear profile monitoring through single index models **103**

6.2 Correlation in profile monitoring methods **105**
6.2.1 A study based on serially correlated nonparametric profiles **105**
6.2.2 Enhanced real-time monitoring with Gaussian process incorporating covariate information **109**
6.3 Approaches for monitoring both regression parameters and profile variance **112**
6.3.1 An adaptive EWMA control chart **113**
6.3.2 An ensemble neural network framework **115**
6.4 Other techniques for monitoring nonparametric profiles **118**
6.4.1 Bayesian sequential monitoring of nonlinear profiles with wavelets **119**
6.4.2 A study for machine condition monitoring **122**
CHAPTER 7 Multivariate profiles **125**
Introduction **125**
7.1 Multivariate principal component analysis methods **128**
7.1.1 Thresholded principal component analysis for Phase I **128**
7.1.2 Multichannel functional principal component analysis in Phase II **133**
7.1.3 A recent study in product portfolio management **136**
7.2 Correlation in profile monitoring methods **139**
7.2.1 Auto-correlated profiles: A MLMM approach **139**
7.2.2 A study for flexible production environments **142**
7.3 Other techniques for monitoring multivariate profiles **144**
7.3.1 The effect of parameter estimation on the performance of control charts in Phase II analysis **144**
7.3.2 Simultaneous monitoring of the mean vector and covariance matrix **148**
7.3.3 Monitoring profiles in multistage processes **152**
CHAPTER 8 Conclusions and further research **155**
References **164**

LIST OF TABLES

Table **Page**

Table 3_1. A brief overview of methods developed to monitor simple linear profiles from 2008 to 2018. **15**

Table 4_1. A brief overview of methods developed to monitor generalized linear profiles from 2008 to 2018. **50**

Table 5_1. A brief overview of methods developed to monitor geometric and polynomial profiles from 2008 to 2018. **74**

Table 6_1. A brief overview of methods developed to monitor nonparametric profiles from 2008 to 2018. **100**

Table 7_1. A brief overview of methods developed to monitor multiple linear profiles from 2008 to 2018. **126**

LIST OF FIGURES

Figure **Page**

Figure 1_1. The profiles of exosomal surface proteins using DNA-PAINT approach for wide-field TIRF images and for super-resolution images. **3**

Figure 1_2. The profiles of gut microbiota in the three age groups. **3**

Figure 1_3. The profile of extracellular vesicles at the single-cell level. **4**

Figure 1_4. Four different cyclic voltammetry profiles. a) ideal profile. b) slanted, c) blunt, and d) mix of blunt and slanted profiles. **4**

CHAPTER 1

Introduction to Profile Monitoring

Introduction

Quality plays a crucial role in the success and prosperity of many production and service organizations. In a competitive market, companies try to differentiate the processes they use or their products from the rest of the market. The implementation of competition policy encourages entrepreneurship, efficiency and improves quality. More specifically, a company that can meet the needs of its customers and at the same time can combine low prices and superior quality in its products, can easily dominate the market. But how can quality be defined? According to a traditional definition, quality means fitness for use. However, a more modern, widely used and attractive definition names quality as inversely proportional to variability. Thus, a product is defined as qualitative when it is adapted to the requirements of the user and has an inverse relationship with its variability. Therefore, reducing the variability of a process or product is a primary interest for market professionals.

A characteristic tool of statistical process control (SPC), that is successfully used in many production and non-production processes and helps professionals improve the quality of a process or product while reducing their sources of variability, is the control chart. A control chart contains a center line, an upper control limit and a lower control limit. Furthermore, a point that plots within the control limits indicates the process is in – control and a point that plots outside the control limits is evidence that the process is out – of – control. In the last case, investigation and corrective action are required to find and eliminate assignable cause(s).

Profile monitoring generally involves the use of various statistical techniques with the control chart playing a major role in monitoring a process or product. Therefore, profile monitoring can be defined as the use of control charts for cases where the quality of a process or product can be characterized by a functional relationship between a response variable (Y) and one or more

explanatory variables (X's). One of the most important considerations for profiling is the distinction between Phase I and Phase II. More specifically, Phase I is a retrospective analysis of process data to construct trial control limits. Charts are effective at detecting shifts in process parameters, outliers, measurement errors, data entry errors, etc. Moreover, Phase I facilitates identification and removal of assignable causes. On the other hand, in Phase II, the control chart is used to monitor the process. Process is assumed to be reasonably stable and emphasis is on process monitoring, not on bringing an unruly process into control. Please note that, either parametric models or non-parametric methods can be used in both phases. Finally, it is emphasized that the aim of the control chart is to quickly identify a possible deviation from a normal profile pattern, which has made it play an important role in profile monitoring.

1.1 Functional relationships qualified as profiles

This section will provide some examples where the quality of a process or product is best modelled by a profile rather than measurements on a single quality characteristic or a vector of quality characteristics. More specifically, they were chosen to discuss practical applications from everyday life, where a profile can characterize the performance of a process or product. Therefore, below are examples from recent research on applications related to everyday life.

1.1.1 Profiles of exosomal biomarkers

Delcanale et al. (2018) utilized DNA-PAINT to quantify the active sites on the surface of nanomaterials. A year later, Chen et al. (2019) applied the above approach to realize the quantitative profiling of exosomal biomarkers. This method allows to profile surface biomarkers at the level of an exosome. Figure 1_1 represents the profile of four extracorporeal surface biomarkers (HER2, GPC-1, EGFR, EpCAM) to detect cancer samples in the blood, where the above biomarkers along with the proteins CD63 and CD81 have undergone fluorescence.

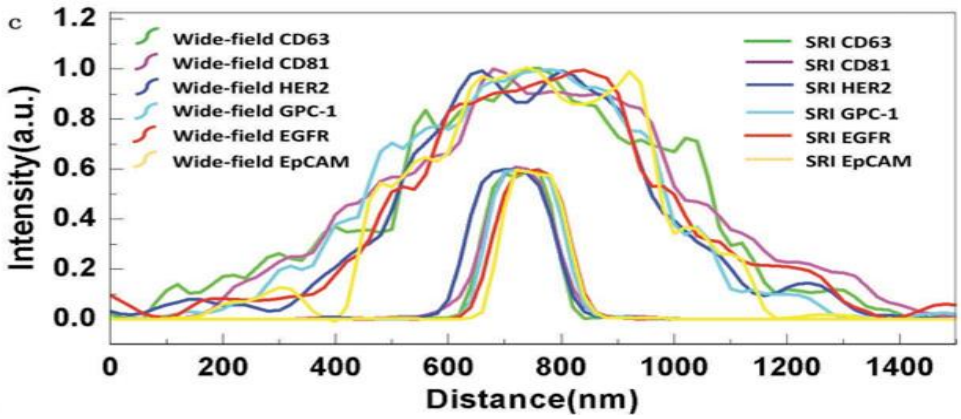

Figure 1_1. The profiles of exosomal surface proteins using DNA-PAINT approach for wide-field TIRF images and for super-resolution images. (Adapted from Chen et al. (2019)).

1.1.2 Profiles of gut microbiota in Sardinian centenarians

Wu et al. (2019) provided a study on the role that the gut microbiota may play in longevity. More specifically, the research analyses the composition profiles of the gut microflora of three age groups. For this reason, a sample population from Sardinia of size 65 (n=65) was used. This sample was classified into the following age groups: young (n_1=19), elderly (n_2=25) and centenarians (n_3=21). Figure 1_2 represents the profiles of gut microbiota in the three age groups. As we can see, the elderly group (E) shared similar profiles with the young group (Y) but differed from the centenarian group (C).

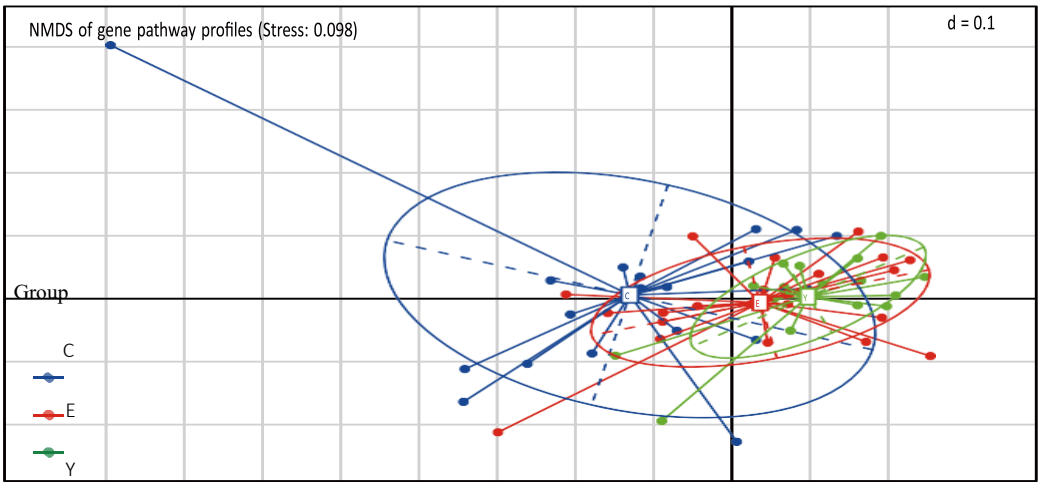

Figure 1_2. The profiles of gut microbiota in the three age groups. (Adapted from Wu et al. (2019)).

1.1.3 Profiles of extracellular vesicles

Huang et al. (2020) provided a study in which they investigated recent approaches to isolate extracellular vesicles. More specifically, their study highlights the importance of the profile and corresponding monitoring of individual extracellular vesicles. Figure 1_3 represents the process of isolating cells and monitoring their profile over time.

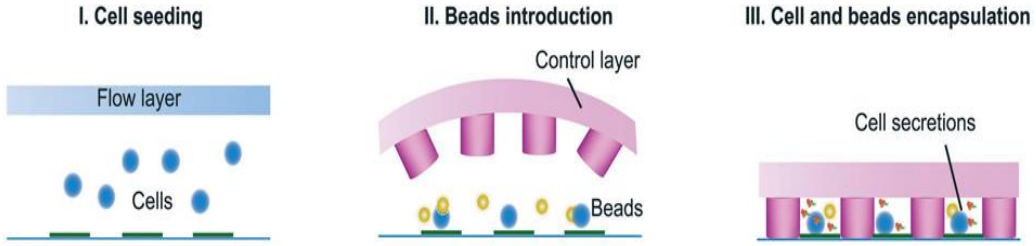

Figure 1_3. The profile of extracellular vesicles at the single-cell level. (Adapted from Huang et al. (2020)).

1.1.4 Profiles of cyclic voltammetry

Boonpakdee et al. (2018) provided a profiling method for cyclic voltammograms. More specifically, by observing the profiles of devices, which have materials with low electrical conductivity, they concluded that the above devices may exhibit non-ideal cycle behavior during cyclic voltammetry (Figure 1_4). Note that the ideal profile of cyclic voltammograms is a rectangular profile.

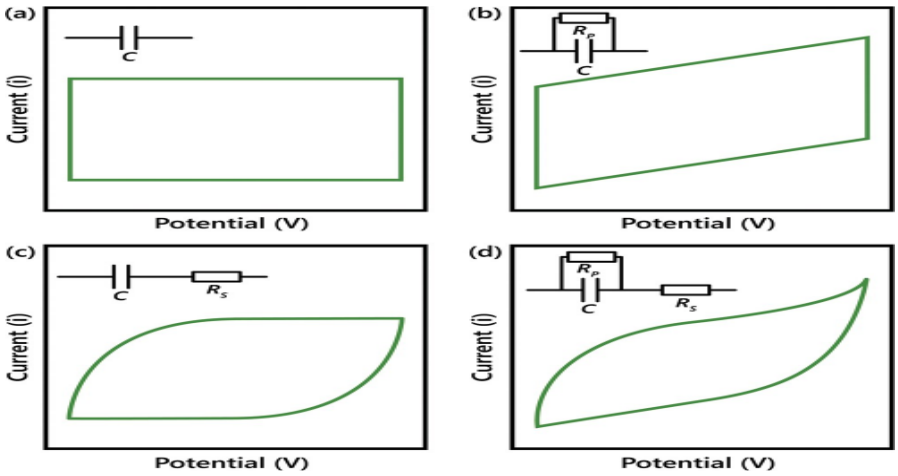

Figure 1_4. Four different cyclic voltammetry profiles. a) ideal profile. b) slanted, c) blunt, and d) mix of blunt and slanted profiles. (Adapted from Mathis et al. (2019)).

1.2 Structure of this thesis

The purpose of this section is to present the structure of this thesis. For this reason, a brief description of each chapter is given below.

- Chapter 2. Statistical concepts will be developed in this chapter, which are used in subsequent chapters and are essential for profiling. For this reason, basic concepts such as the control chart, its structure and its different types, Phase I, Phase II as well as the performance measures used to compare different methods in profiling will be defined and analyzed.
- Chapter 3. In most calibration applications, the functional relationship between the response variable and one or more explanatory variables is given by a simple linear regression model. Since 2007, following Woodall's seminal review paper (2007), more and more papers have come to light on profiling methods, focusing mainly on the applications of simple linear models. In this chapter, after a brief reference to past methods of monitoring simple linear profiles, we will focus on recent methods. More specifically, methods will be discussed in cases where, for example, the assumption of normality does not apply to the linear model data, the estimation of parameters is done with the help of robust estimation methods and the monitoring of linear profiles be possible under the influence of Bayesian approach.
- Chapter 4. This chapter will be divided into two parts, where the first part will refer to modern methods of monitoring generalized linear profiles using appropriate control charts in each case as well as robust estimators will be used to study a method. The second part will discuss recent methods of monitoring generalized linear mixed profiles, discussing three different approaches, two of which use robust estimation methods and the last is done with the help of a weighted score test.
- Chapter 5. This chapter will discuss recent methods of monitoring geometric and polynomial profiles. More specifically, there will be a discussion on circular and cylindrical profiles, followed by recent methods for monitoring polynomial profiles, mentioning interesting cases of them.

- Chapter 6. This chapter will discuss both recent developments in nonparametric nonlinear profiles and more general nonparametric methods applicable to general profiles.
- Chapter 7. This chapter will discuss recent developments in monitoring multivariate profiles. More specifically, appropriate models and control charts will be used to analyze the methods and draw useful conclusions.
- Chapter 8. In this last chapter of the thesis, we will summarize the important parts of the previous chapters and write the conclusions that will have emerged regarding recent developments on profile monitoring.

CHAPTER 2

Basic principles

Introduction

The era of globalization and the rapid development of technology brings to the surface man's need for adaptability and flexibility in the ever-changing environment he lives in. At the same time, its material needs are constantly changing and follow the trends of the seasons, resulting in greater demand and requiring better and better quality in the products of the market. Ensuring high quality seems to be the key to the survival of factories and industries. Thus, each manufactory aims at the continuous improvement of its products, competing with the rest in terms of quality, price and consumer needs. Based on the above philosophy, the main goal of modern industries is the stable or repeated production process of a product, so that it can meet to a significant extent the expectations of customers or exceed them. Therefore, companies introduced the concept of statistical process control (SPC) into their strategic planning, a concept which consists of a powerful collection of problem-solving tools useful for achieving the stability of the production process, differentiation from other industrial units, high quality and product improvement through the reduction of variability. It is worth noting that, no matter how well a production process is structured and designed, there will always be a quantity of natural variability, which in statistical control is called stable system of chance causes. This variability occurs under natural causes and will always take a small percentage of the process, but without being a problem. Thus, the process will be said to be under an in – control situation. However, other types of variability that take place in a production process and significantly affect its qualitative characteristics are called assignable causes of variation. The presence of such assignable causes transforms the process into an out – of – control state. Therefore, SPC is an on-line technique that aims to monitor production processes, reducing variability through elimination of assignable causes and creating an environment of continuous improvement and productivity.

Furthermore, the seven major tools of SPC, often called “the magnificent seven”, are the following: a) histogram or stem-and-leaf plot, b) check sheet, c) Pareto chart, d) cause-and-effect diagram, e) defect concentration diagram, f) scatter diagram, and g) control chart. Among the above tools, the control chart is recognized as the most technologically advanced. Its popularity is due to the fact that is a proven technique for improving productivity and is effective in defect prevention. Moreover, control charts prevent unnecessary process adjustment, provide diagnostic information and provide information about process capability. Finally, control charts have the ability to detect assignable causes that drive the process out – of – control and, after examining these causes, completely or significantly eliminate the variability of the process and turn it into an in – control state.

The continuation of this chapter includes the basic principles and structure of control charts, the separation of Phase I and Phase II, the criteria and measures used to evaluate chart performance. Finally, this section will close by mentioning basic and useful control charts that will be used in future chapters.

2.1 Structure of the control chart

The control chart represents a graphical display of a quality characteristic that has been measured from a sample versus the time. This graphic contains a line, called the center line, which represents the average value of the quality characteristic. Furthermore, two more horizontal lines, called the upper control limit (UCL) and the lower control limit (LCL), are included in the chart. Control limits are particularly useful, as based on them we can determine whether a process is stable over time or has a change. More specifically, if all the sample points that have been observed are within the upper and lower control limits, then this indicates that the process is in – control and no action is necessary. Conversely, if a point is found outside the control limits, then this is evidence that the process is in an out – of – control state, and, so, we should stop the process, find the assignable causes that led the process to such a state, examine them and then eliminate them. It is worth noting that, control charts should be thoroughly investigated, as even if all sample points are within the limits, if they have a systematic or non-random pattern, then this is an

indication that the process is in an out – of – control state. Based on the above information, one could say that control charts have a connection with hypothesis testing, i.e., they examine the null hypothesis that the process is in – control (H_0: in – control) versus the alternative hypothesis that the process is out – of – control (H_1: out – of – control).

As mentioned above, control charts are a useful tool in the field of statistical process control, as they help experts investigate and monitor a production process. Profile monitoring approaches are typically divided into two distinct phases, Phase I (retrospective phase) and Phase II (prospective or monitoring phase). These phases serve different purposes, with Phase I involving the analysis of historical data points. The primary goals of Phase I include assessing process stability, identifying and eliminating assignable causes, and estimating process parameters using in – control samples. The aim in Phase I is on reliably recognizing assignable causes. On the other hand, Phase II is focused on quickly detecting shifts based on the estimated parameters obtained in Phase I. It is reported that the earlier we receive a warning signal about any changes in the production process, the earlier it will stop so that the problem can be examined and corrected. Finally, monitoring approaches employed in these phases differ, utilizing distinct evaluation metrics tailored to their specific objectives and will be discussed in the next section.

2.2 Evaluation criterion

As mentioned in the previous section, the main objective of the Phase I analysis is to understand the process and assess process stability, eliminating any assignable causes of variation. Moreover, control charts are effective at detecting large, sustained shifts in process parameters, outliers and measurement errors. Therefore, below we will briefly see the key measures used in the Phase I analysis to evaluate the control charts in order to ensure that the process is truly in an in – control situation.

- The most popular criterion for evaluating the performance of a control chart in Phase I analysis is the signal probability criterion and is defined as the probability that, at least, one charted statistic falls outside the control limits interval.

- False alarm rate (FAR) is another measure used to evaluate the performance of a control chart in Phase I and is defined as the probability of a false alarm at every sampling stage, which is controlled at a desired level to determine the control limits.
- The false alarm probability (FAP) performance criterion is defined as the overall probability of at least one false alarm during Phase I analysis.

On the other hand, the primary purpose of Phase II is to monitor the production process and identify any shifts in it. The monitoring is done with the help of control charts and their evaluation in Phase II analysis is carried out with the following performance criteria:

- The most widespread and widely known performance criterion is the average run length (ARL). This criterion defined as the average number of samples taken until the chart indicates an out-of-control signal.
- The average time to signal (ATS) defined as the average time required to detect a shift in the process. Please note that, if the samples are taken in fixed intervals of time that are h hours apart, then the average time to signal is equal to the average run length of h, i.e.,

  $$ATS = ARLh, \quad (2.1).$$
- In general, the run length is the number of samples taken until the chart gives an out-of-control signal. Therefore, other popular measures based on the run-length characteristics of control charts are the standard deviation of the run length (SDRL), the standard deviation of ARL (SDARL) which is a very useful metric for measuring the variation of a process and the average of ARL (AARL) metric. Finally, the coefficient of the variation of average run length (CVARL) is another performance criterion and is calculated as:

  $$CVARL = \frac{SDARL}{AARL} \times 100, \quad (2.2).$$

2.3 Basic control charts

This section will present the most basic control charts used in the field of SPC in order to monitor a quality characteristic that behaves as a variable. As already mentioned, in a production process it is necessary to monitor both the mean value of the quality characteristic and its variability. This action is implemented by appropriate control charts, the structure of which is briefly described below.

- The $\bar{x}$ control chart is used to monitor the mean value of the quality characteristic and the formula for its construction is given below.

  Suppose that m samples are collected, each containing n observations of the quality characteristic. Then, the best estimator of the mean value of this characteristic is defined by the following form:

  $$\bar{\bar{x}} = (\bar{x}_1 + \bar{x}_2 + \ldots + \bar{x}_m) / m, \quad (2.3),$$

  where $\bar{x}_i$ represents the average value of sample i, i = 1, …, m.

  Thus, the Eq. (2.3) represents the center line of the $\bar{x}$ chart. Based on this center line, the upper and lower control limits are defined as:

  $$UCL = \bar{\bar{x}} + A_2 \bar{R}, \quad (2.4)$$

  $$LCL = \bar{\bar{x}} - A_2 \bar{R}, \quad (2.5)$$

  where $\bar{R} = [(R_1 + R_2 + \ldots + R_m) / m]$ is the average range and A_2 represents a constant value, depending on the sample size, n, that each professional will use.

- The R control chart is used to monitor the variability of the quality characteristic and the formula for its construction is given below.

  Suppose that m samples are collected, each containing n observations of the quality characteristic. Then, the center line, the upper and lower control limits, respectively, are defined as follows:

  $$UCL = D_4 \bar{R}, \quad (2.6),$$

  $$Center\ line = \bar{R}, \quad (2.7),$$

  $$LCL = D_3 \bar{R}, \quad (2.8),$$

  where $\bar{R} = [(R_1 + R_2 + \ldots + R_m) / m]$ is the average range and D_3, D_4 represent constant values, depending on the sample size, n, that each professional will use.

- The exponentially weighted moving average (EWMA) control chart has the ability to monitor both the mean and variability of the quality characteristic and the formula for its construction is given below.

  Suppose that $\{x_1, x_2, \ldots, x_n\}$ samples are collected. Then, the charting statistic defined as:

  $z_i = \lambda x_i + (1 - \lambda) z_{i-1}$, i = 1, 2, …, n, (2.9)

  where λ $(0 < \lambda < 1)$ represents the smoothing parameter and z_0 is the process target.

  Please note that, if we want to monitor the mean of a quality characteristic, then the process target is equal to the process in – control mean, i.e., $z_0 = \mu_0$. In this case, the center line, the upper and lower control limits, respectively, are given by:

  $$UCL = \mu_0 + L\sigma\sqrt{\frac{\lambda}{1-\lambda}\left[1 - (1 - \lambda)^{2i}\right]}, \quad (2.10),$$

  $$Center\ line = \mu_0, \quad (2.11),$$

  $$LCL = \mu_0 - L\sigma\sqrt{\frac{\lambda}{1-\lambda}\left[1 - (1 - \lambda)^{2i}\right]}, \quad (2.12),$$

  where L represents the width of the control limits and σ is the standard deviation of the independent variables x_i.

It is worth noting that, the first two control charts, $\bar{x}$ and R, are very useful for the Phase I analysis, because the patterns on these charts often provide guidance regarding the nature of the assignable causes. However, these charts use only the information about the process, which is contained in the last point, and so, they ignore any information given by the whole sequence of points. On the other hand, the EWMA control chart is very useful for Phase II analysis, because it takes into account information from previous samples. Furthermore, it has the ability to detect small changes in a production process and is thus more effective than the first two, which are sensitive to large changes. Finally, it is noted that, in the following chapters each new control chart that is analyzed, depending on the type of each profile it represents, its structure is described there.

CHAPTER 3

Simple linear profiles

Introduction

The most common case for monitoring a process or product profile is the simple linear profile, where it is represented through a simple linear regression model. According to this model, the response variable is related to a single explanatory or independent variable through a linear model. Since this is the case, i.e., a single explanatory variable describes the behavior of the response variable, we are talking about univariate response data.

For the j^{th} sample profile, where j = 1, 2, ... is the number of sample profiles, which is denoted by $\{(x_i, y_{ij}), i = 1, 2, ..., n\}$, where n denotes the number of observations in each profile, we get the following model:

$$y_{ij} = \beta_0 + \beta_1 x_i + \varepsilon_{ij}, \quad (3.1)$$

where β_0 and β_1 are the intercept and slope coefficients, respectively and ε_{ij} are the errors of the above model.

The simple linear model in Eq. (3.1) can equivalently be written as:

$$y_{ij} = B_0 + B_1 x_i^* + \varepsilon_{ij}, \quad (3.2)$$

with $B_0 = \beta_0 + \beta_1 \bar{x}$, $B_1 = \beta_1$, and $x_i^* = (x_i - \bar{x})$, where $\bar{x} = \sum_{i=1}^{n} x_i / n$.

A typical assumption in monitoring simple linear regression profiles is that ε_{ij} errors are independent and identically distributed and follow the normal distribution. However, methods have been proposed in the literature that do not use the above assumption for errors, such as the method developed by Noorossana et al. (2007, 2008) in which the simple linear profile for autocorrelated errors was studied, and the method of Noorossana et al. (2011) in which the normal distribution of errors was not used for the monitoring of simple linear profiles, but t-distribution.

To monitor a simple linear profile as a first step is the analysis of Phase I. During Phase I the parameters of the model are estimated, which will later be used to design the control charts for monitoring the Phase II of the model parameters. Moving on to Phase II, the focus is on quickly detecting any

changes in the parameters of the model in relation to the values they had within control in Phase I. Several scientific studies have been cited in the literature, such as the method of Zhu and Lin (2009) in which monitoring the slopes of regression lines for Phase I and Phase II, the method of Zou et al. (2006) and the approach of Mahmoud et al. (2007), who studied the change point method for linear profile data. Based on the above, it is easy to understand that the distinction between the two phases is necessary. It should be noted here that, Zou et al. (2007) investigated a method where they avoided, as far as possible, the distinction between Phase I and Phase II. However, as there is generally a distinction between the two phases as mentioned above, different types of statistical methods have been analyzed in the literature to measure the statistical performance of each chart to monitor the profile of a process or product in either Phase I or Phase II. More specifically, Phase I uses the signal probability criterion in which performance is measured as the probability of obtaining at least one charted statistic falls outside the control limits interval. Finally, the performance of control chart methods for Phase II is usually measured based on a statistic, which is adapted from the run – length characteristics of the control charts. Therefore, such measurements are, for example, the average run length (ARL), the average number of items observed (ANI), the adjusted average time to signal (AATS), the steady-state ARL (SS – ARL), the steady-state SDRL (SS-SDRL), the median absolute deviance (MAD), the inter quantile range (IQR), the average number of samples until a signal (ANS), the extra quadratic loss (EQL), the relative average run length (RARL), the performance comparison index (PCI) and the relative lost in efficiency (RLE), the average ($\bar{\hat{\tau}}$) and the standard deviation of estimated change point (SD($\hat{\tau}$)). It should be noted that, the run length is the number of samples taken until the chart gives an out-of-control signal.

Table 3_1 briefly mentions previous research conducted to monitor simple linear profiles over a decade from 2008 to 2018. More specifically, lists the researchers, whether the expert study concerned Phase I or Phase II of the profile, and the criterion for measuring the performance of the control charts used. It is worth noting that, as we are talking about monitoring simple linear profiles of a process or product, we are talking about univariate response data.

Research	Phase I	Phase II	Performance criterion
Noorossana et al. (2008)	-	Yes	ARL
Saghaei et al. (2009)	-	Yes	ARL
Soleimani et al. (2009)	-	Yes	ARL
Zhang et al. (2009)	-	Yes	ARL
Ho et al. (2010)	Yes	-	Regression metric
Li and Wang (2010)	-	Yes	AATS
Mahmoud et al. (2010)	-	Yes	SS-ARL & SS-SDRL
Noorossana et al. (2010b)	-	Yes	ARL
Noorossana et al. (2010c)	-	Yes	ARL
Noorossana et al. (2011b)	-	Yes	ARL
Hosseinifara and Abbasi (2012a)	-	-	C_{pu}
Hosseinifara and Abbasi (2012b)	-	-	C_{pu}
Mahmoud (2012)	-	Yes	ARL & SDRL
Noghondarin and Ghobadi (2012)	Yes	-	Similarity index
Noorossana and Ayoubi (2012)	-	Yes	ARL & SDRL
			(continued)

Soleimani and Noorossana (2012)	-	Yes	ARL
Wang and Huwang (2012)	-	Yes	ARL, $\bar{\hat{\tau}}$, SD($\hat{\tau}$) & precision
Amiri et al. (2013)	-	Yes	ARL
Ebadi and Shahriari (2013)	-	-	$\widehat{C_{PKA}}$ & $\widehat{C_{PM}}$
Gani and Limam (2013)	-	Yes	ARL
Soleimani et al. (2013b)	-	Yes	ARL
Yeh and Zerehsaz (2013)	Yes	-	Signal probability
Abdella et al. (2014)	-	Yes	ATS
Adibi et al. (2014b)	-	Yes	ARL
Amiri and Mohebbi (2014)	-	Yes	ARL_0, ARL_1, Cost & Optimum variables
Amiri et al. (2014b)	-	Yes	ARL
Farahani et al. (2014)	-	Yes	ARL
Ghahyazi et al. (2014)	-	Yes	ARL
Ghobadi et al. (2014)	Yes	-	Signal probability
Nemati Keshteli et al. (2014a)	-	-	C_P, C_{PK}, C_{PL}
			(continued)

Wang and Tamirat (2014)	-	-	$S_{pkA;AR(1)}$
Soleimani and Noorossana (2014)	-	Yes	ARL
Noorossana et al. (2014b)	-	Yes	ARL_0, ARL_1, Cost & Optimum variables
Zhang et al. (2014a)	-	Yes	ARL
Zhang et al. (2014b)	-	Yes	ARL
Aly et al. (2015)	-	Yes	SDARL
Khedmati and Niaki (2015)	-	Yes	$\bar{\hat{\tau}}$, SD($\hat{\tau}$) & precision
Moghadam et al. (2015)	-	Yes	ARL
Niaki et al. (2015)	Yes	-	Signal probability
Noorossana et al. (2015a)	-	Yes	ARL
Noorossana and Zerehsaz (2015)	-	Yes	ARL
Vakilian et al. (2015)	-	Yes	$\bar{\hat{\tau}}$, SD($\hat{\tau}$) & precision
Wang and Tamirat (2015)	-	-	$S_{pkA;AR(1)}$
Abdella et al. (2016)	-	Yes	ARL
Chen et al. (2016)	-	Yes	ARL
			(continued)

De Magalhaes and Von Doellinger (2016)	-	Yes	ARL
Jensen et al. (2016)	Yes	Yes	-
Huwang et al. (2016)	-	Yes	ARL, $\bar{\hat{\tau}}$, SD($\hat{\tau}$) & correct classification
Kamranrad and Amiri (2016)	-	Yes	ARL, MAD & IQR
Karimi Ghartemani et al. (2016)	-	-	MC_pM
Wang (2016)	-	-	TS_{pKA}
Kazemzadeh et al. (2016b)	-	Yes	$\bar{\hat{\tau}}$, SD($\hat{\tau}$) & precision
Moghadam et al. (2016)	-	Yes	Process state
Noorossana et al. (2016)	-	Yes	ARL
Tamirat and Wang (2016)	-	-	Lot acceptance probability
Kazemzadeh et al. (2016a)	-	Yes	ATS, ANI & ANS
Wang and Tamirat (2016)	-	-	C^T_{puA}, C^T_{pLA}, $C^T_{puA;PC}$ & $C^T_{pLA;PC}$
Zhang et al. (2016)	-	Yes	ARL & SDRL
Chiang et al. (2016)	-	Yes	BC_p & BC_{pk}
			(continued)

Esmaeeli et al. (2017)	-	Yes	ARL & correct diagnosis
Kalaei et al. (2017)	Yes	-	Signal probability
Riaz et al. (2017)	-	Yes	ARL, EQL, RARL & PCI
Sayyad et al. (2017)	Yes	Yes	ARL, SDRL & RLE
Taghipour et al. (2017)	Yes	-	Signal probability
Wang and Huang (2017)	-	Yes	ARL
Zhang et al. (2017a)	-	Yes	ARL
Zhang et al. (2017b)	-	Yes	ARL & SDRL

Table 3_1. A brief overview of methods developed to monitor simple linear profiles from 2008 to 2018. (Adapted from Maleki, M. R., Amiri, A., & Castagliola, P. (2018)).

Finally, based on the fact that, following the detailed review papers of Woodall (2007) and Maleki et al. (2018) almost a decade later, there is no review paper available from 2018 onwards, the continuation of this chapter aims to present recent studies, research and developments for monitoring simple linear profiles.

3.1 Methods for simultaneous shifts in the profile parameters

In this section, two recent studies on simultaneous monitoring of linear profile parameters will be discussed. In the first place, a study by Saeed et al. (2018), who examined the monitoring of simple linear profiles based on progressive mean, will be introduced. Then, the study by Yeganeh et al. (2021), who developed a new scheme based on a combination of multivariate exponentially weighted moving average (MEWMA) control chart, which is introduced by Zou

et al. (2007), and novel run – rules to improve the performance of monitoring a simple linear profile in Phase II, will be mentioned.

3.1.1 A memory type structure based on progressive mean

In this subsection we will mention the study of Saeed et al. (2018), who designed a new memory type control chart based on progressive mean in order to simultaneously monitor the parameters of the simple linear model. Therefore, for the j^{th} profile of the Eq. (3.2), the j^{th} progressive statistics for intercept, slope and error variance, respectively, are defined as follows:

$$PM_I(j) = \sum_{k=1}^{j} b_{0k} \,/\, j, \tag{3.3}$$

$$PM_S(j) = \sum_{k=1}^{j} b_{1k} \,/\, j, \tag{3.4}$$

$$PM_E(j) = \sum_{k=1}^{j} [\sum_{i=1}^{n} (y_{ij} - \widehat{y_{ij}})^2 \,/\, (n-2)] \,/\, j, \tag{3.5}$$

where b_{0k} and b_{1k} are the estimates of B_0 and B_1 of the simple linear model in Eq. (3.2),respectively, while $\widehat{y_{ij}}$ is the i^{th} predicted value for the j^{th} profile.

In addition, upper control limits (UCL) and lower control limits (LCL), respectively, for each progressive statistic are in the form of:

For intercept: $B_0 \pm L_I \sigma \sqrt{1/n}\, f(j)$, (3.6)

For slope: $B_1 \pm L_S \sigma \sqrt{1/\sum_{i=1}^{n} (x_i - \bar{x})^2}\; f(j)$, (3.7)

For error variance: $\sigma^2 \pm L_E \sigma^2 \sqrt{2/(n-2)}\, f(j)$, (3.8)

where $f(j) = j^{-(0.5 + q)}$ be the penalty function and L_I, L_S, L_E are the charting constants for intercept, slope, error variance of the new progressive mean control chart, respectively.

Saeed et al. (2018) compared through their study the new progressive mean chart with already existing and known control charts. So, the comparison was made with: a) the EWMA/R chart, which is a combination between the exponentially weighted moving average EWMA chart used to monitor the average deviation from the in – control profile and the range R control chart used to monitor the variation about this profile, b) the Hotelling T^2 control chart which has as lower control limit the zero and upper control limit the α^{th} quantile

of χ^2 distribution, c) the EWMA_3 chart which has the three individual EWMA statistics for each parameter of the simple linear model of Eq. (3.2) and, d) the Shewhart_3 chart which has the individual Shewhart chart for intercept, slope and error variance, respectively. The performance measures ARL, RARL, SRARL, EQL and SEQL were used to compare the above control charts. Finally, it is worth noting that, during their simulation study, they set an overall in – control average run length $ARL_0 = 200$ and therefore the value of q in the penalty function was set equal to 0.2.

The conclusions reached were as follows:

- For small and moderate shifts in the intercept of the Eq. (3.2), according to the ARL performance measure, the new progressive mean control chart performs better than the EWMA_3 and EWMA/R charts, while these in turn perform better than the Hotelling T^2 and Shewhart_3 charts.
- For large shifts in the intercept of the Eq. (3.2), the new progressive mean control chart performs better than the Hotelling T^2 and Shewhart_3 charts, while these in turn perform better than the EWMA_3 and EWMA/R charts.
- In general, for any value in the intercept shift in the Eq. (3.2), the values of ARL, RARL and EQL metrics, which are smaller than those of the other charts examined, indicate that the progressive mean control chart performs better at identifying shifts.
- For slope shifts of the Eq. (3.1), the values of ARL, EQL and RARL are lower for the new control chart than for the rest. Therefore, in this case too, it seems that the progressive mean control chart performs better.
- For small shifts in the error variance of the Eq. (3.1), it was observed that the ARL value for the new control chart was lower than for the others, while for moderate and large shifts the Shewhart_3 chart has a smaller ARL value. However, for any value in the shift of the error variance, the progressive mean chart shows smaller values in EQL and RARL, which indicates that it has better detection ability.

- For slope shifts of the Eq. (3.2), based on the performance measures ARL, EQL and RARL, it was observed that these values are lower on the new control chart than EWMA_3, EWMA/R, Hotelling T^2 and Shewhart_3 charts.
- When in the Eq. (3.2) exist joint shifts in intercept and slope, then according to the ARL the performance of the new progressive control chart is better than other charts. It is noted that, second in a row comes the EWMA_3 control chart for simultaneous detection of shift in the intercept and the slope of the model.

3.1.2 MEWMA control chart with innovative run – rules

In this subsection a novel approach is introduced by Yeganeh et al. (2021) for enhancing the efficacy of Phase II monitoring of simple linear profiles. This innovative scheme integrates multivariate exponentially weighted moving average control charts with a set of new run-rules. Therefore, MEWMA statistic and the idea of run – rules are briefly given below.

The MEWMA control chart introduced by Zou et al. (2007), is used to monitor linear profiles and MEWMA statistic, based on simple linear model in Eq. (3.1), is defined as:

$$U_j = W_j^T \Sigma^{-1} W_j, \text{ j} = 1, 2, \ldots \quad (3.9)$$

with $W_j = \theta Z_j + (1-\theta)W_{j-1}$, where W_j represents the exponentially weighted moving average of the vector Z_j for the j^{th} profile, θ ($0 \leq \theta \leq 1$) represents the smoothing parameter and Z_j is multivariate normally distributed vector with mean vector 0 and covariance matrix $\Sigma = \begin{pmatrix} (X'X)^{-1} & \mid 0 \\ 0 & \mid 1 \end{pmatrix}$.

Furthermore, run – rules can be defined with a rule matrix of dimension $S \times 3$, where S represents the number of rules, as follows:

$$\begin{pmatrix} r_1 & p_1 & m_1 \\ \cdots & \cdots & \cdots \\ r_S & p_S & m_S \end{pmatrix}, \quad (3.10)$$

where r_k ($1 \leq k \leq S$) represents the regions of each rule so that, region 1 belongs to interval (r_1, UCL_{rule}), …., and region S belongs to interval (r_S, UCL_{rule}),

where UCL_{rule} is the upper control limit of MEWMA chart using run – rules, p_k $(1 \leq k \leq S)$ is the maximum acceptable ratio of the number of points in each region to the total number of points until the current sample and m_k $(1 \leq k \leq S)$ represent the maximum number of points in each region for satisfied rules. As an interpretation we could say for example that, the first rule shows that if the ratio of the number of points in region 1 to the total number of points is greater than p_1 and at least $(m_1 + 1)$ points is in this region then , the rule fires, i.e., satisfied, and the chart signals an out – of – control situation.

Remarkably, the process is in an out-of-control state when the Uj statistic is outside the upper or lower control limits, even if the rule has not fired. The results obtained in Phase II are extracted through a simulation study, where the new MEWMA scheme is compared with the following known schemes: a) T^2 control chart by Kang and Albin (2000), b) EWMA_3 control chart by Kim et al. (2003), c) multivariate exponentially weighted moving average (MEWMA) control chart by Zou et al. (2007), d) the three distinct cumulative sum (CUSUM_3) charts to detect step shifts in the model parameters, i.e., intercept, slope, and error variance, by Saghaei et al. (2009), e) likelihood rate test (LRT), which is a statistical test of the goodness – of – fit, by Zhang et al. (2009), f) artificial neural network (ANN1) by Hosseinifard et al. (2011), g) generalized likelihood ratio (GLR) control chart by Xu et al. (2012), h) variable simultaneous confidence set (VSCS) by Huwang et al. (2014), i) EWMA – area control chart, which represents an area-based approach for monitor general linear profile slopes and intercept simultaneously, by Motasemi et al. (2017) and j) proposed scheme (PM) by Saeed et al. (2018), which developed in the previous subsection. Finally, the above comparisons are made in terms of ARL criterion.

The conclusions drawn are as follows:

- For small positive shifts in the regression parameters of the alternative linear model in Eq. (3.2), the proposed new method based on both MEWMA control chart and run – rules were observed to perform better than the other examined methods, as it receives smaller ARL values and thus has the ability to detect a change faster. However, for moderate and

large shifts, other methods were a bit better. Specifically for moderate and large positive shifts in intercept, CUSUM_3 performs better than other methods. Moreover, for moderate and large positive shifts in slope both CUSUM_3 and VSCS methods are better than the others and for large shifts in error variance CUSUM_3 performs better, again. Finally, it should be noted that, for small positive changes in the error variance the proposed method has better results than the PM approach, while for moderate and large shifts in the error variance the PM was more efficient.

- For positive shifts in the profile parameters, i.e., intercept, slope and error variance, it was observed that the ANN1 method takes longer to detect a shift. Therefore, this makes it less effective compared to other methods.
- For decreasing shifts in the profile parameters of model in Eq. (3.2), the new method seems to work effectively, particularly for small and moderate shifts.
- For uncoordinated shifts in intercept and slope of model in Eq. (3.2), the EMWA – area method performed significantly better than all other methods examined in this study for any size of shift, i.e., small, moderate and large shift, respectively. Moreover, for small shifts, the new proposed method based on MEWMA control chart and run – rules as well as the EWMA_3 scheme performed equally well compared to the remaining methods.
- For coordinated shifts in two parameters in the model of Eq. (3.1), the new approach performs best for small and moderate shifts, as it receives the smallest ARL values.
- For coordinated shifts in two parameters in the model of Eq. (3.2), the new method performs best in all situations and has absolute superiority over all the considered approaches in the joint shifts. It is worth mentioning that the PM method by Saeed et al. (2018) shows the second-best performance, but the ARL values are considerably greater than the ARL values of the proposed approach, which prevails in performance.

3.2 Robust estimation methods for simple linear parameters

In this section we will present three methods, which for the estimation of regression parameters use robust estimators. In the first place, a study by Hassanvand et al. (2019), who examined the monitoring two stages of a process or product, where quality characteristics are represented as simple linear profiles, will be introduced. Then the study of Salmasnia et al. (2019) will be discussed, who examined the monitoring of simple linear profiles with the simultaneous help of EWMA and R control charts under an economic-statistical design approach, and finally, the research of Moheghi et al. (2020) will be presented, who monitored simple linear profiles in the presence of outliers.

3.2.1 Robust two – stage process control chart

Considering the well-known cascade property, in which the quality of a process or product at its current production stage is affected by the quality of its previous stage, Hassanvand et al. (2019) examined multistage (two-stage) process monitoring. Specifically, their research focuses on the performance of the least square estimation method, which is compared to that of Huber's and bi – square robust estimation methods considering the effect of outliers and autocorrelations between the two stages. Furthermore, they examined through a simulation study the performance of least – square, Huber's and bi – square estimation methods and then proceeded to a comparison of the above methods.

In Phase I of statistical process control, twenty (20) sample profiles were collected of which each profile contained ten (10) different points and the process stages were two – stages process. Additionally, the error term in each profile assumed to follow normal distribution and be independently distributed. Furthermore, it was assumed that the values of the explanatory variable are constant for both steps of the procedure. Finally, to generate outliers or contamination in each run of simulation, each data point is produced according to a new model with probability p. Thus, p is defined as the probability of contamination. The hypothetical two-stage process used is the following:

$$y_{i,j,1} = 1 + x + \varepsilon_{i,j,1}, \tag{3.11}$$

$y_{i,j,2} = \varphi y_{i,j,1} + 1 + x + \varepsilon_{i,j,2},$ (3.12)

with i = 1, …, 10, j = 1, …,20, x = 1, 2, 3, 4, 5, 6, 7, 8, 9, 10, where φ is the AR(1) model parameter (autocorrelation coefficient of the two stages of process) and $\varepsilon_{i,j,1} \sim N(0, \sigma_1^2)$, $\varepsilon_{i,j,2} \sim N(0, \sigma_2^2)$, $\sigma_1^2 = \sigma_2^2$.

After generating the data, the profile parameters at each stage for each run were estimated using both the least square method and the robust estimation methods. Here it is noted that, the number of simulation runs was equal to ten thousand (10.000). In summary, the parameter estimates are as follows:

- The least square estimator for $\hat{\beta} = (X'X)^{-1} X' Y$.
- For robust estimation methods:

Step 1. Calculate the residuals $e_i = y_i - x_i\hat{\beta}$, where $\hat{\beta}$ is the least square estimator.

Step 2. Calculate the robust scale $\hat{\sigma}_r$. A popular choice for $\hat{\sigma}_r$ is the median absolute deviation (MAD), which is an unbiased and robust estimator. Therefore, $\hat{\sigma}_r$ = 1.4826*median $|e_i - \text{median}(e_i)|$.

Step 3. Calculate the standardized residuals $u_i = e_i / \hat{\sigma}_r$.

Step 4. Calculate the weights (w_i) of the Huber´s and bi – square estimators. For Huber´s estimators we have, if $|u_i| < 1.345$ then $w_i = 1$ and if $|u_i| \geq 1.345$ then $w_i = 1.345 / |u_i|$.

For bi – square estimators, if $|u_i| \leq 1.345$ then $w_i = (1 - (u_i / 1.345)^2)^2$ and if $|u_i| > 1.345$ then $w_i = 0$.

Note that, we choose 95% efficiency for the above methods.

Step 5. Calculate the weights functions of the Huber´s and bi – square estimators as W = diag(w_1, …, w_n). Here, we have W = diag(w_1, …, w_{10}).

Step 6. Calculate the new values of the model parameters as:

$\hat{\beta}_{new} = (X'W\,X)^{-1} X' W Y$ (weighted least square method).

Step 7. If $|| \hat{\beta}_{new} - \hat{\beta} || / ||\hat{\beta}_{new}|| < \varepsilon$ then $\hat{\beta}_{Final} = \hat{\beta}_{new}$ and end, else $\hat{\beta} = \hat{\beta}_{new}$ and go back to the Step 1 again.

The interested readers are referred to the comprehensive article for the detailed calculation of estimated parameters with the above methods for multistage process monitoring by Hassanvand et al. (2019).

Next, the criterion of the mean bias matrix (MBM) and the mean square error matrix (MSEM) was used to check whether the estimated results are close to the actual value of the parameters. Obviously, smaller values of these criteria signal to more reliable and accurate estimators. Jain et al. (2011) defined these criteria as:

$$MBM(\hat{B}) = E(\hat{B} - B), \tag{3.13}$$

$$MSEM(\hat{B}) = E\{vec(\hat{B} - B)' \times (vec(\hat{B} - B)')'\}, \tag{3.14}$$

where $\hat{B}$ is the matrix of estimated values and B is the matrix of the desired values of the regression parameters.

For comparison of the MBM values of the estimators, the Frobenius norm $||MBM||_F = \sqrt{tr\{MBM' \times MBM\}}$, which is known as mean absolute bias (MAB), and the trace of MSEM are calculated.

The research examined the following hypothetical scenarios for the value of the parameter of the new model: (a) change in the profile intercept, (b) change in the profile slope and (c) change in the profile standard deviation error. The conclusions drawn are as follows:

- When there is no contamination in the initially data, i.e., p = 0, then all three methods perform similarly in both stages of profiling.
- For the first stage of the process, as the probability of contamination and the value of the model parameters increase, robust estimation methods perform better than the least square method, i.e., robust methods show lower values. In fact, Huber's method is a bit better than the bi-square method.
- When there is contamination in the profile intercepts in both stages of process, for large values of φ, i.e., when strong autocorrelation occurs, then the three methods work similarly in both stages of the process. However, for contamination in both stages of the process and weak

autocorrelation, robust estimation methods perform better in the second stage of the process, as the probability of contamination takes greater values and the value of the intercept increases, compared to the least square method. In fact, the bi-square method is better than the Huber´s method.

- When there is contamination in the profile slopes in both stages of process, as the probability of contamination gets higher values and the slope value increases, Huber's method performs better in the second stage compared to the bi-square method, which in turn performs better than the least square method. Finally, the value of φ does not affect the performance of the three methods, and thus, their performance is similar in both stages for the various autocorrelation values.
- When there is contamination in the profile standard deviation errors in both stages of process, as p gets higher and the standard deviation error increases, robust estimation methods perform better in the second stage of the process than the least square method. In fact, for strong autocorrelation Huber's method is better, while for weak autocorrelation the bi-square method is better.
- At the first stage there are better performances, due to the absence of the cascade property, compared to the second stage of the process.

As the model parameters have been evaluated in Phase I, the T^2 control chart is used to monitor the model parameter estimated in Phase II for the two stages of process. Hassanvand et al. (2019) through a simulation calculated the upper limit of the T^2 control chart. Note that, the upper limit was calculated in such a way for each of the three methods examined that type – I error does not exceed 0.01. When the process is under statistical control for each stage, then the T^2 statistic follows a chi-square distribution with two (2) degrees of freedom. Therefore, for the upper control limit (UCL) it applies that, UCL = $\chi^2_{2,\alpha}$, where α is the probability of type – I error. The next step is to create out – of – control samples after a shift in the parameters of the model. It is noted that, the

parameters in both stages are shifted equally and simultaneously. A brief description for calculating the probability of signal in Phase II is as follows:

Step 1. Suppose that the initial probability of signal of the T^2 control chart for both the first and second stages it is equal to zero, that is, $s_1 = s_2 = 0$.

Step 2. Generate m samples and estimate the initial parameters for each method separately (least square, Huber, bi – square method, respectively).

Step 3. Generate one sample without contamination, i.e., p = 0, but with a shift. Then, calculate the parameters of this sample using the least square method, i.e., $\hat{A}_S$, s = 1, 2 (two – stages process).

Step 4. Calculate the $\widehat{U}_1$ and $\widehat{U}_2$ using the U statistic, with the value of $\widehat{U}_1$ be the same for all the three methods. Thus, for the j^{th} profile in the first and second stages are as follow:

$U_{j,1} = \hat{A}_{j,1}$ (1^{st} stage), (3.15)

$U_{j,2} = \hat{A}_{j,2} - \sum_{2,1} \sum_{1,1}^{-1} \hat{A}_{j,1}$ (2^{nd} stage), (3.16)

where $\sum_{2,1}$ represents the matrix of covariance between $\hat{A}_{j,2}$ and $\hat{A}_{j,1}$, while $\sum_{1,1}^{-1}$ is the covariance matrix of $\hat{A}_{j,1}$.

Step 5. Calculate the T^2 statistic for each stage.

Step 6. For stage 1, if $T_{1new}^2 > UCL_1$ then $s_1 = s_1 + 1$, else $s_1 = s_1$.

For stage 2, $T_{2new}^2 > UCL_2$ then $s_2 = s_2 + 1$, else $s_2 = s_2$.

In each case, he repeated this process 10,000 times, which is the number of simulation runs.

Step 7. We have, $S_1 = s_1 / 10.000$ and $S_2 = s_2 / 10.000$,

where S_1 is the probability of signal of the T^2 control chart for the stage 1 and S_2 is the probability of signal of the T^2 control chart for the stage 2.

The conclusions drawn are as follows:

- In general, when there is no contamination, i.e., p = 0, then all three methods perform similarly in detecting shift in the parameters in each

stage. In fact, the performance of the least squares method is a bit better than the robust methods.

- When contamination is present, robust methods appear to perform better at detecting different types of shifts in the first stage of the process, as p, intercept, slope and standard deviation error values of the contamination data in Phase I increase. In fact, the bi-square method is a bit better than the Huber´s method.
- When there is contamination in the profile intercepts in both stages and shifts in the profile intercepts in both stages, for small values of φ, i.e., when weak autocorrelation occurs, robust methods perform better at detecting shifts in the second stage of the process, as the probability of contamination gets higher values and the value of the intercept increases, with the bi-square method performing slightly better than that of Huber's.
- When there is contamination in the profile slopes in both stages and shifts in the profile slopes in both stages, whether for weak or strong autocorrelation, robust methods perform better at detecting a shift in slopes in the second stage of the process, as p gets higher values and the value of the slope increases, with the bi-square method performing a little better than that of Huber's.
- When there is contamination in the profile standard deviation errors in both stages and shifts in the profile standard deviation errors in both stages, whether for weak or strong autocorrelation, robust methods perform best in detecting a shift in model parameters in the second stage of the process. In fact, both the bi-square and the Huber method perform similarly.
- In the combined case, where there is contamination in slopes in the second stage and shifts in intercepts in both stages, robust methods perform better than the least square method, either for weak or for strong autocorrelation. In fact, bi-square method performs a little better than Huber's.

3.2.2 A robust economic – statistical design

In this subsection the monitoring of simple linear profiles with the simultaneous help of EWMA and R control charts under an economic-statistical design approach will be discussed. This approach is looking for a scheme that can minimize the expected total cost under uncertain conditions. The expected total cost is defined as the ratio of the expected cycle cost, due to sampling costs, false alarms, the detection of an assignable cause, the correction of the process and its integration from the out – of – control state to the in – control state, divided to the sum of in – control and out – of – control states considering that the process at the initial stage was in – control and after some steps a shift was created. In order to address the above uncertainties of the parameters mentioned through the definition of the expected total cost, a robust economic – statistical design (RESD) was presented. For the development of the RESD, the residual approach was used in which the EWMA and R charts are used for monitoring the residuals of the simple linear model of Eq. (3.1). Therefore, based on the simple linear model, the statistic for the EWMA chart for the j^{th} profile is defined as:

$$Z_j = \lambda\, \overline{e_j} + (1 + \lambda)\, \overline{e_{j-1}}, \tag{3.17}$$

where λ ($0 \leq \lambda \leq 1$) is the weighted constant parameter, the initial value of this statistic is equal to zero, i.e., $Z_0 = 0$ and $\overline{e_j} = \sum_{i=1}^{n}(y_{ij} - \hat{y})/n$ with $\hat{y}$ be the predicted value of the model in Eq. (3.1).

The upper and lower control limits of the above statistic are respectively:

$$l\sigma \pm \sqrt{\lambda/(2-\lambda)n}\,, \tag{3.18}$$

where l is the control limit coefficient, σ and n να είναι the standard deviation of error term and number of observations in each profile based on the simple linear model in Eq. (3.1), respectively.

The statistic for the R chart for the j^{th} profile is defined as:

$$R_j = max_i(e_{ij}) - min_i(e_{ij}),\ i = 1, 2, \ldots, n, \tag{3.19}$$

The upper and lower control limits of the above statistic are respectively:

$\sigma d_2 \pm \sigma l d_3$, (3.20)

where d2 and d3 are constants that depend on n.

Therefore, based on simple linear model, the RESD model defined as:

$min_{x\epsilon X}\, max_{s\epsilon S}\, E(C^S)$, (3.21)

with $ARL_0 \geq ARL_L$, $ARL_1 \leq ARL_U$ for every s ϵ S, where $E(C^S)$ is the expected total cost for scenarios s per each solution x, ARL_L and ARL_U are the lower and upper bounds for ARL_0 and ARL_1, receptively.

In the above model, as mentioned in the definition of expected total cost, the parameters of expected time to sample the profile, fix cost of each false alarm, cost of repairing an assignable cause, quality loss cost in per time unit while the process is in – control state and out – of – control, respectively, fix cost of sampling and variable cost of sampling, are considered as uncertain. In fact, these parameters are not exactly estimated and as a result they deviate from their estimated values. Finally, to draw conclusions two scenarios are investigated: a) the above uncertain parameters take 10% deviation from their corresponding nominal values, and b) the above uncertain parameters take 20% deviation from their corresponding nominal values.

The results of the survey are as follows:

- Under 10% shift scenario in Phase II where there is a shift of size 0.5 in the mean residual, for a small increase in uncertainty in the set of parameters it was observed that the expected total cost increases significantly. On the other hand, for a greater increase in the uncertain condition, the $E(C^S)$ does not increase greatly and, so, there is no significant effect on it.
- Under 20% shift scenario, the results obtained on the effect of uncertainty on the expected total cost are equivalent to the 10% shift scenario.
- Comparing the above two scenarios shows that the expected total cost gets higher values at 20% than in the 10% shift scenario.

- In the 10% shift scenario, as the size of the shift in the mean residual increases from 0.5 to 0.75 and 1, respectively, the expected total cost gets smaller values. A similar relationship arises with the other scenario.

3.2.3 Simple linear profiles in the presence of outliers

Because of the outliers, the study of Moheghi et al. (2020) deals with robust parameter estimation and a comparison are made between robust and least squares estimators. In addition, the control charts used to monitor the simple linear profile and compare the robust method with the least square estimation method were:

- Stover and Brill's T^2 chart, introduced by Stover and Brill (1998), is based on the simple linear model of Eq. (3.1), referred to as SB method and the T^2 statistic follows the Beta distribution with upper control limit as follows:

  $$UCL_{SB} = (m-1)^2 B_{1,\,(m-3)/2,\,(1-\alpha)/m}, \quad (3.22)$$

  where m represents the number of profiles and $B_{\alpha,b,1-\alpha}$ is the 100(1 – a) percentile of Beta distribution with parameters α and b.

- Kang and Albin's control chart, introduced by Kang and Albin (2000), is based on the simple linear model of Eq. (3.1), referred to as KA method and the T^2 statistic follows the F distribution with upper control limit as follows:

  $$UCL_{KA} = 2\,F_{2,\,m(n-2),\,1-\alpha}, \quad (3.23)$$

  where $F_{2,m(n-2),1-\alpha}$ represents the 100(1 – α) percentile for the F distribution with 2 degrees of freedom in nominator and m(n – 2) degrees of freedom in denominator.

- Kim, Mahmoud and Woodall's control chart, introduced by Kim, Mahmoud and Woodall (2003), is based on the alternative simple linear model of Eq. (3.2), referred to as KMW method and the t statistics which follow the t – distribution with m (n – 2) degrees of freedom, defined as:

t_{oj} = $(\widehat{B_{0J}}$ - $\overline{\widehat{B}_0})$ / $\sqrt{(m-1)MSE/mn}$, (3.24)

t_{1j} = $(\widehat{B_{1J}}$ - $\overline{\widehat{B}_1})$ / $\sqrt{(m-1)MSE/mS_{xx}}$, (3.25)

where $\widehat{B_{0J}}$ is the estimated parameter of B_0, $\widehat{B_{1J}}$ is the estimated parameter of B_1, $\overline{\widehat{B}_0} = \sum_{j=1}^{m}\widehat{B_{0J}}/m$, $\overline{\widehat{B}_1} = \sum_{j=1}^{m}\widehat{B_{1J}}/m$, $S_{xx} = \sum_{i=1}^{n}(xi - \bar{x})^2$ and MSE represents the mean square error.

The interested readers are referred to the comprehensive articles for the detailed calculation of statistics with the above methods for profile monitoring by Stover and Brill (1998), Kang and Albin (2000), and Kim, Mahmoud and Woodall (2003), respectively.

Furthermore, the performance of robust and least square estimators is compared with the following performance measures: a) probability of signal (POS), b) fraction correctly classified (FCC), c) specificity, d) sensitivity, e) false positive rate (FPR), f) false negative rate (FNR) and g) index SOC which is used to measure the amount of sensitivity for the profile which should be explored as an out – of – control profile. Please note that, the ideally best performance occurs when FCC, specificity and sensitivity values increase and at the same time FNR and FPR values decrease. Finally, it is worth noting that the parameters of the simple linear model during the robust estimation method were estimated using the Huber function and the steps of this estimation are described in subsection 3.2.1.

The conclusions that emerged through a Monte Carlo simulation study are the following:

- In the SB method, the distribution of the T^2 statistic is not greatly affected when robust estimators are used instead of least square estimators. Therefore, in this method the effect of the choice of estimation method on the distribution of the statistic is negligible.
- When presented shift in profile intercept and if 10% of observations are contaminated (i.e., outliers) then the robust estimators give better estimates in Phase I for profile intercept and error variance.
- When a shift in profile intercept is presented and under the assumption that 10% of observations are contaminated (i.e., outliers) then the

estimated Phase I performance measurements are not significantly affected by the choice of estimation method, i.e., robust or least square estimation methods, except for the POS performance measure.

- When a shift in profile slope is presented and under the assumption that 10% of observations are contaminated (i.e., outliers) then the robust estimators outperform the estimates from least square method.
- When a shift in profile slope is presented and under the assumption that 10% of observations are contaminated (i.e., outliers) then the POS and SOC performance measures show better (larger) values for the robust method.
- When presented shift in profile error variance and if 10% of observations are contaminated (i.e., outliers) then robust estimators yield better estimates in Phase I for profile error variance than least square estimators. However, there is no significant difference between the two estimation methods for the rest of the model parameters.
- When a shift in profile error variance is presented and under the assumption that 10% of observations are contaminated (i.e., outliers) then it was observed that for POS and FPR performance measures the model parameter estimates during Phase I with the least square method show better performance.
- In general, it was observed that when parameters have been evaluated in Phase I with robust estimation methods, then ARL values in Phase II are smaller and therefore can detect shifts in model parameters faster than least square estimators.
- ARL values were lower in both robust SB and robust KA methods when a shift in profile intercept is created in Phase II compared to ARL values for least square SB and KA methods, respectively.
- When the slope shifts in Phase II, then for a large shift the ARL values of least square methods perform a little better than robust methods.

- In general, the combination of robust estimators with the KA method is preferable to the SB approach.
- For a small number of out – of – control profiles, least square estimators perform better than the KA method.

3.3 Other techniques for monitoring simple linear profiles

In this section we will talk about three different approaches, where the monitoring of simple linear models occurs under a specific framework. In more detail, initially, the study developed by Aytaçoğlu, B., and Bayrak, Ö. T. (2019), who monitor simple linear profiles in the case where the error term of the simple linear model does not follow the normal distribution, will be discussed. Then a method for monitoring linear profiles under Bayesian framework, which was examined by Abbas et al. (2019), will be reported and, finally, a very recent study will be given by Yeganeh et al. (2023), who implemented a groundbreaking approach to financial market surveillance with a perspective on statistical process control charts.

3.3.1 Influence of estimation on simple linear profile monitoring in non – normal conditions

In this subsection will discuss the study developed by Aytaçoğlu, B., and Bayrak, Ö. T. (2019), who assumed that the error terms of Eq. (3.1) follow Student's t-distribution and investigated the estimation of unknown model parameters when in Phase I there are m profiles with the same constant of observations in each of them. Furthermore, their study investigates the effect of both estimation and violation of normality assumption in Hotelling T^2, EWMA/R and EWMA_3 control charts. Average run length (ARL) and standard deviation of run length (SDRL) are used as performance measures to compare the above control charts. Finally, it is noted that, when the number of profiles used in the study to estimate the parameters tends to infinity, i.e., $m = \infty$, then

the parameter values of the simple linear model are simulated using true parameter values rather than their estimates.

The results obtained from the study were the following:

- For Phase I, when m = ∞ then, as the distribution deviates from the normality, the values of in – control ARL decrease for all the charts considered, i.e., Hotelling T^2, EWMA/R and EWMA_3 control charts.
- Under the assumption of normality for estimating model parameters in Phase I, when the number of profiles is bigger than ten, i.e., m > 10, then the Hotelling T^2 and EWMA/R charts show larger in – control ARL values than the EWMA_3 control chart. This shows that the first two charts have fewer false alarm rates.
- Assuming normality for estimating model parameters in Phase I, when the number of profiles is ten, i.e., m = 10, then the EWMA_3 control chart shows ARL values closer to the theoretical value than the other two charts, which indicates that it performs better.
- In general, under normal conditions, the EWMA has lower ARL values with known parameters than when m > 10 and its SDRL is much less than the other charts. Therefore, EWMA method performs better than the others.
- Under the assumption of nonnormality for estimating model parameters in Phase I, it was observed that as the number of Phase I profiles used in estimation is small then the values of the ARL performance measure for all control charts examined increase. Conversely, when the number of Phase I profiles used in estimation increases, the ARL values decrease.
- Under the assumption of nonnormality for estimating model parameters in Phase I, something similar happens with SDRL values, i.e., as m increases, SDRL values decrease. Therefore, for a larger number of profiles, the control charts perform better.

- Under normal distribution, for large shifts in the profile intercept during Phase II all charts have similar ARL values for the known parameter case, regardless of the number of profiles used in Phase I. Therefore, for large shifts in the intercept the effect of estimation is negligible and, so, any number of profiles can be used, even small number.
- Under normal distribution, for small shifts in the intercept it was observed that ARL values increase requiring a larger number of Phase I profiles used in estimation to eliminate the estimation effect.
- For any shift in the profile parameters and under t-distribution, the ARL values are heavily influenced by estimation, resulting in control chart performance being downgraded. It is worth noting that, when the degrees of freedom of t-distribution increase, this effect is less.
- Under normality, when there is a large shift in the intercept then the Hotelling T^2 chart has large SDRL values, while the SDRL values are similar and smaller in the EWMA/R and EWMA_3 control charts.
- Under normality, when there is a small shift in the intercept then the SDRL values of the charts are equivalent to those of the ARL, i.e., the values increase so that a larger number of Phase I profiles used in estimation to eliminate the estimation effect are needed.
- In general, under normality, EWMA_3 is less affected by estimation and performs better than EWMA/R, which in turn performs better than Hotelling T^2 chart, which needs more profiles to detect a large shift in intercept.
- Under normality, when there is a shift in profile slope then EWMA_3 is less affected by estimation and performs better than the rest of the charts.
- Under Student's t – distribution, when a slope profile shift occurs then the estimate affects both ARL and SDRL values as the distribution deviates from normality. Therefore, since the effect of the estimate is not negligible, the performance of the control charts is downgraded.

- Generally, when there is a shift in profile error variance, then as the distribution deviates from normality there is an increasing estimation effect. However, it was observed that the examined control charts are less sensitive to estimation compared to cases where there is a shift in intercept or slope.

3.3.2 A Bayesian approach with random variables

In a profiling process, parametric uncertainty, which occurs when changes occur on a frequent basis aiming at the efficiency of the process, can be incorporated in the form of probability. In the view of Bayesian approach, this parametric uncertainty is called prior distribution and was used in the study by Abbas et al. (2019), where they investigated profiling by considering both process parameters and the explanatory variable as random (rather than fixed).

In Phase I of statistical process control, the task is to evaluate the parameters of the model. Abbas et al. (2019), tested the parameter estimation based on the Bayesian framework. For this reason, the first step is the choice of prior distribution. It is known that, for the selection of the prior in Bayesian set there are the following approaches: a) subjective approach, b) pragmatic approach (conjugate prior), and c) objective approach. In this study, both the subjective and pragmatic approaches were used, while assumed non-conjugate and conjugate priors for the integration of parametric uncertainty.

For Bayesian estimation using non-conjugate priors, the non-conjugate priors of Bramwell, Holdsworth, Pinton (BHP) distribution, introduced by Bramwell, Holdsworth and Pinton (1998) and used for the intercept and slope of the model, were examined, while for the variance errors the non-conjugate Levy prior distribution was used. Therefore, let it be $B_0 f\tilde{}(\nu_0,\xi_0)$, $B_1 f\tilde{}(\nu_1,\xi_1)$, $\sigma^2 f\tilde{}(\zeta_0)$ the priors for intercept, slope, errors variance, respectively, where $(\nu_0,\nu_1,\xi_0,\xi_1,\zeta_0)$ are the hypers parameters. The following estimates then arise for intercepts and slopes of posterior distributions for the j^{th} profile:

$b_{0nj} = [(n_j\bar{y}_j\xi_0 + \frac{\pi}{2}\sigma_j^2)\xi_0^3 exp(\frac{\nu 0}{\xi 0}) + (\nu_0 - \xi_0^2)\sigma_j^2] / [n_j\xi_0^4 exp(\frac{\nu 0}{\xi 0}) + \sigma_j^2]$, with variance $\sigma_{0nj}^2 = [\sigma_j^2\xi_0^4 exp(\frac{\nu 0}{\xi 0})] / [n_j\xi_0^4 exp(\frac{\nu 0}{\xi 0}) + \sigma_j^2]$, (3.26)

$b_{1nj} = [(\xi_1\sum_{i=1}^{n}(x_{ij} - \bar{x}_j)y_{ij} + \frac{\pi}{2}\sigma_j^2)\ \xi_1^3 exp(\frac{\nu 1}{\xi 1}) + (\nu_1 - \xi_1^2)\sigma_j^2] / [\sum_{i=1}^{n}(x_{ij} - \bar{x}_j)^2\ \xi_1^4 exp(\frac{\nu 1}{\xi 1}) + \sigma_j^2]$, with variance $\sigma_{1nj}^2 = [\sigma_j^2\xi_1^4 exp(\frac{\nu 1}{\xi 1})] / [\sum_{i=1}^{n}(x_{ij} - \bar{x}_j)^2\xi_1^4 exp(\frac{\nu 1}{\xi 1}) + \sigma_j^2]$, (3.27)

where σ_j^2 is the variance of the error terms ε_{ij} for the j^{th} profile.

However, this research studies a model in which the explanatory variable is random. Therefore, due to this randomness, Eqs. (3.26) and (3.27) are transformed as follows:

$b_{0nj}^* = b_{0nj} + b_{1nj}\,\mu_{xj}$, with variance $\sigma_{0nj}^{2*} = \sigma_{0nj}^2 + b_{1nj}^2\,\sigma_{xj}^2$, (3.28)

$b_{1nj}^* = (b_{1nj} - B_{1j}) / \sqrt{\sigma_{1nj}^2}$, with the same variance σ_{1nj}^2 as above, (3.29)

where μ_{xj} and σ_{xj}^2 is the mean and variance of the explanatory variable, respectively.

Finally, the estimates of the posterior distribution for errors variances are as:

$\alpha_{nj} = (n_j + 1) / 2$, and $\beta_{nj} = \{(\zeta_0 / 2) + [(n - 2)\sigma_j^2] / 2\}$, (3.30)

where $\sigma_j^2 = \sum_{i=1}^{n}(y_{ij} - B_{0j} - B_{1j}x_{ij}^*)^2 / (n_j - 2)$.

For Bayesian estimation using conjugate priors, the conjugate prior distributions of normal for the intercept and slope coefficients was used, while for error variance the conjugate prior of inverse gamma was used. Therefore, let it be $B_0N(b_0,\lambda_0^2)$, $B_1N(b_1,\lambda_1^2)$, $\sigma^2IG(\varphi_0,\varphi_1)$ the priors for intercept, slope, errors variance, respectively, where $(b_0,\lambda_0^2,\ b_1,\lambda_1^2,\varphi_0,\varphi_1)$ are the hypers parameters. The following estimates are then obtained for intercepts and slopes of posterior distributions for the j^{th} profile:

$b_{0nj}' = (n_j\bar{y}_j\lambda_0^2 + b_0\,\sigma_j^2) / (n_j\lambda_0^2 + \sigma_j^2)$, with $\sigma_{0nj}'^2 = \lambda_0^2\sigma_j^2 / (n_j\lambda_0^2 + \sigma_j^2)$, (3.31)

$b_{1nj}' = [\sum_{i=1}^{n}(x_{ij} - \bar{x}_j)y_{ij}\ \lambda_1^2 + b_1\,\sigma_j^2] / [\sum_{i=1}^{n}(x_{ij} - \bar{x}_j)^2\ \lambda_1^2 + \sigma_j^2]$, with variance $\sigma_{1nj}'^2 = \lambda_1^2\,\sigma_j^2 / [\sum_{i=1}^{n}(x_{ij} - \bar{x}_j)^2\ \lambda_1^2 + \sigma_j^2]$. (3.32)

However, this research studies a model in which the explanatory variable is random. Therefore, due to this randomness, Eqs. (3.31) and (3.32) are transformed as follows:

$b_{0nj}^{\sim} = b_{0nj}^{'} + b_{1nj}^{'} \mu_{xj}$, with variance $\sigma_{0nj}^{\sim 2} = \sigma_{0nj}^{'2} + b_{1nj}^{'2} \sigma_{xj}^{2}$, (3.33)

$b_{1nj}^{\sim} = (b_{1nj}^{'} - B_{1j}) / \sqrt{\sigma_{1nj}^{'2}}$, with the same variance $\sigma_{1nj}^{'2}$ as above. (3.34)

Finally, the estimates of the posterior distribution for errors variances are as:

$\alpha_{nj}^{'} = \varphi_0 + \frac{n}{2}$, and $\beta_{nj}^{'} = \varphi_1 + [(n - 2)\, \sigma_0^2] / 2$. (3.35)

As the model parameters have been evaluated in Phase I, the Bayesian exponentially weighted moving average (EWMA) control chart is used to monitor the simple linear profiles, when the independent variable is random. To structure this control chart, Abbas et al. (2019) used posterior estimates under conjugate priors of the profile intercepts, slopes and errors variance, respectively, which have been estimated in Phase I of the process. Below is defined the EWMA statistic along with the control limits for each parameter of the model under Bayesian framework. Therefore, for the j^{th} profile intercepts EWMA statistic is defined as:

$EWMA_I(j) = \theta b_{0nj}^{\sim} + (1 - \theta) EWMA_I(j - 1)$, (3.36)

where θ is the smoothing constant ($0 < \theta \leq 1$) and $EWMA_I(0) = \beta_0 + \beta_1 \mu_x$. Moreover, the lower control limit (LCL_I) and the upper control limit (UCL_I) for the j^{th} profile intercepts are defined as:

$LCL_I = \beta_0 + \beta_1 \mu_x - L_I\, \sigma_{0nj}^{\sim} \sqrt{\frac{\theta}{(2 - \theta)}}$, $UCL_I = \beta_0 + \beta_1 \mu_x + L_I\, \sigma_{0nj}^{\sim} \sqrt{\frac{\theta}{(2 - \theta)}}$, (3.37)

where L_I is the initial value of control limits intercept coefficient (fixed).

For the j^{th} profile slopes EWMA statistic is defined as:

$EWMA_S(j) = \theta b_{1nj}^{\sim} + (1 - \theta) EWMA_S(j - 1)$, (3.38)

where $EWMA_S(0) = 0$.

Moreover, the lower control limit (LCL_S) and the upper control limit (UCL_S) for the profile slopes are defined as:

$$LCL_S = -L_S\sqrt{\frac{\theta}{(2-\theta)}},\ UCL_S = +L_S\sqrt{\frac{\theta}{(2-\theta)}}, \quad (3.39)$$

where L_S is the initial value of control limits slope coefficient (fixed).

For the j^{th} profile errors variance EWMA statistic is defined as:

$$EWMA_E(j) = max\{\theta\ ln(MSE_j) + (1-\theta)EWMA_E(j-1),\ ln(\sigma_j^2)\}, \quad \text{(statistic using log scale)}, \quad (3.40)$$

where MSE_j is the mean square error for the j^{th} profile and $EWMA_E(0) = \ln(\sigma_0^2)$.

Moreover, the upper control limit (UCL_E) using the log scale for the profile errors variance is defined as:

$$UCL_E = L_E\sqrt{[\theta/(2-\theta)]\,Var\{ln(MSEj)\}}, \quad (3.41)$$

where L_E is the initial value of control limits slope coefficient (fixed).

Finally, for the profile errors variance, again, the EWMA statistic defined as:

$$EWMA_{E^*}(j) = max\{\theta(MSE_j - 1) + (1-\theta)EWMA_{E^*}(j-1),\ 0\}, \quad \text{(statistic using nature scale)}, \quad (3.42)$$

where $EWMA_{E^*}(0) = 0$.

The upper control limit (UCL_{E^*}) using the nature scale for the profile errors variance is defined as:

$$UCL_E = L_{E^*}\sqrt{[\theta/(2-\theta)]\,Var\{ln(MSEj)\}}, \quad (3.43)$$

where L_{E^*} is the initial value of control limits slope coefficient (fixed).

Notably, the Bayesian EWMA control chart will indicate an out – of – control signal either when the EWMA statistic is greater than the UCL or when it is smaller than the LCL. As we saw in the introduction to this chapter, the performance of control chart methods for Phase II is usually measured based on a statistic, which is adapted from the run – length characteristics of the control chart and is suitable for evaluating split shifts. However, Abbas et al. (2019) studied the case of monitoring linear profiles with a random explanatory variable, where a sequence of shifts occurs under the Bayesian framework. For this reason, their research was based on the Monte Carlo simulation method, the steps of which are summarized below. Therefore, the procedure for implementing the method is as follows:

Step 1. Designed the Bayesian EWMA statistics along with the corresponding control limits for each model parameter (intercept, slope, variance errors), as defined in Eq. (3.36) – (3.43).

Step 2. Decide about the value of constant θ and the size of each profile (n).

Step 3. Generate error terms from the normal distribution with mean equal to zero and standard deviation equal to one, i.e., $\varepsilon_{ij} \sim N(0,1)$, where i = 1, …, n (n is fixed from the previous step) and j = 1, 2, …

Step 4. Generate values for explanatory variable, which assumed to follow normal distribution with mean μ_x and standard deviation σ_x.

Step 5. Decide about the values of the parameters B_0 and B_1 under in – control situation.

Step 6. Calculate the response variable y using both the Eq. (3.2) and the values of parameters from the previous steps.

Step 7. Decide about the values of hyper parameters.

To select the most appropriate values for hyper parameters b_0, λ_0^2, b_1, λ_1^2 a method was applied, introduced by Garthwaitea et al. (2013) and concerned variables that follow normal distributions, while for hyper parameters φ_0, φ_1 a method was applied, introduced by Elfadalya and Garthwaitea (2014) and concerned variables that follow the inverse gamma prior distribution. Therefore, $B_0 \sim N(20, 35)$, $B_1 \sim N(2.5, 12)$ and $\sigma^2 \sim IG(0.68, 0.3)$.

Step 8. Select the initial values of L_I, L_S, and L_E.

Step 9. Calculate the $b_{0nj}^{\sim}$ and $b_{0nj}^{\sim}$ as defined in Eq. (3.33) – (3.34).

Step 10. Compute the Bayesian EWMA statistics together with the corresponding control limits for each profile as defined in Eq. (3.36) – (3.43) using the values obtained from the previous steps of the procedure.

Step 11. If the statistics of Step 10 are greater than either the corresponding UCL or smaller than the LCL, then there is an out-of-control signal, and the value of the ARL is recorded.

Step 12. Repeat the process a large number of times and find the value of in – control ARL (ARL_0). In each iteration if the value of new in – control ARL is the same as the specified ARL_0 value, then continue to the next step. Otherwise, go back to Step 8, redefine the values of L_I, L_S, and L_E, and then continue the process again.

Step 13. After calculating the value of ARL_0, it incorporated into the process a sequence of shifts in its parameters.

Step 14. Evaluate the out – of – control ARL value (ARL_1).

Step 15. Recalculate the EWMA statistics for the profile intercepts, slopes and errors variance, respectively, under out – of – control situation.

Step 16. Repeat the Step 15 to a point which is out – of – control.

Step 17. Count the values that fall outside the control limits for intercepts, slopes and errors variance.

Step 18. Repeat the above process a large number of times to get the ARL value, which is under out – of – control state.

The conclusions drawn are as follows:

- As we know, the values of smoothing constant θ fluctuate in the interval (0, 1]. Following the study conducted by Abbas et al. (2019) through a simulation, it was observed that for smaller values of θ the performance of Bayesian EWMA control charts improves.
- Bayesian EWMA control charts, which were used to monitor linear profiles with a random explanatory variable, are better suited to detect small shifts in process parameters than large shifts. It is worth noting that, quickly detection of small shifts in the parameters of a process is extremely useful in the field of production, as profiling professionals can obtain a timely out – of – control signal and examine the causes and whether they need to fix anything for the smooth continuation of the process.

- Whether log scale or natural scale is used to design Bayesian EWMA control charts, this does not affect chart performance for intercept and slope, and it does affect performance for errors variance.

3.3.3 A novel approach to financial market monitoring

This subsection will discuss the study by Yeganeh et al. (2023), who proposed a new control chart to monitor the price variability of a cryptocurrency pair, consisting of Bitcoin (BTC) and Ethereum (ETH). Due to the existence of autocorrelation in financial markets, the new approach proposed in this study to monitor the economic and financial market (financial surveillance) is referred to as control chart based on profile monitoring (CCPM). More specifically, the aim of this new method is to examine the profiles of two coins, i.e., Bitcoin and Ethereum, predict how the relationship of this currency pair changes over time, and generate buy and sell signals. Notably, these signals are equivalent to changing the assets from Bitcoin to Ethereum (for buy) and Ethereum to Bitcoin (for sell). Therefore, the daily relationship between the considered assets is referred to as a profile and can be written in the form of a simple linear model as follows:

$$ETH_{ij} = A_0 + A_1 BTC_{ij} + \varepsilon_{ij},\ i = 1, 2, \ldots, 24 \quad j = 1, 2, \ldots \tag{3.44}$$

where ETH_{ij} represents a variable of the hourly price of ETH at the i^{th} hour of the j^{th} day, BTC_{ij} is a variable of the hourly price of BTC at the i^{th} hour of the j^{th} day, A_0, A_1 and ε_{ij} are the intercept, slope and error variance of the linear model, respectively.

To account for both between and within autocorrelation effects, the model in Eq. (3.44) is converted to an Autoregressive time series of order one model, i.e., AR(1) model, as follows:

$$ETH_{ij} = A_0 + A_1 BTC_{ij} + \varepsilon_{ij},\ i = 1, 2, \ldots, 24 \quad j = 1, 2, \ldots \tag{3.45}$$

with $\varepsilon_{ij} = p\varepsilon_{(i-1)j} + a_{ij}$, $a_{ij} = \varphi\varepsilon_{i(j-1)} + u_{ij}$, $i = 1, 2, \ldots, 24$ and $j = 1, 2, \ldots$, where ε_{ij} and a_{ij} are the correlated error terms, u_{ij} are the independently and identically normally distributed errors, $|\rho| < 1$ and $|\varphi| < 1$ are the coefficients of AR(1)

model in a way that ρ is used within-profile autocorrelation, while φ accounts for between-profile autocorrelation.

The Hotelling T^2 control chart was used to monitor the model in Eq. (3.45). Briefly the steps for the CCPM method are as follows:

- Estimation step. In this step we classify the profile parameters into a dataset where the rows represent the days and the twenty-four columns the hourly values of BTC and ETH assets. If the process is in – control condition, the parameters are estimated and the limits of the T^2 control chart are calculated. It is noted that the chart statistics for each model profile are not independent of each other due to the between profile autocorrelation and, thus, do not follow geometric distribution. The interested readers are referred to the comprehensive article for choosing an appropriate distribution for the above statistics by Knoth et al. (2021).

- Monitoring step. In this step, the process profile is monitored, and the process is terminated when a warning signal is reached, i.e., when the T^2 statistic has gone outside the control limits. It is recommended to detect at least (NOC + 1) statistically out of control, where NOC represents the number of consecutive out – of – control profiles, to terminate the process.

- Decision step. In this step we calculate both the average of ETH/BTC prices (CP) based on the number of profiles we have just before the process is terminated and the reference price (RP) which is based on the number of profiles of the estimation step. Therefore, the following decisions are made:

  If CP > RP then sell and if CP < RP then buy, (3.46).

The measure of performance used for the CCPM method was the target ratio (TR), defined as the relative decrease (increase) in ETH/BTC price based on the sell (buy) signal. Based on this measure, the following criteria were defined: a) ratio of uncompleted signals (RUS), b) average of days to desired price (ADDP), c) standard deviation of days to desired price (SDDP), and d) median of days to desired price (MDDP).

The results obtained through a simulation study with 1,000 iterations were the following:

- In most cases, as TR values grew, the values of the four criteria mentioned above were getting larger values, too.
- When we want to achieve more benefit/profit, i.e., TR price to increase, then we need more time, i.e., the prices of ADDP, SDDP and MDDP increase, and therefore the risk increases, i.e., the price of RUS increases.
- The relationship between the ADDP, SDDP and MDDP criteria and the NOC is negligible. Therefore, the days it takes to reach the target value do not depend significantly on the waiting time to reach the necessary number of signals.
- Out – of – control profiles with larger NOC values imply an increase in instability in the process and the expectation of it to return to the original in – control situation.
- Large NOC values signal smaller ADDP, SDDP and MDDP values, compared to smaller NOC values.
- For larger model parameter shifts, i.e., intercept, slope and error variance, the average of run length (ARL), standard deviation of run length (SDRL) and median of run length (MRL) performance measures had better detection ability. In fact, the variance error was detected more quickly due to the smaller effect on autocorrelation compared to profile intercept and slope.

CHAPTER 4

Generalized linear and generalized linear mixed profiles

Introduction

Generalized linear profiles are an extension of the simple linear profiles we developed in the previous chapter and are used when the normality assumption of the response variable is violated, and the characteristics of the process can be represented as a discrete response data. For this reason, generalized linear models (GLM) were developed and used to express a profile in which the distribution of the response variable belongs to the family of exponential distributions. Therefore, to describe and monitor a generalized linear profile, a generalized linear model should be used, the form of which is described below.

Suppose y_i, i = 1, 2, …, n, denotes the response values, then the form of GLM is as follows:

$$g[E(y_i)] = g(\mu_i) = \eta_i = \boldsymbol{x}_{i'}\boldsymbol{\beta} = \beta_1 x_{i1} + \beta_2 x_{i2} + \ldots + \beta_p x_{ip}, \quad (4.1)$$

where $\mathbf{x}_i = (x_{i1}, x_{i2}, \ldots, x_{ip})'$ is a vector of independent variables for the i^{th} observation, $\boldsymbol{\beta} = (\beta_1, \beta_2, \ldots, \beta_p)'$ is the vector of regression coefficients, i.e., profile parameters, and $g(\cdot)$ represents a link function, which relates the linear predictor $\mathbf{x}_{i'}\boldsymbol{\beta}$ to the mean of response variable (μ_i).

Note that the expected value of response variable is in the form of:

$$\mu_i = E(y_i) = g^{-1}(\eta_i) = g^{-1}(\boldsymbol{x}_{i'}\boldsymbol{\beta}), \quad (4.2).$$

Furthermore, one of the most widespread types of GLM profiles, used in many applications of everyday life and has an excellent position in various fields, such as medicine and pharmacy, is the so-called logistic regression profile. According to the logistic regression model, the response variables are binomial variables, and the logistic regression model is in the form of:

$$ln[\pi_i / (1-\pi_i)] = g(\mu_i) = g(\pi_i) = \boldsymbol{x}_{i'}\boldsymbol{\beta}, \; i = 1, 2, \ldots, n \quad (4.3)$$

where $g(\cdot)$ is the logit link function and $\pi_i = Pr(y_i = 1)$ represents the probability of success for the i^{th} observation.

On the other hand, linear mixed profiles will be mentioned in this chapter, which are also an extension of simple linear profiles. More specifically, linear mixed models (LMM) are models that combine fixed and random effects, and their form is as follows:

$y_i = X_i\beta_i + Z_i b_i + \varepsilon_i$, i = 1, 2, …, n (4.4).

Equivalently, the above model can be given using a general form of LMM as follows:

$Y = X\beta + Zb + \varepsilon$, (4.5)

where Y is a vector of response variables for all the profiles, X is a matrix which contains all the X_i´s, β represents the fixed effects vector, Z is a diagonal matrix with Z = diag(Z_i), b is the random effects vector and ε is the vector of error terms.

Table 4_1 briefly mentions previous research conducted to monitor generalized linear profiles from 2008 to 2018. Thus, lists the researchers, whether the expert study concerned Phase I or Phase II of the profile, and the criterion for measuring the performance of the control charts used.

Research	Phase I	Phase II	Performance criterion
Yeh et al. (2009)	Yes	-	Signal probability
Shang et al. (2011)	-	Yes	ARL & SDRL
Paynabar et al. (2012)	Yes	-	Signal probability, $\bar{\hat{\tau}}$, SD($\hat{\tau}$)
Saghaei et al. (2012)	-	Yes	ARL
			(continued)

Sharafi et al. (2012)	-	Yes	$\bar{\hat{\tau}}$, SD($\hat{\tau}$) & precision
Koosha and Amiri (2013)	Yes	-	Signal probability
Sharafi et al. (2013b)	-	Yes	$\bar{\hat{\tau}}$, SD($\hat{\tau}$) & precision
Soleymanian et al. (2013)	-	Yes	ARL & SDRL
Zand et al. (2013)	Yes	-	$\bar{\hat{\tau}}$, SD($\hat{\tau}$) & precision
Sharafi et al. (2014)	-	Yes	$\bar{\hat{\tau}}$, SD($\hat{\tau}$) & precision
Sogandi and Amiri (2014a)	-	Yes	$\bar{\hat{\tau}}$, SD($\hat{\tau}$) & precision
Sogandi and Amiri (2014b)	-	Yes	$\bar{\hat{\tau}}$, SD($\hat{\tau}$) & precision
Shadman et al. (2015)	Yes	-	Signal probability, $\bar{\hat{\tau}}$, SD($\hat{\tau}$)
Abbasi Charkhi et al. (2016)	-	-	C_p
Shang et al. (2016)	Yes	-	Signal probability, bias of $\bar{\hat{\tau}}$, precision & accuracy of identifying shift directions
			(continued)

Amiri et al. (2017)	-	Yes	ARL
Hakimi et al. (2017)	Yes	Yes	Estimated regression parameters, ARL
Maleki et al. (2017a)	-	Yes	ARL
Maleki et al. (2017b)	-	Yes	$\bar{\hat{\tau}}$, SD($\hat{\tau}$) & precision
Shadman et al. (2017)	-	Yes	ARL, SDRL, $\bar{\hat{\tau}}$, SD($\hat{\tau}$) & diagnostic probability
Sogandi and Amiri (2017)	-	Yes	$\bar{\hat{\tau}}$, SD($\hat{\tau}$) & precision
Khosravi and Amiri (2018)	Yes	Yes	ARL

Table 4_1. A brief overview of methods developed to monitor generalized linear profiles from 2008 to 2018. (Adapted from Maleki, M. R., Amiri, A., & Castagliola, P. (2018)).

Finally, considering the gap that exists after the year 2018, after the review contributions by Woodall (2007) and Maleki et al. (2018), the continuation of this chapter aims to present some recent studies, research and developments for monitoring generalized linear and generalized linear mixed profiles, to provide an up-to-date exploration of the field's contemporary developments.

4.1 Robust estimation methods for generalized linear and generalized linear mixed profiles

In this section, three recent developments will be discussed, one of which concerns the monitoring of generalized linear model (GLM) profiles, while the last two approaches concern generalized linear mixed model (GLMM) profiles, using robust estimation methods. In the first place, the study of Moheghi et al. (2021), who monitored two types of GLM profiles under the influence of outliers, will be developed. Then, we will discuss the study by Nassar and Abdel-Salam (2022), who monitored linear mixed model (LMM) profiles using the model robust regression 2 (MRR2) method for Phase II analysis. This section will close with the research of Bandara et al. (2020) in which the assumption that, the response variable can be correctly modelled using generalized linear models, is unknown or uncertain.

4.1.1 Robust estimators for logistic and Poisson profiles

As mentioned in the introduction to this chapter, generalized linear models are used to describe and monitor models where the distributions of response variables belong to the family of exponential distributions, such as Bernoulli, Binomial, Poisson, Exponential and Gamma distributions. Thus, the study of Moheghi et al. (2021) investigates logistic/Binomial and Poisson profiles and, due to the presence of outliers in Phase I, uses the robust method to reduce the effect of outliers and to estimate the parameters of the above profiles. Finally, of particular interest is the comparison of the robust estimation method with the maximum likelihood estimation (MLE) method in terms of average run length (ARL) criterion.

Before giving a brief description of the robust and MLE methods, it is recalled that for the logistic profile the model will be used in Eq. (4.3), while the model for the Poisson profile is described below.

Suppose Y_i, i = 1, 2, …, n, are Poisson response variables with parameter λ_i. Then, the Poisson model, which uses the log link function, is of the form:

$g(\mu_i) = ln(\mu_i) = ln(\lambda_i) = x_i'\beta$, i = 1, 2, …,n (4.6)

with $\lambda_i = \exp(x_i'\beta)$.

Therefore, based on the general formula of the generalized linear model of Eq. (4.1), the maximum likelihood estimators (MLEs) are as follow:

$\hat{\beta}^* = (X'\widehat{W}\,X)^{-1}\,X'\widehat{W}q$, (4.7)

with $q = X\hat{\beta} + \widehat{W}^{-1}(y - \hat{\mu})$, where $\hat{\beta}$ represents a vector of the least square estimator of β, $\hat{\mu}$ is the vector of expected estimation value of response variables and $\widehat{W}$ represents a diagonal matrix that includes estimators for the $\sigma_i^2 = var(y_i)$.

The above formula of Eq. (4.7) can be used appropriately for any GLM profile. In the present study it was used through a Monte Carlo simulation study with the use of R software for the logistic and Poisson profiles.

On the other hand, the robust method developed in this study is inspired by Cantoni and Ronchetti (2001), who assessed the parameters of GLM using the quasi – probability approach. Thus, this method is known as the robust C – R estimation method and results from the following form:

$\sum_{i=1}^{n}[\psi(r_i)\omega(x_i)\,\frac{1}{\sigma_i}\frac{d\mu_i}{d\eta_i} - \Omega(\beta)] = 0$, (4.8)

with $\Omega(\beta) = (1/n)*\sum_{i=1}^{n} E[\psi(r_i)]\omega(x_i)\frac{1}{\sigma_i}\frac{d\mu_i}{d\eta_i}$, where ψ represents the Huber function which was defined in the Section 3.3, $r_i = (y_i - \mu_i) / \sigma_i$, $\sigma_i^2 = var(y_i)$ and $\omega(x_i)$ represents the weight of the i^{th} observation.

Note that the T^2 control chart is used to monitor GLM profiles. The conclusions that emerged through a simulation study were the following:

- For the estimation of the parameters of a Poisson profile in Phase I, it was observed that either in the case where outliers are generated by shifts in profile intercept or in the case where outliers are generated by shifts in slope, the robust C – R estimators are not sensitive to the presence of outliers, while MLEs are very sensitive to contamination (i.e., to outliers).
- For the ability to detect shifts in the parameters of the Poisson model in Phase II, it was observed that the T^2 control chart based on C – R

estimation method is more efficient and detects a shift faster than the T^2 control chart based on the MLE method.

- For the estimation of the parameters of a logistic profile in Phase I, where data have generated with 10% contamination, it was observed that C-R estimators are more accurate and effective than MLEs, which are very sensitive to the presence of outliers.
- For the ability to detect shifts in the parameters of the logistic model in Phase II, it was observed that the T^2 control chart based on C – R estimation method is more efficient and detects a shift faster than the T^2 control chart based on the MLE method.
- In general, it is concluded that the C – R estimation method is insensitive to the presence of outliers in Phase I data and has better performance for quickly detecting shifts in the profile parameters than the MLE method.

4.1.2 A semiparametric technique for Phase II analysis via residuals

In this subsection we will discuss the study by Nassar and Abdel-Salam (2022), who monitored linear mixed model (LMM) profiles using the model robust regression 2 (MRR2) method for Phase II analysis. More specifically, the MRR2 method is a semiparametric approach, which combines a parametric fit with a segment dedicated to nonparametric residuals fit. Furthermore, as the study focused on the Phase II analysis, the multivariate cumulative sum (MCUSUM) control charts were used to monitor the slope of linear mixed models, incorporating random – effects considerations. Of particular interest is the comparison made between the MCUSUM charts, which are used appropriately for parametric, nonparametric and semiparametric approaches, respectively, in terms of their effectiveness and ability to detect a shift quickly. Finally, the results are obtained with the help of average run length (ARL) and average time to signal (ATS) performance criteria.

Before proceeding to the conclusions that have emerged from the above study, we will briefly give the estimates of the parameters of LMM, using the

parametric, nonparametric and semiparametric methods, respectively. Therefore, the estimators of linear mixed models are given as follows:

- Based on LMM in Eq. (4.5), parameter estimates using the parametric approach have the following form:

  $\widehat{\beta_p} = (X'V^{-1}X)^{-1}\,(X'V^{-1}y)$ and $\widehat{b_{ip}} = DZ_i'V^{-1}\,(y_i - X_i\widehat{\beta_p})$, (4.9)

  with $V = ZBZ' + R$, be a positive definite matrix, where R represents a matrix of the variances of the error terms, B is a diagonal matrix with elements the variance terms of b, i.e., $B = diag(D)$, $\widehat{\beta_p}$ represents the vector of the fixed – effects β and $\widehat{b_{ip}}$ represents the vector of the random – effects b.
- Using the nonparametric residuals estimation method, according to which the response variable y fits with the residuals r parametrically, i.e., $y = f(r) + \xi_i(r) + \varepsilon$, $i = 1, 2, \ldots, n$, random – effects estimators for the i^{th} profile have the following form:

  $\widehat{\gamma_i} = [\widehat{b_i}, \widehat{t_i}]'$ (4.10)

  where $\widehat{b_i}$ represents the estimated random – effects for the spline component vector y and $\widehat{t_i}$ represents the estimated knots.
- Using the semiparametric estimation method, according to which estimators will be derived with the help of the MRR2 approach introduced by Mays et al. (2000), estimated parametric random – effects for the i^{th} profile are defined as:

  $\widehat{\psi_i} = [\widehat{b_{ip}}, \hat{\lambda}\widehat{\gamma_i}]'$, $i = 1, 2, \ldots, n$ (4.11)

  where $\hat{\lambda}$ represents the estimated mixing parameter.

The last step before commenting on the results of the given research is the definition of MCUSUM control chart statistics. Thus, these statistics are defined as follows:

- The parametric MCUSUM statistic $S_{i,p}$ for the i^{th} profile is defined as:

  If $d_i > k$ then $S_{i,p} = (S_{i-1} + \widehat{b_{ip}} - \overline{\widehat{b_p}})(1 - k/d_i)$, else $S_{i,p} = 0$, (4.12)

  with $S_{0,p} = 0$ and $d_i = [(S_{i-1} + \widehat{b_{ip}} - \overline{\widehat{b_p}})'\,\Sigma^{-1}\,(S_{i-1} + \widehat{b_{ip}} - \overline{\widehat{b_p}})]^{1/2}$, where k represents a predetermined constant, Σ is the variance – covariance matrix of $\widehat{b_{ip}}$ and $\overline{\widehat{b_p}}$ represents the vector of the mean parametric estimated random – effect $\widehat{b_{ip}}$.

- The nonparametric MCUSUM statistic $S_{i,non}$ for the i^{th} profile is defined as:

  If $d_i > k$ then $S_{i,non} = (S_{i-1} + \hat{\gamma}_i - \bar{\hat{\gamma}})(1 - k/d_i)$, else $S_{i,non} = 0$, (4.13)

  with $S_{0,non} = 0$ and $d_i = [(S_{i-1} + \hat{\gamma}_i - \bar{\hat{\gamma}})' \Sigma^{-1} (S_{i-1} + \hat{\gamma}_i - \bar{\hat{\gamma}})]^{1/2}$, where k represents a predetermined constant, Σ is the variance – covariance matrix of $\hat{\gamma}_i$ and $\bar{\hat{\gamma}}$ represents the vector of the non-parametric residuals estimated random – effect $\hat{\gamma}_i$.
- The semiparametric MCUSUM statistic $S_{i,sp}$ for the i^{th} profile is defined as:

  If $d_i > k$ then $S_{i,sp} = (S_{i-1} + \widehat{\psi_i} - \bar{\hat{\psi}})(1 - k/d_i)$, else $S_{i,sp} = 0$, (4.14)

  with $S_{0,sp} = 0$ and $d_i = [(S_{i-1} + \widehat{\psi_i} - \bar{\hat{\psi}})' \Sigma^{-1} (S_{i-1} + \widehat{\psi_i} - \bar{\hat{\psi}})]^{1/2}$, where k represents a predetermined constant, Σ is the variance – covariance matrix of $\widehat{\psi_i}$ and $\bar{\hat{\psi}}$ represents the vector of the semi-parametric MRR2 estimated random – effect $\widehat{\psi_i}$.

The conclusions that emerged through a Monte Carlo simulation study were the following:

- If the misspecification parameter, denoted as γ, is equal to zero, i.e., γ = 0, and so, the estimated semiparametric profiles are equivalent to the parametric profiles, then the ARL values of the parametric method are smaller and better than the ARL values of the nonparametric approach using residuals. However, as the values of parameter γ increase, the nonparametric method becomes better than the parametric approach, as the ARL values become smaller and thus has a better ability to detect a shift quickly.
- For γ = 0 the semiparametric method is characterized as the best and most effective estimation approach.
- For values of γ close to zero, the performance of the parametric with the semiparametric method is close, while for values of the misspecification parameter near the unit the performance of the semiparametric method with that of the nonparametric show similar results.
- Generally, the semiparametric estimation approach, which is based on MRR2 technique, was the most sensitive method in detecting shifts for all the γ levels and provided the best estimates.

4.1.3 Robust profile monitoring for Phase I Analysis

GLMM are extremely popular, as they model many applications from everyday life and have an important place in the field of product production, and mainly are used when the response variable follows a nonnormal distribution. Studies conducted until recently investigated profiling under the assumption that the response variable can be correctly modelled using generalized linear models. Bandara et al. (2020) studied the case where the above hypothesis is unknown or uncertain. For this reason, they proposed two methods for monitor generalized linear mixed profiles from the exponential family: a) Nonparametric regression method, and b) Semiparametric method.

4.1.3.1 A nonparametric method for Phase I

A generalized linear mixed model can be expressed nonparametrically as:

$$g[E(Y_{ij})] = f(x_{ij}) + \zeta_i(x_{ij}),\ i = 1, 2, \ldots, m \text{ and } j = 1, 2, \ldots, n_i \quad (4.15)$$

where $g[E(Y_{ij})]$ represents the link function applied to the expected value of Y_{ij}, i represents the different profiles, while j represents the different observations within each profile, $f(x_{ij})$ is the fixed but unknown smooth function that captures the overall profile average curve, which represents the average behavior of the functional relationship between response and explanatory variable and $\zeta_i(x_{ij})$ is the i^{th} profile random smooth function that captures the random difference between the i^{th} profile specific curve and the profile average curve.

Both $f(x_{ij})$ and $\zeta_i(x_{ij})$ can be accessed from the following relationships:

$$f(x_{ij}) \approx \beta_0 + \sum_{l=1}^{p} \beta_1 x_{ij}^l + \sum_{K=1}^{K_1} u_{iK} (x_{ij} - k_K)^p,\ i = 1, \ldots, m\ j = 1, \ldots, n_i \quad (4.16)$$

$$\zeta_i(x_{ij}) \approx b_{i0} + \sum_{l=1}^{p} b_{i1} x_{ij}^l + \sum_{K=1}^{K2} t_{iK} (x_{ij} - k_K)^p,\ i = 1, \ldots, m\ \ j = 1, \ldots, n_i \quad (4.17)$$

where $\beta_0 + \sum_{l=1}^{p} \beta_1 x_{ij}^l$ is the parametric component and $\sum_{K=1}^{K_1} u_{iK} (x_{ij} - k_K)^p$ is the spline component for the profile average curve, while $b_{i0} + \sum_{l=1}^{p} b_{i1} x_{ij}^l$ represents the random parametric component and $\sum_{K=1}^{K2} t_{iK} (x_{ij} - k_K)^p$ represents the random spline component for the i^{th} profile.

The Eq. (4.15) can equivalently be written as:

$$g[E(Y_{ij})] = X_i\beta + Z_i u + X_i b_i + E_i t_i,\ i = 1, \ldots, m\ \ j = 1, \ldots, n_i \tag{4.18}$$

where $\beta = (\beta_0, \beta_1, \ldots, \beta_p)^T$, $u = (u_1, u_2, \ldots, u_{K1})^T$, $b_i = (b_{i0}, b_{i1}, \ldots, b_{ip})^T$, $t_i = (t_{i1}, t_{i2}, \ldots, t_{iK2})^T$, K_1 is the number of knots for the profile average curve and K_2 is the number of knots for the profile specific curve. Moreover, the matrices X_i, Z_i and E_i have the follow fit:

$$X_i = \begin{bmatrix} 1 & x_{i1} & \cdots & x_{i1}^p \\ \vdots & & \ddots & \vdots \\ 1 & x_{ini} & \cdots & x_{ini}^p \end{bmatrix}, \qquad Z_i = \begin{bmatrix} (x_{i1} - k_1)^p & \cdots & (x_{i1} - k_{K1})^p \\ \vdots & \ddots & \vdots \\ (x_{ini} - k_1)^p & \cdots & (x_{ij} - k_{K1})^p \end{bmatrix},$$

$$E_i = \begin{bmatrix} (x_{i1} - k_1)^p & \cdots & (x_{i1} - k_{K2})^p \\ \vdots & \ddots & \vdots \\ (x_{ini} - k_1)^p & \cdots & (x_{ij} - k_{K2})^p \end{bmatrix}.$$

Equivalently, Eq. (4.18) can be written as:

$$g[E(y)] = X\beta + Z B, \tag{4.19}$$

where $Z = \begin{bmatrix} Z_1 & X_1 & 0 & \cdots & 0 & E_1 & 0 & \ldots & 0 \\ \vdots & & & \ddots & & & \vdots & & \\ Z_m & 0 & 0 & \cdots & X_m & 0 & 0 & \ldots & E_m \end{bmatrix}$ and $B = \begin{bmatrix} u \\ b \\ t \end{bmatrix}$, with $u = (u_1, u_2, \ldots, u_{K1})^T$, $b = (b_1, b_2, \ldots, b_m)^T$, $t = (t_1, t_2, \ldots, t_m)^T$.

Then, using the maximum likelihood method, estimates for model parameters $\hat{\beta}$ as well as forecasts $\hat{B}$ are in the form of:

$$\hat{\beta} = (X^T D^{-1} X)^{-1} X^T D^{-1} d, \tag{4.20}$$

$$\hat{B} = M Z^T D^{-1} (d - X\hat{\beta}), \tag{4.21}$$

with $D = Z M Z^T + \Delta^{-1} A^{1/2} R A^{1/2} \Delta^{-1}$, where M is the covariance matric of B, Δ is a block diagonal matrix of the first derivatives of the conditional mean evaluated at the fixed effects estimate and the random effects estimate, A is a block diagonal matrix containing the variance functions in the diagonal blocks, R is a correlation matrix and d represents the pseudo-responses vector representing pseudo responses from all clusters.

Once the parameters of the model have been estimated, it is easy to understand that the estimates of Eqs. (4.18), (4.19) are in the form of:

$$g(\hat{y}_i) = X_i \hat{\beta} + Z_i \hat{u} + X_i \hat{b}_i + E_i \hat{t}_i,\ i = 1, \ldots, m\ \ j = 1, \ldots, n_i \tag{4.22}$$

$$g(\hat{y}^*) = X\hat{\beta} + Z\hat{u}, \tag{4.23}$$

where $g(\hat{y}_i)$ represents the p-spline estimator of the expected values for the i^{th}

profile and $g(\hat{y}^*)$ represents the p-spline estimation for the expected values of the profile average curve. Note that, both $g(\hat{y}_i)$ and $g(\hat{y}^*)$ were estimated using the link scale.

The next step is the calculation of the T^2 statistic in order to detect outlying profiles, which are characterized in an out – of – control situation. Bandara et al. (2020) defined the T^2 statistic as follows:

$$T_1^2 = (g(\hat{y}_i) - g(\hat{y}^*))^T \hat{S}^{-1} (g(\hat{y}_i) - g(\hat{y}^*)), \text{ i} = 1, 2, \ldots, \text{m} \quad (4.24)$$

or,

$$T_2^2 = (\hat{\varphi}_i - \bar{\varphi})^T \hat{S}^{-1} (\hat{\varphi}_i - \bar{\varphi}), \text{ i} = 1, 2, \ldots, \text{m} \quad (4.25)$$

where $\hat{S}$ is the estimated variance-covariance matrix for $g(\hat{y}_i)$ and $\hat{\varphi}_i = (\hat{b}_i, \hat{t}_i)^T$.

Therefore, a profile is classified as outlying when it applies:

$$T_s^2 \geq \chi^2_{df,\alpha}, \text{ s} = 1, 2 \quad (4.26)$$

where α represents the significance level and df are the degrees of freedom of the χ^2 distribution, which are equal to the sum of the numbers of random effects and knots numbers of each model.

4.1.3.2 A semiparametric method for Phase I

In this subsection, a study, examined by Bandara et al. (2020), will be introduced, concerning profiling for generalized linear mixed models using a semiparametric approach. More specifically, their research involved the introduction of a robust generalized linear mixed model (MRGLMM), which refer to a statistical framework that integrates both robust regression and mixed model. In Phase I, where model parameter estimates are made, Bandara et al. (2020) used a mixed model in which both the parametric and non-parametric methods are incorporated through a convex combination. Therefore, the form of MRGLMM in the link scale is defined as:

$$g(\hat{y}_i^{\sim}) = (1 - \lambda)\, g(\hat{y}_i^{p}) + \lambda\, g(\hat{y}_i), \text{ i} = 1, 2, \ldots, \text{m} \quad (4.27)$$

where $g(\hat{y}_i^{\sim})$ represents the MRGLMM fit, $g(\hat{y}_i^{p})$ represents the parametric fit, $g(\hat{y}_i)$ represents the nonparametric mixed model fit defined by Eq. (4.22) and λ $(0 \leq \lambda \leq 1)$ is the mixing parameter.

Mays et al. (2000) estimated λ as follows:

$$\hat{\lambda} = [g(\widehat{y_{i,-i}}) - g(\widehat{y_{i,-i}}^{p})] - [g(y) - g(\hat{y}^{p})] / [g(\hat{y}^{*}) - g(\hat{y}^{p})]^{T} [g(\hat{y}^{*}) - g(\hat{y}^{p})], \quad (4.28)$$

where $g(\widehat{y_{i,-i}})$ and $g(\widehat{y_{i,-i}}^{p})$ represent the nonparametrically and parametrically estimated expected values for the i^{th} profile without the observations from the i^{th} profile, respectively, $g(\hat{y}^{*})$ and $g(\hat{y}^{p})$ represent the nonparametrically and parametrically estimated profile average curve, respectively. Finally, the vector (y) is the observation vector of the model.

The next step is the calculation of the T^2 statistic in order to detect outlying profiles, which are characterized in an out-of-control situation. Bandara et al. (2020) defined the T^2 statistic as follows:

$$T_3^2 = [g(\tilde{y}_i) - g(\hat{y}^{MRGLMM})]^T \hat{S}^{-1} [g(\tilde{y}_i) - g(\hat{y}^{MRGLMM})], \; i = 1, 2, \ldots, m \quad (4.29)$$

where $\hat{S}^{-1}$ is an appropriate estimate of the variance-covariance matrix (for example, pooled sample variance-covariance matrix) and $g(\hat{y}^{MRGLMM}) = \sum_{i=1}^{m} g(\tilde{y}_i) / m$.

A second way of defining the T^2 statistic is in the form:

$$T_4^2 = (\widehat{\psi_i} - \bar{\psi})^T \{[\sum_{i=1}^{m-1} (\widehat{\psi_{i+1}} - \hat{\psi})(\widehat{\psi_{i+1}} - \hat{\psi})^T] / 2(m-1)\}^{-1} (\widehat{\psi_i} - \bar{\psi}), \quad (4.30)$$

with $\widehat{\psi_i} = ((1 - \hat{\lambda})\hat{b_i}, \hat{\lambda}\hat{\varphi_i})^T$, i = 1, 2, …,m, where $\hat{b_i}$ is the predicted random effect for the i^{th} profile of the parametric GLMM, which estimated using the pseudo-probability method of Wolfinger and O'Connell (1993), $\hat{\varphi_i}$ represents the vector of estimated random coefficients as defined through Eq. (4.25) and $\bar{\psi} = \sum_{i=1}^{m} \widehat{\psi_i} / m$.

Therefore, a profile is classified as outlying when it applies:

$$T_s^2 \geq \chi^2_{df,\alpha}, \; s = 3, 4 \quad (4.31)$$

where α represents the significance level and df are the degrees of freedom of the χ^2 distribution, calculated as $(1 - \hat{\lambda})df_p + \hat{\lambda}df_{np}$, with df_p represent the degrees of freedom of the parametric model and df_{np} are the degrees of freedom of the nonparametric model.

4.1.3.3 A comparison of methods

This subsection will report conclusions drawn from the study by Bandara et al. (2020). More specifically, a performance comparison was made between the nonparametric approach and the semiparametric method. While their performance research, conducted through a Monte Carlo simulation study, focused on the univariate regressor situation using a binary response variable, the resulting conclusions can be generalized to the multiple regressor situation using any distribution from the exponential family. The model used derived from Bandara et al. (2020) is in the form of:

$$G_{ij}(x_{ij}) = (1 - \gamma)(A) + \gamma(B),\ i = 1, 2, \ldots, m \quad j = 1, 2, \ldots, n_i \tag{4.32}$$

where $G_{ij}(x_{ij})$ is the probability of success for the i^{th} profile at the j^{th} level of x_{ij}, γ ($0 \leq \gamma \leq 1$) represents the misspecification parameter, A is a logistic probability density function and B represents a mix of two logistic probability density functions.

Therefore, the measures used in this study to measure the performance of the above methods were simulated integrated mean square error (SIMSE) and simulated probability of signal (POS) for the analysis of Phase I. SIMSE, which is a measure of the goodness of fit, is defined as:

$$SIMSE = 1/m\ [\sum_{i=1}^{m} (\hat{y}_i - \mu_i)^T (\hat{y}_i - \mu_i)],\ i = 1, 2, \ldots, m \tag{4.33}$$

where $\hat{y}_i$ represents a vector of estimated values for the i^{th} profile using either the nonparametric or semiparametric methods and μ_i is a vector of the probability of success for the i^{th} profile.

POS is defined as the probability that at least one of the T^2 statistics, defined for both the nonparametric and semiparametric methods, are outside the limits in a simulation study. The upper control limit (UCL), in which the independence of T_i^2, i = 1, 2, ..., m was assumed, was defined as follows:

$$UCL = \chi^2_{1-\alpha,df}, \tag{4.34}$$

where $\chi^2_{1-\alpha,df}$ represents the $(1 - \alpha)$ quantile of the χ^2 distribution.

In this study, α was set equal to 0.05 and represents the significance level.

The conclusions drawn are as follows:

- As the number of observations in each profile increases, SIMSE takes smaller values and thus estimates become more accurate.
- When the misspecification parameter is equal to zero, i.e., $\gamma = 0$ (so, the model used in the simulation study is equal to the real model), the adaptation of the model by the semiparametric method consists mainly of the parametric fit.
- When $\gamma = 1$ then the model adaptation from the semiparametric method consists mainly of the nonparametric fit.
- For intermediate values of γ, the semiparametric method model performs better than that of the nonparametric method.
- In general, MRGLMM performs better for misspecification of models.
- Control limits increase for each T^2 statistic as the number of repetitions decreases.
- POS was used as a performance measure to detect step shift in intercepts in both the nonparametric and semiparametric methods. It was observed that as the size of the shift increased, the price of the POS became larger, regardless of the value of γ. Therefore, T^2 statistics can be considered sensitive to step shift.
- The probability of signal value for all T^2 statistics increases as the number of repetitions increases.
- MRGLMM method performance is better than nonparametric method for partially misspecified models.
- According to the probability of signal criterion, when $\gamma = 1$ then for small shifts the performance of the nonparametric method is better, while for large shifts the MRGLMM method performs better.
- According to the POS for drift shift in profile intercepts, the performance of the semiparametric method is better for partially misspecified models, while for $\gamma = 1$ the nonparametric method performs better.

- According to the POS performance measure for temporary shifts in the profile intercepts, it was observed that the T^2 statistic results of the two methods are similar to those to step and drift shifts for small values of parameter γ (specifically, for γ values = 0, 0.25, 0.5).

4.2 Other techniques for monitoring generalized linear and generalized linear mixed profiles

In this section we will talk about three different approaches, where the monitoring of GLM and GLMM occurs under a specific framework. In more detail, initially, we will refer to the study of Mohammadzadeh et al. (2021), who monitored logistic profiles using the variable sample interval method in order to examine whether or not to increase the sensitivity of change detection in Phase II. Then, we will discuss the study by Mohamed et al. (2022), who monitored a known type of GLM profile, namely gamma regression model (GRM) profile, based on identity and log link function. This section will close with the study by Liu et al. (2018), who investigated the monitoring of generalized linear mixed model (GLMM) profiles for surgical data.

4.2.1 Adapting to variable sampling intervals: A VSI approach

In this subsection logistic profiles, which are the most popular type of GLM profiles, were monitored in Phase II with the help of control charts, under the assumption that one chart parameter, namely the sampling interval, is not fixed but behaves as a variable. The above method is referred to in the literature as the variable sample interval (VSI) approach, introduced by Mohammadzadeh et al. (2021) and is used to test the stability of a process over time in Phase II. Furthermore, the above study is of particular interest as it proceeds to a comparison between T^2, multivariate exponentially weighted moving average (MEWMA), deviance (DEV) control chart, generalized likelihood ratio (GLR) and support vector regression (SVR) methods, drawing conclusions about their performance where the VSI approach is used and where the sampling intervals

are fixed. It is noted that the last two methods, i.e., generalized likelihood ratio and support vector regression, although developed and used in other types of profiles, for monitoring logistic profiles with binary responses in Phase II are used for the first time. Finally, the above comparison is made with the help of the average time to signal (ATS) criterion, which represents the expected time until a signal occurred. Below are briefly given the statistics of the above methods, which are based on the logistic regression model of Eq. (4.3).

- The general form of T^2 chart statistic for t^{th} profile is:

  $$T_t^2 = (\widehat{\beta_t} - \beta_0)' \Sigma_0^{-1} (\widehat{\beta_t} - \beta_0), \quad (4.35)$$

  where j is the maximum number of profiles, $\widehat{\beta_t}$ represents the vector of estimated parameters for the t^{th} profile, β_0 is the vector of in – control model parameters and Σ_0 is the in – control variance – covariance matrix.

- The general form of MEWMA chart statistic for t^{th} profile is:

  $$MEWMA_t = (Z_t - \beta_0)' \Sigma_{Zt}^{-1} (Z_t - \beta_0), \quad (4.36)$$

  with $Z_t = \theta\widehat{\beta_t} + (1 - \theta) Z_{t-1}$, where Σ_{Zt} represents the variance – covariance matrix of Z_t, θ ($0 \leq \theta \leq 1$) represents the smoothing parameter, β_0 is the vector of in – control model parameters and $\widehat{\beta_t}$ represents the maximum likelihood estimation of profile parameters (β_t) using IWLS algorithm.

- The general form of DEV chart statistic for t^{th} profile is:

  $$DEV_t = \{-2[\sum_{i=1}^{n} log(m/y_{it}) + \sum_{i=1}^{n} y_{it}(x_i'\widehat{\beta_t}) - \sum_{i=1}^{n} mlog(1 + exp(x_i'\widehat{\beta_t}))]\} - \{-2[\sum_{i=1}^{n} log(m/y_{it}) + \sum_{i=1}^{n} y_{it}(x_i'\beta_0) - \sum_{i=1}^{n} mlog(1 + exp(x_i'\beta_0))]\}, \quad (4.37)$$

  where $\widehat{\beta_t}$ represents the maximum likelihood estimation of full profile parameters (β_t) using IWLS algorithm, β_0 is the maximum likelihood estimation of reduced profile parameters (β_t) using IWLS algorithm and m represents the total number of trials.

- The general form of GLR chart statistic for t^{th} profile is:

  $$GLR_{\tau,t} = -2[\sum_{i=1}^{n} \sum_{j=\tau+1}^{t} y_{ij}(x_i'\beta_0) - \sum_{i=1}^{n} \sum_{j=\tau+1}^{t} mlog(1 + exp(x_i'\beta_0)) + \sum_{i=1}^{n} \sum_{j=\tau+1}^{t} y_{ij}(x_i'\widehat{\beta_1}) - \sum_{i=1}^{n} \sum_{j=\tau+1}^{t} mlog(1 + exp(x_i'\widehat{\beta_1}))], \quad (4.38)$$

  where τ ($1 \leq \tau \leq t$) is the unknown time, β_0 represents the in – control

parameters' vector and $\widehat{\beta_1}$ represents the estimated out – of – control parameters' vector.

- The SVR method is a machine learning technique, and the general steps are as follow:

  Step 1. Determine the sample size (n), number of trials (m), fixed sampling interval (d_0) and the other parameters of the control chart.

  Step 2. Specify the upper control limit of the chart using simulation.

  Step 3. Determine the sampling intervals d_1 and d_2 so that $d_1 \leq d_0 \leq d_2$.

  Step 4. Calculate the percentage of p as $p = [(d_2 - d_0) / (d_2 - d_0)]$.

  Step 5. Generate in – control profiles, which are determined to achieve a specific in-control ATS and calculate the chart statistic for each one.

  Step 6. Count the number of times that d_1 and d_2 is utilized.

  Step 7. Adjust a warning limit based on the generated profiles to reach p.

The results obtained through a simulation study were the following:

- For shift in the profile intercept, it was observed that, both in the scenario where the sampling interval is fixed and, in the scenario, where the sample interval is variable, GLR and SVR methods perform better as they have lower ATS values compared to T^2, MEWMA and DEV control charts. In fact, GLR and SVR methods have better ability to detect a shift under the VSI approach.

- For shift in the profile slope, it was observed that, both in the scenario where the sampling interval is fixed and, in the scenario, where the sample interval is variable, GLR and SVR methods perform better as they exhibit lower ATS values compared to T^2, MEWMA and DEV control charts. However, for very large shifts in the profile slope the DEV method seems to perform equally well in both scenarios.

- For simultaneous shifts in the intercept and slope, the VSI approach performs better and in fact, GLR and SVR methods have lower ATS

values compared to other methods, which makes them more effective at detecting shifts.

- T^2 control chart is the least efficient chart for small shifts, both when the sampling interval is constant and when it behaves as a variable.
- The bias effect, which means that ATS values in some shifts exceed specific in-control ATS values, was observed on the T^2 and MEWMA control charts.
- In general, it was observed that the VSI method improves the performance of all charts examined, mainly for small and moderate shifts.
- For smaller values of d_1 and for larger values of d_2 it was observed that the examined control charts perform better and are more efficient under the VSI method.
- As the number of trials increases, chart´s performance becomes better, with GLR and SVR methods showing better performance at detecting shifts in intercept than others.

4.2.2 Residuals control chart profiling in gamma regression models

In this subsection the gamma regression model (GRM) profile is examined and monitored during Phase II, where monitoring is based on residuals exponentially weighted moving average (residuals EWMA) control charts in order to detect any out – of – control situation. It is noted that the estimation of the model parameters in Phase I has been performed with the maximum probability estimation (MLE) method, which was mentioned in the previous section of this chapter. Furthermore, this study draws conclusions about the EWMA control charts, as it compares the EWMA chart using deviance residuals with the EWMA using Pearson residuals. Thus, the comparison is performed on the EWMA control charts using different residuals, i.e., deviance and Pearson residuals, and different link function, i.e., identity and log link functions.

Finally, the results are obtained with the help of average run length (ARL) and relative average run length (RARL) performance criteria.

Initially, it should be mentioned that the gamma regression model (GRM) is applied when the response variable, y, is continuous and positively skewed. Furthermore, the gamma distribution, which belongs to the family of exponential distributions with mean $1/\varphi$, $\varphi>0$, is used to model the time between events or the failure times. Therefore, in this model y represents the waiting time until an event occurred.

Based on the generalized linear model in Eq. (4.1) the two types of residuals that will be examined in this study will be briefly presented. Therefore, we have the following two categories of residuals:

- Pearson residuals are used for the purpose of checking the model for each observation and are defined as follows:

  $r_i^p = (y_i - \hat{\mu}_i) / \sqrt{var(\hat{\mu}_i)}$, i = 1, 2, …, n (4.39)

  with $var(\hat{\mu}_i) = [\hat{\mu}_i (\eta_i - \hat{\mu}_i) / \eta_i]$, where $\hat{\mu}_i$ is the fitted mean value.
- Deviance residuals are a likelihood ratio statistic for detecting a mean shift and are defined as follows:

  $r_i^d = -2\sum_{i=1}^{n} log(y_i / \hat{\mu}_i) - ((y_i - \hat{\mu}_i) / \hat{\mu}_i)$, i = 1, 2, …, n (4.40)

  with $\hat{\mu}_i = g^{-1}(x_i'\hat{\beta})$, where $\hat{\beta}$ represents the vector of estimators for parameters β.

Therefore, below are defined the GRM profiles that would be used in the study by Mohamed et al. (2022).

The GRM with mean and shape structures, using the identity link function for the mean structure, defined as:

- $\mu_i = xi'\theta$, i = 1, 2, …, n (4.41)

  $\log(\theta_i) = Z_i'y$, i = 1, 2, …,n (4.42)

  where Eq. (4.41) represents the mean structure and Eq. (4.42) represents the regressors Z for the shape structure, with log link function.

The GRM with mean and shape structures, using the log link function for the mean structure, defined as:

- $\log(\mu_i) = x_i'\theta$, i = 1, 2, …, n (4.43)

  $\log(\theta_i) = Z_i'y$, i = 1, 2, …, n (4.44)

where Eq. (4.43) represents the mean structure and Eq. (4.44) represents the regressors Z for the shape structure, with log link function.

The conclusions of the research are drawn through a simulation study, where four, five and ten sample sizes (n), respectively, were used, and the number of samples (m) was twenty-five, thirty and thirty-five, respectively. Therefore, the results were as follows:

- When using the identity link function, ARL values of deviance residuals are smaller than ARL values of Pearson residuals for any value in the sample size.
- As the number of samples used in the study increased, the ARL values became smaller, resulting in better performance for any link function and type of residuals.
- It was observed that for number of sample size equal to four or five, the highest ARL value - and therefore the worst - was presented for Pearson residuals, for both kind of link function.
- Through this study, it was realized that smaller ARL values occurred under deviance residuals for both types of link function.
- For number of samples equal to thirty and number of sample size equal to five, the best RARL values were observed in the EWMA statistic for scenario where it includes log link function and deviance residuals.
- For number of samples equal to twenty-five and number of sample size equal to ten, the best RARL values were observed in the EWMA statistic for scenario where it includes log link function and Pearson residuals.
- Overall, at m = 25 the best RARL values were observed for the log link function and Pearson residuals, while at m = 30 became the worst RARL values.
- In general, the deviance residuals results have greater effectiveness and are more accurate compared to Pearson residuals results.

4.2.3 Real-time monitoring of surgical outcomes

Liu et al. (2018) proposed a new efficient control chart, which will be able to detect shifts both in average levels (i.e., location parameters) and in scale

parameters (i.e., volatility within the same group), to monitor surgical performance. Therefore, a weighted score test (WST) statistic was developed to construct an exponentially weighted moving average (EWMA) control chart to simultaneously monitor location and scale parameters. The research ends with a comparison between the above new method and an existing approach based on the risk – adjusted cumulative sum (RA – CUSUM) control chart.

In studies of surgical outcomes, the model used is based on GLMM and has the following form:

$$\omega(\pi_n) = x_n'\beta + \alpha, \tag{4.45}$$

where $\omega(\cdot)$ is the logit link function, x_n represents a vector of a set of risk factors of the binary outcomes y_n, β is a vector of parameters, α represents the intercept parameter and $\pi_n = Pr(y_n = 1) = 1 - Pr(y_n = 0)$ represents the surgical failure rate.

Furthermore, to monitor the 30-day mortality risk of surgical outcomes, Liu et al. (2018) assumed that for every independent binary outcome y_i, i = 1, 2, ..., n, there will be a random effect γ_i. Therefore, based on this assumption, the WST statistic S(0) for the model in Eq. (4.45) is defined as follows:

$$S(0) = 0.5\sum_{i=1}^{n} \lambda(1 - \lambda)^{n-i} [(y_i - \pi_i)^2 - \pi_i(1 - \pi_i)], \; i = 1, 2, \ldots, n \tag{4.46}$$

where λ ($0 \leq \lambda \leq 1$) is a smoothing parameter and π_i is the surgical failure rate with logit link function $\text{logit}(\pi_i) = x_i'\beta + \alpha + \gamma_i$.

Therefore, based on the WST statistic the pairs (x_n, y_n) are collected and thus the EWMA control statistic Z_n for the n^{th} observation (x_n, y_n) is defined as:

$$Z_n = (1 - \lambda) Z_{n-1} + \lambda Y_n, \; n = 1, 2, \ldots \tag{4.47}$$

with $Y_n = (y_n - \pi_n)^2 - \pi_n(1 - \pi_n)$ and $Z_0 = 0$, where $\text{logit}(\pi_n) = x_n'\beta + \alpha$.

The control chart, which uses Z_n for its statistic, is referred to in the literature as the EWMA chart for surgical outcome (ESOP) and is used to detect upward shifts and downward shifts simultaneously. Finally, before proceeding to draw conclusions, we will define the RA-CUSUM chart, as the research compares the returns of the above control charts. Therefore, the RA-CUSUM chart, which was introduced by Steiner et al. (2000) and is based on the Wald sequential probability ratio test, can be written as:

$Z_n = \max(0, Z_{n-1} + X_n)$, n = 1, 2, … (4.48)

$Z_n = \min(0, Z_{n-1} - X_n)$, n = 1, 2, … (4.49)

with $Z_0 = 0$ and $X_n = \log\{[\pi_R^{yn} (1 - \pi_R)^{1-yn}] / [\pi_n^{yn} (1 - \pi_n)^{1-yn}]$, where $\pi_n = Pr(y_n = 1)$ represents the surgical failure rate, $\pi_R = R\pi_n / (1 + (R - 1)\pi_n)$ and R represents an initial value adapt to the minimal clinically important effect in a clinical trial. Note that Eq. (4.48) presents the form of the upper – sided RA-CUSUM chart, while Eq. (4.49) the lower – sided of this control chart.

The conclusions that emerge through a simulation study are the following:

- For the lower-sided charts, when the ESOP receives small values of the λ parameter, then it performs better for small shifts, as the ARL values are smaller resulting in the ability to quickly detect shifts, while when the ESOP receives large λ values then it has a better detection capability of large shifts. Finally, the RA-CUSUM chart performs better when actual shifts mainly match those initial R values that the above control chart was designed to detect, which take small values. Therefore, the above control charts are most effective when λ and R values decrease.
- For the upper – sided charts, when the ESOP receives small values of the λ parameter, then it performs better for small shifts, as the ARL values are smaller resulting in the ability to quickly detect shifts, while when the ESOP receives large λ values then it has a better detection capability of large shifts. Finally, the RA-CUSUM chart performs best when actual shifts mainly match those initial R-values that the above control chart was designed to detect, which take large values.
- When the scale parameter is greater than zero, observed that both the ESOP and the RA-CUSUM charts are effective for detecting shifts by a large margin.
- In general, the ESOP control chart is more sensitive either for smaller mean shifts or when shifts are performed in the scale parameters, compared to the RA-CUSUM chart. Therefore, the ESOP is characterized as more effective for monitoring random effects belonging within the same group, than the RA-CUSUM control chart.

CHAPTER 5

Geometric and Polynomial profiles

Introduction

A geometric profile, encompassing roundness, flatness, and cylindricity, pertains to the characteristics of a two or three-dimensional space. This profile is derived by assessing the quality features of interest at multiple locations. It involves the examination and measurement of the dimensional attributes, ensuring precision and conformity across the specified geometric parameters. This comprehensive approach provides a understanding of the object's form and alignment, enabling a thorough evaluation of its geometric integrity. Therefore, the geometric profile can be modeled in its general form as:

$$y = f(x) + \varepsilon, \tag{5.1}$$

where y represents the observed deviation from the nominal value, f(x) corresponds to the system error and ε is the error term of the model.

It is noted that the following sections will report recent research on two known types of geometric profiles, the circular and the cylindrical profiles, which will be appropriately analyzed in the respective sections. Finally, the remaining sections of this chapter will present studies on monitoring polynomial profiles. The polynomial profile is a type of profile that belongs to the category of linear profiles and incorporates a mathematical framework known as polynomial regression, establishing a model that illuminates the relationship between explanatory and response variables. The form of a polynomial model is described below.

Considering $\{(x_i, y_{ij}), i = 1, 2, \ldots, n \text{ and } j = 1, 2, \ldots\}$ as the j^{th} random sample and $\beta_0, \beta_1, \ldots, \beta_p$ as the nominal values of the in – control parameters, the polynomial regression model of order p is defined as:

$$y_{ij} = \beta_0 + \beta_1 x_i + \beta_2 x_i^2 + \ldots + \beta_p x_i^p + \varepsilon_{ij}, \tag{5.2}$$

where x_i represents the explanatory variable and ε_{ij} is the error terms between

profiles, which are independent and identically distributed with a normal distribution, i.e., $\varepsilon_{ij} \sim N(0, \sigma^2)$.

In order to eliminate the effect of multicollinearity, Eq. (5.2) can be written equivalently as follows:

$y_{ij} = b_0 + b_1 x_i^* + b_2 x_i^{*2} + \ldots + b_p x_i^{*p} + \varepsilon_{ij}$, i = 1, 2, …, n and j = 1, 2, … (5.3)

where $x_i^* = x_i - \bar{x}$, $b_i = \sum_{s=k}^{p} \beta_s \binom{s}{k} x^{-(s+k)}$, $\bar{x} = (1/n) \sum_{i=1}^{n} x_i$ and $\varepsilon_{ij} \sim N(0, \sigma^2)$.

Table 5_1 briefly mentions previous research conducted to monitor geometric and polynomial profiles from 2008 to 2018. Thus, lists the researchers, whether the expert study concerned Phase I or Phase II of the profile, and the criterion for measuring the performance of the control charts used.

Research	Phase I	Phase II	Performance criterion
Colosimo et al. (2008)	-	Yes	ARL & estimated parameters
Kazemzadeh et al. (2008)	Yes	-	Signal probability, $\bar{\hat{\tau}}$, SD($\hat{\tau}$) & precision
Kazemzadeh et al. (2009)	-	Yes	ARL
Amiri et al. (2010)	Yes	-	Regression metric & R_{adj}^2
Pacella and Semeraro (2011)	-	Yes	ARL
Abdella et al. (2012)	-	Yes	ARL
Keramatpour et al. (2013)	-	Yes	ARL, $\bar{\hat{\tau}}$, SD($\hat{\tau}$) & precision
Colosimo et al. (2014)	-	Yes	ARL & SDRL
			(continued)

Keramatpour et al. (2014)	-	Yes	ARL
Nemati Keshteli et al. (2014b)	-	-	C_P & C_{PK}
Viveros – Aguilera et al. (2014)	Yes	Yes	ARL
Chen et al. (2015b)	Yes	-	Probability of signal, sensitivity & specificity
Noorossana and Nikoo (2015)	-	Yes	ARL
Zeng and Chen (2015)	Yes	-	Regression metric & chart statistic
Abdella et al. (2016)	-	Yes	ARL
Chen et al. (2016)	-	Yes	ARL
Awad (2017)	Yes	Yes	Estimated regression parameters & R_{adj}^2
Nie and Du (2017)	Yes	-	Identification accuracy of change point & non – signal probability
Pacella et al. (2017)	Yes	Yes	ARL & SDRL

Table 5_1. A brief overview of methods developed to monitor geometric and polynomial profiles from 2008 to 2018. (Adapted from Maleki, M. R., Amiri, A., & Castagliola, P. (2018)).

Considering the scholarly gap identified beyond 2018, following the contributions of Woodall (2007) and Maleki et al. (2018), the remainder of this chapter seeks to bridge this void. The objective is to present recent studies, research and advancements pertaining to the monitoring of geometric and polynomial profiles. This continuation aims to offer an updated exploration by bringing together some contemporary developments within this field.

5.1 Correlation in profile monitoring methods

In this section we will present three methods, which use correlated data to monitor geometric and polynomial profiles, respectively. In the first place, the study of Zhao et al. (2020), who attended an extremely useful type of profile for the field of geometric specifications, the circular profile, which contribute to the reliability and durability of products, will be discussed. Then, we will discuss the study by Zhao et al. (2020) on monitoring cylindrical profiles under spatial correlations, who proposed a new approach using T^2 and Shewhart control charts for monitor the variance of error term. This chapter will close with the study by Song et al. (2023), who examined the monitoring of polynomial profiles in the case where response variables behave as attribute data (categorical or count data) and the observations between profiles are correlated, i.e., there is between-profile correlation.

5.1.1 Monitoring circular profiles under spatial correlations

In modern manufacturing, the precision of rotary parts relies heavily on geometric specifications like circularity and cylindricity. As the number of measurement points increases, traditional statistical process control methods struggle due to highly correlated measurements. Therefore, Zhao et al. (2020) studied monitoring circular profiles under spatial correlations and proposed a new approach using T^2 and Shewhart control charts for monitor the variance of error term. Below, the model used to describe circular profiles is given.

Suppose that there are m profiles and each profile j (j = 1, 2, …, m) consists of n observation points. The deviation of each i^{th} (i = 1, 2, …, n) point in the j^{th} circular profile is denoted by y_{ij} and the model is defined as follows:

$$y_{ij} = \sum_{s=1}^{p} \rho_{sj} W^{(s)} y_{ij} + x_i'\beta_j + \varepsilon_{ij}, \quad (5.4)$$

where ρ ($0 \leq \rho \leq 1$) is the unknown lag coefficient (for spatial correlations), x_i are the independent variables, β_j represent the coefficient parameters, $W^{(s)}$ is the s-order spatial weight matrix and ε_{ij} represent the error terms, which follow the normal distribution as $\varepsilon_{ij} \sim N(0, \sigma^2)$.

Of particular interest is the comparison made between the new proposed method described above under spatial correlations and other known methods. Specifically, the new method is compared with the following methods: a) out of roundness (OOR) method, which is used to test the accuracy of circularity and is monitored using the Shewhart chart, b) location control charts (LOC) method, which monitors data by designing it in the same coordinate system and is monitored using the Shewhart chart, c) spatial autoregressive regression (SARX) approach, which examines the effect of spatial correlations on residuals, is monitored using T^2 and residuals charts and the difference with the new method presented above is that the SARX approach include the error terms while in the new method they exist in a separate term, and d) principal component analysis (PCA) method, which is used to monitor T^2 statistics.

The conclusions obtained through simulation studies, where the results are obtained with the help of average run length (ARL) performance criterion, are the following:

- The new method appears to perform better compared to LOC and SARX methods, which in turn perform better than OOR and PCA approaches.
- For small shifts, it was observed that the new method as well as the SARX methods perform better and are more effective than the others, because they have the lowest ARL values. Therefore, the ability to detect a small shift is faster than the rest of the examined methods.
- Through this study it was observed that the PCA method is not sensitive to minor shifts and the OOR approach is the least effective.

- In general, methods using spatial correlations were shown to perform better than other methods, with the new proposed approach achieving slightly better results than SARX.

5.1.2 Monitoring cylindrical profiles under spatial correlations

The cylindrical profile is a geometric structure composed of circular profiles. Using cylindrical coordinates, which extend polar coordinates into three dimensions, it incorporates a height dimension. Measurement points are evenly distributed along the axis, forming layers of points with the same height that constitute circular profiles. The radial position of a point is defined by the angle (θ), and the radius is denoted as r(z, θ), determined by both height (z) and angle (θ). Zhao et al. (2020) studied monitoring cylindrical profiles and they proposed the following model to take into account the spatial correlations:

$$y_{ij} = \sum_{s=1}^{p} \rho_{sj} W^{(s)} y_{ij} + x_i'\beta_j + \varepsilon_{ij}, \quad (5.5)$$

with $x_i'\beta_j = \sum\sum [A_{ij}P_j(z)\cos(i\theta) + B_{ij}P_j(z)\sin(i\theta)]$, where $z \in [-1, 1]$, $\theta \in [-\pi, \pi]$, $P_j(z)$ represents the j^{th} Legendre polynomial, A_{ij} and B_{ij} are the coefficients in the systematic error $x_i'\beta_j$, ρ $(0 \leq \rho \leq 1)$ is the unknown lag coefficient (for spatial correlations), $W^{(s)}$ is the weight matrix, which is represented by the rook-based contiguity or the queen-based contiguity and ε_{ij} represent the error terms, which follow the normal distribution as $\varepsilon_{ij} \sim N(0, \sigma^2)$.

Of particular interest is the comparison made between the new method under spatial correlations with other known methods. Specifically, the new proposed method is compared to the OOR, LOC, SARX and PCA approaches, which were developed in subsection 5.1.1, simply as we are talking about cylindrical profiles, axial and radial errors were added to evaluate their performance in Phase II.

The conclusions obtained through simulation studies, where the results are obtained with the help of average run length (ARL) performance criterion, are the following:

- The new method under spatial correlations and the SARX approach seems to perform better than the rest of the examined methods, because they exhibit the lowest ARL values, with the new proposed method prevailing slightly more.

- For large shifts the LOC method gives similar results to the new and SARX methods.
- Through this study it was observed that the PCA method is not sensitive to minor shifts and the OOR approach is the least effective.
- It was observed that the axial error can be detected faster than the radial shift error. Based on this observation and since both in subsection 5.1.1 and here, the new proposed methods presented for circular and cylindrical profiles, respectively, were compared with common geometric approaches, we can finally conclude that, comparing circular and cylindrical methods the detection rate for the cylindrical profiles is higher.

5.1.3 Monitoring polynomial profiles based on attribute data

This subsection will discuss the study by Song et al. (2023), who examined the monitoring of polynomial profiles in the case where response variables behave as attribute data and there is between-profile correlation. The motivation for the development of their research was a real example of automobile warranty data, where through it they note a trend where new car models experience a decline in warranty claims over time, signaling improved reliability in early manufacturing stages. This reduction in claims offers manufacturers insights into field reliability, enabling them to enhance product quality and customer satisfaction. Examining the data from a profile monitoring perspective reveals a correlation between different profiles. Inspired by learning effects, their study applies the learning curve model to illustrate the connection between profiles, particularly the decreasing claim rates or increasing production quantities of new products. Therefore, below is given the form of the proposed model developed by Song et al. (2023) based on learning effects/curves, i.e., on the phenomenon of production and time reduction.

Suppose y_{ij} and x_{ij} are the j^{th} observations, j = 1, 2, …, n, for the i^{th} profile response and explanatory variables, respectively. Then, assuming that, $\{y_{i1}, y_{i2}, \ldots, y_{in}\}$ are independent but the between-profile observations are correlated, the second-order polynomial model is defined as follows:

$g(\mu_{ij}) = \beta_0 + \beta_1 x_{ij} + \beta_2 x_{ij}^2 + \varphi log(D_i)$, j = 1, 2, …, n, i = 1, 2, … (5.6)

where g(·) represents a link function, $\mu_{ij} = E(y_{ij})$, $\beta = (\beta_0, \beta_1, \beta_2)$ is the vector of the regression coefficients and $\varphi log(D_i)$ represents the failure rate decreases for the i^{ih} profile, with $\varphi > 0$.

Furthermore, the proposed control chart for monitoring and evaluating model performance is based on the model of Eq. (5.6) and its statistic is defined as:

$$E_i = \lambda(\widehat{\beta}_i - \beta_{IC}) + (1 - \lambda)E_{i-1}, \quad (5.7)$$

where λ ($0 < \lambda < 1$) is the smoothing parameter, $\widehat{\beta}_i$ represents the estimate of vector β for the i^{th} profile, β_{IC} is the in – control vector of the regression coefficients and $E_0 = 0$.

It is worth noting that, as the size of products manufactured on the same day for i^{th} profile, i.e., the batch size, is time – varying, it is advisable to use dynamic control limits and not constant-fixed. Therefore, a series of dynamic control limits are used for each profile and thus, the charting statistic of Eq. (5.7) was named dynamic exponentially weighted moving average (dEWMA) chart. Finally, it is interesting to compare the simulation study between the new proposed dEWMA control chart and two other charts. Specifically, dEWMA is compared to a) the generalized likelihood ratio (GLR) chart, which is used for independent profiles and its control limits are constant, and b) the iEWMA control chart, which is identical to the new proposed dEWMA chart, just ignores between-profile correlation.

The conclusions obtained through a Monte Carlo simulation study using a second-order polynomial model, where the results are obtained with the help of average run length (ARL) performance criterion, are the following:

- For shifts in the profile intercept, it was observed that the dEWMA chart performs best, as it has the smallest ARL values and thus can detect a change in profile parameters faster than the other control charts examined. Also, iEWMA provides better results in turn than the GLR chart. Note that the effectiveness of dEWMA is due to the fact that it takes into account between-profile correlation and does not use constant control limits.

- As the value of $|\varphi|$ increases, the ARL values of dEWMA chart increase, which signals a decrease in chart´s performance, primarily for detecting small shifts in the profile intercept.
- For small values of λ, the dEWMA is capable of detecting a small change in the profile parameters more quickly, while for larger values of λ it is more efficient for detecting large shifts.
- The iEWMA chart proved to be very poor since between-profile correlation is ignored and thus, the out – of – control ARL values are much larger than the in – control ARL values. Furthermore, GLR control chart was deemed defective for monitoring polynomial profiles using attribute data and between-profile correlation and exhibits the worst performance.
- The control limits of dEWMA do not show a trend, they are random and small, while the control limit values of iEWMA chart are very large, have a trend and after an upward trend they stabilize (not random).
- Integrating the learning effect term into the model proves essential in characterizing the between-profile correlation and effectively mitigating the influence of correlated factors on control limits. In general, the dynamic nature of the control limit in the proposed dEWMA control chart enhances its accuracy in assessing the product state, effectively reducing the occurrence of false alarms.
- The study reveals that the variation in within-profile sample size (n) does not impact the in – control performance of the proposed dEWMA chart. Even when there are differences in the within-profile sample sizes, the run length distribution of the dEWMA chart consistently approximates a geometric distribution. It is worth noting that as n increases, the ARL values decrease, so that the chart can more quickly and efficiently detect a change in the profile parameters.

5.2 Methods for simultaneous shifts in the profile parameters

In this section, two methods will be discussed, which refer to the monitoring of polynomial profiles for the ability to detect simultaneous changes in the profile

parameters. In the first place, we will discuss the study of Yao et al. (2020), who proposed a new control chart for monitoring polynomial profiles during the analysis of Phase II, while at the end of this section will be presented the study of Atashgar and Abbassi (2021), who presented a new polynomial profile monitoring technique designed to effectively detect small shifts during Phase II analysis.

5.2.1 Development of a Phase II control chart using the weighted likelihood ratio test

Yao et al. (2020) proposed a control chart based on the weighted likelihood ratio test (WLRT) scheme and, in addition to the ability to detect changes in the parameters of the polynomial profile, has the ability to detect the decrease of model variance. Moreover, interestingly, the new proposed method based on the WLRT scheme is compared to other known approaches. Specifically, the WLRT control chart is compared with a) T^2 control chart, b) MCUSUM\χ^2 control chart, c) MEWMA control chart and d) Ortho chart. Below are briefly given the statistics for each method. Therefore, we have that:

- T^2 charting statistic, introduced by Kang and Albin (2000), is based on the polynomial model in Eq. (5.2) and has the following form:

  $$T_j^2 = (\widehat{\beta}_J - \beta)' \, \Sigma^{-1} \, (\widehat{\beta}_J - \beta), \quad (5.8)$$

  where $\widehat{\beta}_J$ represent the vector of the estimated parameters for the j^{th} profile, $\beta = (\beta_0, \beta_1, \ldots, \beta_p)'$ is the vector of the nominal values of the in – control parameters and Σ represents the covariance matrix of $\widehat{\beta}_J$.

- MCUSUM charting statistic, introduced by Noorossana and Amiri (2007), is based on the polynomial model in Eq. (5.2) and has the following form:

  $$S_j = \max\{S_{j-1} + B'(\widehat{\beta}_J - \beta) - 0.5D, 0\}, \quad (5.9)$$

  with $B = (\widehat{\beta}_J - \beta)' \, \Sigma^{-1} / D$, where $D = \sqrt{(\beta^* - \beta)' \, \Sigma^{-1} (\beta^* - \beta)}$, β is the vector of the nominal values of the in – control parameters, β^* is the vector of the nominal values of the out – of – control parameters and Σ represents the covariance matrix of $\widehat{\beta}_J$.

But, to assess error variance concurrently with the MCUSUM control chart, a suggested approach involves introducing a χ^2 statistic. Thus, the proposed χ^2 charting statistic is defined as follows:

$$\chi_j^2 = (1/\sigma^2) \sum_{i=1}^{n} e_{ij}^2, \quad (5.10)$$

where $e_{ij} = y_{ij} - \beta_0 - \beta_1 x_i - \beta_2 x_i^2 - \ldots - \beta_p x_i^p$ and σ^2 represents the variance of the error terms.

- MEWMA charting statistic, introduced by Zou et al. (2007), is based on the polynomial model in Eq. (5.2) and has the following form:

$$U_j = W_j' \, \Sigma_Z^{-1} \, W_j, \quad (5.11)$$

with $W_j = \lambda Z_j + (1 - \lambda) W_{j-1}$ be the EWMA statistic, where λ $(0 < \lambda < 1)$ is the smoothing parameter, $Z_j = (Z_j'(\beta), Z_j(\sigma_0))'$, σ_0 is the in – control standard deviation of the error terms, $W_0 = 0$, $Z_j(\beta) = [(\widehat{\beta_J} - \beta) / \sigma_0]$, Σ_Z is the covariance matrix of Z_j, $Z_j(\sigma_0) = \Phi^{-1}\{F(n\text{-}p) \, \widehat{\sigma_J}^2 / \sigma_0^2, n\text{-}p)\}$, Φ is the inverse standard normal cumulative distribution function and F represents the chi-square distribution function.

- Ortho charting statistic, introduced by Kazemzadeh et al. (2009), is based on the transformed orthogonal model:

$$y_{ij} = b_0 P_0(x_i) + b_1 P_1(x_i) + \ldots + b_p P_p(x_i) + \varepsilon_{ij}, \quad (5.12)$$

where $b_0, b_1, \ldots, b_p$ are the regression parameters such in Eq. (5.3) under in – control situation and $P_0(x_i), P_1(x_i), \ldots, P_p(x_i)$ are the orthogonal polynomials. Thus, the EWMA statistics based on the transformed model are defined as:

$$EWMA(j) = \lambda \widehat{b_{lJ}} + (1 - \lambda) EWMA(j\text{-}1), l = 1, \ldots, p \quad (5.13)$$

$$EWMA^*(j) = \max\{\lambda(MSE_j - 1) + (1 - \lambda) EWMA^*(j\text{-}1), 0\}, \quad (5.14)$$

with $EWMA(0) = b_l$, $l = 1, 2, \ldots, p$, and $EWMA^*(0) = 0$, where Eq. (5.13) represents the EWMA statistic for the regression parameters of the model, Eq. (5.14) represents the EWMA statistic for the in – control error variance of the error terms, MSE is the mean square error and $\widehat{b_{lJ}}$ represent the vector of the least square estimators of regression parameters for the j^{th} profile.

- WLRT charting statistic, proposed by Yao et al. (2020) for monitoring polynomial profiles, where in addition to identifying shifts in the

regression parameters, has the ability to detect variance decrease, is based on the polynomial model in Eq. (5.3) and has the following form:

$R_{j,\lambda} = (Y_{c,j} / \sigma_0^2) + n \log(n \sigma_0^2 / \widehat{Y_{c,J}}) - n,$ (5.15)

where $Y_{c,j} = (1 - \lambda)Y_{c,j-1} + \lambda\sum_{i=1}^{n}(y_{ij} - b_0 - b_1 x_i^* - \ldots - b_p x_i^{*p})^2$, λ is the smoothing parameter, σ_0^2 is the in – control variance of the error terms, $\widehat{Y_{c,J}} = (1 - \lambda)\ \widehat{Y_{c,J-1}} + \lambda\sum_{i=1}^{n}(y_{ij} - \widehat{b_0} - \widehat{b_1}\ x_i^* - \ldots - \widehat{b_p}\ x_i^{*p})^2$, $b_0, b_1, \ldots, b_p$ are the in-control regression parameters, $\widehat{b_0}, \widehat{b_1}, \ldots, \widehat{b_p}$ are the estimators of the in – control regression parameters, $Y_{c,0} = n$ and $\widehat{Y_{c,0}} = n$.

The conclusions obtained through simulation study using a second-order polynomial model, where the results are obtained with the help of average run length (ARL) performance criterion, are the following:

- For small shifts in the profile intercept, the MCUSUM\χ^2 chart performs best, while for larger changes it was observed that the Ortho control chart performs best. Finally, the T^2 chart shows the worst performance for any size change in the profile intercept.
- For small shifts in the first slope, the recommended WLRT method performs best, as it has the smallest ARL values and thus could detect small changes faster than other methods. However, for moderate shifts it was observed that the Ortho chart performs slightly better than WLRT. In general, for large changes both Ortho and WLRT approaches perform equally well and prevail over other methods.
- For any size shift in the second slope, the WLRT chart performs better than the rest of the charts, except in the case of moderate and large shifts, where the WLRT and Ortho charts show similar returns. Furthermore, second in performance and efficiency come the MEWMA and MCUSUM\χ^2 control charts and last comes T^2 which shows the worst performance.
- In detecting the upward shift of error standard deviation, Ortho control chart was observed to perform better for small and moderate shifts and the WLRT performed better for larger shifts. But, in detecting the downward shift of error standard deviation, WLRT performs best for small and moderate shifts, while for large changes the MEWMA control chart shows the best performance.

- For simultaneous change in the intercept and second slope, T^2 performs worst of all the control charts examined. Moreover, for moderate and large shifts in the intercept and at the same time for small changes in the second slope, Ortho chart performs better than the others, while for small shift in the intercept and at the same time for small shift in the second slope the WLRT chart shows the best performance. In general, as the change in the second slope gets bigger, then the WLRT performs better than all other charts.
- In general, for simultaneous changes in the intercept, first and second slopes, WLRT and Ortho charts perform best, while the T^2 control chart performs the worst. Finally, MCUSUM\$\chi^2$ and MEWMA control charts perform similarly, with MCUSUM\$\chi^2$ performing better for larger changes in first slope and for any change in second slope, while for smaller shifts in the first slope the MEWMA chart performs a little better.
- In general, for simultaneous changes in the intercept, first slope, second slope and error standard deviation, WLRT and Ortho charts perform best, while the T^2 control chart is the least efficient. Finally, the MCUSUM\$\chi^2$ and MEWMA charts perform similarly, with MCUSUM\$\chi^2$ performing better for larger changes in the error standard deviation and for any change in the second slope, while for smaller shifts in the error standard deviation the MEWMA chart performs a little better.

5.2.2 A method for enhancing sensitivity to minor changes

Atashgar and Abbassi (2021) presented a new polynomial profile monitoring technique designed to effectively detect very small shifts during Phase II analysis. Specifically, for Phase II monitoring, a newly introduced control chart simplifies the process by employing a single statistic and a singular control limit to simultaneously oversee all profile parameters. Therefore, based on the polynomial model in Eq. (5.2), they developed the so-called multivariate generally weighted moving average polynomial profile (MGWMA-PF) method, which uses the following statistic in j^{th} profile analysis:

$W_j = \sum_{i=1}^{n}[(q^{(i-1)^\alpha} - q^{i^\alpha})V_{j-i+1}] + q^{j^\alpha}W_0$, j = 1, 2, … (5.16)

with $V_j = (V_j'(\beta), V_j(\sigma))'$ and $W_0 = 0$, where $V_j(\beta) = (\widehat{\beta_J} - \beta) / \sigma$, $V_j(\sigma) = \Phi^{-1}\{F((n-p)\widehat{\sigma_J}^2 / \sigma^2, n-p)\}$, $\widehat{\beta_J}$ represents the vector of the estimated coefficients of model in Eq. (5.2), β is the vector of the profile parameters, σ represents the variance of the error term, Φ is the inverse standard normal cumulative distribution function, F represents the chi-square distribution function, α (α>0) is the adjustment parameter, q ($0 \leq q < 1$) represents the design parameter and $\widehat{\sigma_J}^2 = [1 / (n-p-1)] (y_j - x\widehat{\beta_J})' (y_j - x\widehat{\beta_J})$.

Moreover, the above method will indicate a signal that the process is in an out-of-control state when:

$L_G < W_j' [Var(W_j)]^{-1} W_j$, (5.17)

where L_G ($L_G > 0$) represents the upper control limit, which is determined each time by the researcher, depending on the in-control average run length (ARL) value to be used.

Finally, of particular interest is the fact that, through a Monte Carlo simulation study, the new MGWMA-PF method, which uses W_j statistic, is compared with other known methods using T^2, MEWMA, and multivariate cumulative sum along with χ^2 control chart (MCUSUM/χ^2) statistics, respectively. The format of these statistics has been given earlier in this section, but the interested readers are referred to the comprehensive articles for the detailed calculation of statistics with the above methods for profile monitoring by Kang and Albin (2000), Zou et al. (2007) and Noorossana and Amiri (2008), respectively.

The conclusions obtained through simulation study using a second-order polynomial model, where the results are obtained with the help of average run length (ARL) and standard deviation run length (SDRL) performance criteria, are the following:

- For small and moderate shifts in the profile intercept, the new proposed MGWMA-PF method performs better than the others, as it has lower ARL and SDRL values, respectively, and thus has the ability to detect a change faster.
- For shifts in the first slope (mainly for small and moderate changes), the new method performs better than the MEWMA approach, which in turn performs better than the T^2 and MCUSUM/χ^2 methods.

- For small and moderate shifts in the second slope, the MGWMA-PF approach performs uniformly better than the other methods under consideration. Furthermore, it was observed that, the MCUSUM/χ^2 method shows better results than T^2 and MEWMA methods.
- For small and moderate changes in the standard deviation, the new proposed method presents the smallest ARL and SDRL values, respectively, which marks its best performance.
- For large shifts in model parameters, all examined methods show similar performances, with the new method appearing to perform more efficiently.
- Under very small simultaneous shifts in the profile parameters, it was demonstrated through the simulation study that the new MGWMA-PF method performs better than the MEWMA approach.
- Finally, an interesting position in the study by Atashgar and Abbassi (2021) is that the MGWMA-PF method performs better when shifts occur in the profile intercept than the approach presented in the subsection 5.2.1, namely WLRT.

5.3 Methods regarding the effects on the Phase II performance

In this section, approaches to monitoring polynomial profiles will be presented, where they will examine how various factors affect the performance of Phase II analysis in the fullness of time. In the first place, we will discuss the study by Ghasemi Eshkaftaki et al. (2021), who sought to evaluate how parameter estimation in Phase I affects the performance of Phase II control charts. Furthermore, the study by Liu et al. (2023), who evaluated monitoring polynomial profiles under the assumption that observed data are not accurate, will be presented and, finally, the study by Netshiozwi et al. (2023), who introduced a monitoring framework that utilizes the concept of polynomial profile monitoring as a data-driven method for overseeing the internet usage of a telecommunications company, will be discussed.

5.3.1 The impact of estimation methods on Phase II performance

In various applications, there is a common assumption that process parameters are known, but this isn't always the case. In such instances, parameter estimation becomes necessary, utilizing in – control data collected during Phase I. The study of Ghasemi Eshkaftaki et al. (2021) aims to assess the impact of parameter estimation during Phase I analysis on the effectiveness of control charts in Phase II, specifically focusing on polynomial profiles, an area not extensively explored previously. Furthermore, the investigation delves into the influence of sample size in Phase I parameter estimation on the performance of Phase II methods and the study seeks to identify optimal methods for parameter estimation in Phase I for polynomial profiles, aiming to enhance the overall performance of Phase II control charts. Therefore, initially, the two estimation approaches that will be used for monitoring polynomial profiles during Phase I will be briefly given below. The choice of two estimation methods, namely F and T^2 approaches, stems from their demonstrated superior performance compared to alternative methods and are defined as follows:

- The F approach introduced by Kazemzadeh et al. (2008) for polynomial profiles Phase I monitoring, the idea is based on the fact that all m samples, each having n_j size, merge into a common sample size $N = \sum_{j=1}^{m} n_j$ and the model based on Eq. (5.2) is converted as follows:

  $y_{ij} = \beta_{0j} + \beta_{1j}x_{ij} + \beta_{2j}x_{ij}^2 + \ldots + \beta_{pj}x_{ij}^p + \varepsilon_{ij}$, $i = 1, \ldots, n_j \quad j = 1, \ldots, m$ (5.18).

  Therefore, based on the transformed model, the statistic used for the F approach is of the form:

  $$F_j = [((n_j - p - 1)MSE_j / \sigma^2(n_j - p - 1)] / \sum_{i \neq j}^{m}(n_j - p - 1)MSE_j / \sigma^2 \sum_{i \neq j}^{m}(n_j - p - 1), \quad (5.19)$$

  where MSE_j represents the mean square error for the j^{th} profile.
- The T^2 approach was introduced by Kazemzadeh et al. (2008) for polynomial profiles Phase I monitoring, is based on the polynomial model of Eq. (5.2) and the statistical of the method is of the form:

  $$T_j^2 = (\hat{\beta}_J - \bar{\hat{\beta}})' \, \widehat{\Sigma^{-1}} \, (\hat{\beta}_J - \bar{\hat{\beta}}), \quad (5.20)$$

  where $\hat{\beta}_J$ represents the vector of the estimated parameters for the j^{th}

profile, $\bar{\hat{\beta}}$ is the average mean of $\hat{\beta}_j$ and $\hat{\Sigma}$ is the estimated covariance matrix.

After assessing the parameters of the model in Phase I, it is the turn to monitor the stability of the model over time and the ability to detect any shifts in the profile parameters in Phase II. Therefore, the methods to be used in Phase II analysis are the following: a) MEWMA method, which was discussed earlier in this chapter, b) Ortho method, which was also mentioned earlier, and c) the double EWMA based on orthogonal model (dEWMA-OR) approach, which is briefly described below.

- The dEWMA-OR method introduced by Shamma et al. (1991), is based on the orthogonal model of Eq. (5.12), each parameter of the model is monitored by a separate control chart and so, the dEWMA-OR statistics for monitoring regression coefficients and error variance, respectively, are defined as:

  $$dEWMA\text{-}OR(j) = \lambda EWMA(j) + (1-\lambda)dEWMA\text{-}OR(j-1), \quad (5.21)$$

  $$dEWMA\text{-}OR^{*}(j) = max\{\lambda EWMA^{*}(j) + (1-\lambda)dEWMA\text{-}OR^{*}(j), 0\}, \quad (5.22)$$

  with $EWMA(j) = \lambda b_{lj} + (1-\lambda)EWMA(j-1)$, $dEWMA\text{-}OR(0) = b_l$, $EWMA(0) = b_1$, $EWMA^{*}(j) = \lambda(MSE_j-1) + (1-\lambda)EWMA^{*}(j-1)$, where MSE_j represents the mean square error for the j^{th} profile, λ $(0 < \lambda < 1)$ is the smoothing constant parameter and b_{lj}, $l = 1, 2, \ldots, p$, are the in – control regression parameters for the j^{th} profile.

The conclusions obtained through a Monte Carlo simulation study using a second-order polynomial model, where the results are obtained with the help of average run length (ARL), standard deviation run length (SDRL), average ARL (AARL) and standard deviation ARL (SDARL) performance criteria, are the following:

- When the parameters of the polynomial model are estimated with either the F or T^2 methods, then according to the AARL criterion the MEWMA approach performs better than the other methods under study.
- According to the SDARL metric, estimating the profile parameters with the F approach in Phase I we observe that the Ortho method shows the best performance for any number of samples (m). Furthermore, dEWMA-OR method also has good performance, like that of Ortho.

However, when the T^2 approach is used to assess parameters, then the MEWMA control chart shows the best performance and effectiveness.

- It was observed that as the number of samples used in the study increases, the in – control ARL and AARL values increase, while the in-control SDARL values decrease. This results from the fact that, as we consider more samples, then the estimation error decreases and thus, the in – control ARL and AARL values approach their specified value (usually the value is 200).
- In general, the accuracy of Phase II monitoring greatly depends on the initial parameter estimation in Phase I. Additionally, when using the estimated parameters, the ARL values under in – control conditions are consistently lower than the ARL values based on known parameters. Therefore, employing estimated parameters not only influences the performance under in – control conditions but also exerts significant effects on the ARL and SDRL performance in out – of – control scenarios across the methods.
- In Phase II analysis, when the number of samples tend to infinity, i.e., the profiles parameters are known, then for small shifts in the profile intercept the dEWMA-OR chart performs better than the other control charts under ARL metric, while for moderate and large changes in the intercept it was observed that the Ortho method has smaller ARL values and thus, is considered more effective. However, according to the SDRL criterion, the dEWMA-OR chart shows better results for detecting a shift than the other charts.
- When profile parameters are estimated using the F method in Phase I, then for small shifts in the profile intercept in Phase II the dEWMA-OR chart shows better results for any m, in terms of ARL and SDRL metrics. On the other hand, for larger changes in the profile intercept, greater effectiveness is noted by the Ortho approach.
- When the estimates of profile parameters are made with the T^2 method in Phase I, then for small shifts in the profile intercept in Phase II and small or moderate number of samples the MEWMA chart shows better results while for large m the Ortho approach has better results, in terms of ARL metric. Moreover, for moderate and large changes in the

intercept the MEWMA method outperforms in relation to the other methods. Finally, based on SDRL metric, for any sample size it was observed that MEWMA and dEWMA-OR control charts have the best performance for fast detection of a shift.

- In general, applying the F method for parameter estimation during Phase I typically leads to enhanced performance of charts during Phase II.
- In Phase II analysis, when the number of samples tend to infinity, i.e., the profiles parameters are known, then for moderate and large shifts in the standard deviation the Ortho chart performs better than the other control charts under ARL metric, while for small changes in the standard deviation it was observed that the dEWMA-OR method has smaller ARL values and thus, is considered more effective. However, according to the SDRL criterion, the dEWMA-OR chart shows better results for detecting a shift than the rest of the charts and so, this chart has the best performance.
- For any number of samples m and for any estimation method in Phase I, the dEWMA-OR chart is characterized as the best control chart for detecting small shifts in the profile standard deviation, while for larger changes the Ortho chart shows better results.
- In general, ARL and SDRL values derived from the F estimation method are consistently lower than those obtained through the T^2 method. Consequently, it is highly advisable to select the F method when estimating parameters during Phase I, particularly when the profile parameters are unknown.

5.3.2 The effect of measurement errors on Phase II performance

Control charts for profile models assume data accuracy, but this is rare in manufacturing and service settings due to measurement errors. A recent study, introduced by Liu et al. (2023), explores how neglecting these errors affects monitoring control charts, and specifically, it focuses on examining the following well-known charts: a) the double multivariate exponentially weighted moving average (dMEWMA) control chart, proposed by Alkahtani and Schaffer (2012) to monitor polynomial profiles during Phase II, b) the

multivariate cumulative sum (MCUSUM) control chart, introduced by Crosier (1988) to identify shifts in the polynomial profile parameters, c) the multivariate exponentially weighted moving average (MEWMA) control chart, which was introduced by Lowry et al. (1992) to monitor any change in the regression parameters of a polynomial model, and d) the Hotelling´s T^2 control chart, which was introduced by Kang and Albin (2000) to monitor simple linear profiles and then extended its formula for polynomial profiles by other researchers. Below are briefly given the charting statistics of the control charts mentioned above.

- The dMEWMA charting statistic for the j^{th} profile, based on the polynomial model of Eq. (5.2), it has the following form:
  $$dMEWMA_j = d_j' \, \Sigma^{-1} \, d_j, \tag{5.23}$$
  with $d_j = \lambda z_j + (1 - \lambda) d_{j-1}$, where λ ($0 < \lambda < 1$) is the smoothing parameter, $z_j = \lambda(\widehat{\beta}_J - \beta) + (1 - \lambda) z_{j-1}$, $\widehat{\beta}_J$ represents the vector of the ordinary least square estimated parameters for the j^{th} profile, β is the in – control regression parameters, Σ represents the variance – covariance matrix of d_j and $z_0 = d_0 = 0$.
- The MCUSUM charting statistic for the j^{th} profile, based on the polynomial model of Eq. (5.2), it has the following form:
  $$If \; c_j > c \; then \; s_j = (s_{j-1} + \widehat{\beta}_J - \beta)(1 - c/c_j), \; else \; s_j = 0, \tag{5.24}$$
  with $c_j = [(s_{j-1} + \widehat{\beta}_J - \beta)' \, \widehat{\Sigma^{-1}} \, (s_{j-1} + \widehat{\beta}_J - \beta)]^{1/2}$, where $s_0 = 0$ and c represents a constant value.
- The MEWMA charting statistic for the j^{th} profile, based on the polynomial model of Eq. (5.2), it has the following form:
  $$MEWMA_j = w_j' \, \Sigma^{-1} \, w_j, \tag{5.25}$$
  with $w_j = \lambda(\widehat{\beta}_J - \beta) + (1 - \lambda) w_{j-1}$, where $w_0 = 0$.
- The Hotelling´s T^2 charting statistic for the j^{th} profile, based on the polynomial model of Eq. (5.2), it has the following form:
  $$T_j^2 = (\widehat{\beta}_J - \beta)' \, \widehat{\Sigma^{-1}} \, (\widehat{\beta}_J - \beta), \tag{5.26}$$

In real-world scenarios, obtaining precise observations is often challenging due to the presence of measurement errors. Consequently, an error-prone variable, denoted as ξ, is observed and utilized instead of the true variable x. It is

assumed that the connection between the variable x and the observed variable ξ can be captured by the model:

$$\xi = x + u, \tag{5.27}$$

For this reason, the polynomial model used to account for the measurement errors is transformed into the form:

$$y_{ij} = \beta_0 + \beta_1 x_i + \beta_2 x_i^2 + \ldots + \beta_p x_i^p + \varepsilon_{ij}, \; with \; \xi_{ij} = x_{ij} + u_{ij}, \tag{5.28}$$

where the errors u_{ij} and ε_{ij} are independent.

Through a simulation study, the conclusions regarding the effect of measurement errors on the performance of the examined control charts, in terms of ARL, were the following:

- The influence of measurements errors on the in – control ARL values show that, as the standard deviation of measurement errors increases, there is a corresponding rise in the false-alarm rate. Moreover, the detection capability of each chart remains nearly unchanged despite variations in sample size (n).
- The influence of measurements errors on the out – of – control ARL values show that, in the presence of measurement errors, all the above control charts have a delay in indicating an alarm compared to scenarios where measurement errors are absent.

The above conclusions reveal a negative impact on control chart performance, which may be due to the fact that, when the measurement errors exist then the vector of the estimated regression parameters for the j^{th} profile, i.e., the $\widehat{\beta_J}$, is biased. To address this problem, Liu et al. (2023) used: a) the adjusted least square (ALS) estimators, introduced by Cheng and Schneeweiss (1998), the idea is based on finding unbiased estimates t_{ij} of x_{ij} and replacement of x_{ij} by t_{ij}, but with the limitation that the ALS estimator, denoted as $\widehat{\beta_A}$, is unstable for small or moderate samples and b) the modified adjusted least square (MALS) estimators, denoted as $\widehat{\beta_M}$, introduced by Cheng et al. (2000), have the same asymptotic properties as the $\widehat{\beta_A}$ and are suitable for both small and moderate samples and larger sample sizes. Thus, the above estimators were used for control charts reconstruction, where the ordinary least square estimator, $\widehat{\beta_J}$, was

replaced with $\widehat{\beta_A}$ or $\widehat{\beta_M}$. The conclusions for the performance of reconstructed charts obtained through a simulation study, using a second-order polynomial model, where the results are obtained with the help of average run length (ARL) performance criterion, are the following:

- The control charts based on MALS demonstrate superior performance compared to those based on ALS. This different becomes more pronounced as the magnitude of measurement errors increases.
- For shifts in the profile intercept and first slope, the dMEWMA and MCUSUM charts show the best returns for any value in measurement error standard deviation.
- For shift in the second slope, it was observed that the dMEWMA chart is more efficient than the other control charts under review.
- In general, the dMEWMA and MCUSUM control charts show better results for changes in the profile parameters than MEWMA, which in turn performs better than Hotelling's T^2 chart, for various values of the measurement error standard deviation (σ_u).
- For shifts in the standard deviation, the T^2 control chart has the best performance for $\sigma_u \leq 0.2$, while for $\sigma_u > 0.2$ the MEWMA chart performs better and more efficiently.

Based on the above conclusions, it is understood that the reconstructed charts remain affected by measurement errors. For this reason, the following two solutions have been proposed: a) a multiple measurement approach, and b) increasing sample size, aiming to minimize the impact of measurement errors. Please note that, adopting multiple measurements for each sample point has the potential to decrease the variance of the error component. However, this comes at the expense of higher measurement costs and additional time. Conversely, an augmentation in the sample size results in a reduction of the variance in the monitoring statistic. Finally, the conclusion that emerges from this study, which focuses on MALS-based charts through a simulation study, particularly the dMEWMA-MALS scheme is the following:

- In the multiple measurement approach, employing eleven (11) measurements per observation effectively addresses measurement errors

when monitoring process parameters. Moreover, it was observed that, the ARL values are smaller than those without errors, indicating faster alarms on detecting shifts in the regression parameters. Furthermore, increasing sample size enhances the dMEWMA–MALS chart's ability to detect regression parameters. However, for shifts in profile variance, the proposed remedial approaches prove ineffective in monitoring profile error variance.

5.3.3 The impact of a practical application on the profile monitoring

Netshiozwi et al. (2023), motivated by the fact that most profiling research focuses mainly on constructing various new theories, approaches, control charts and assumptions, focused on the lack of practical application of the above concepts and wanted to provide an answer by proposing the direction of attention to real applications of profile monitoring. Therefore, they introduce a monitoring framework that adopts a data-driven approach to oversee the internet usage of a telecommunications company. This framework is based on the polynomial model of Eq. (5.2), where the explanatory variables represent hours, i.e., $x_i = 1, 2, \ldots, 24$, and response variables, y_{ij}, represent the usage of internet in a specific hour. Notably, there appears to be a lack of research addressing the tangible application of polynomial profiles, as far as the researchers are aware.

In general, in certain companies such as telecom company, the purchasing patterns, product consumption, or other quality characteristics exhibit variations at different hours throughout the day. These fluctuations can carry significant consequences for the overall performance of the company. Therefore, the proposed framework aims to enable the daily monitoring of internet usage, facilitating the detection of any abnormal trends or patterns and includes the following five (5) stages:

- Model estimation. At this initial stage, the polynomial model is adjusted and estimated, and then residuals for each profile are calculated.
- Model verification. As a next step, the basic assumptions that the model should meet are tested. Specifically, the assumption of normality is

tested through the Kolmogorov – Smirnov test, the equality of variances between the profiles is checked using the Levene test and, finally, the existence of within or/and between profile autocorrelation is checked. Note that, in cases where the assumption of normality or equality of variances are violated, then an appropriate transformation of the response variables is applied, while for the existence of autocorrelation the use of a linear mixed model is recommended.

- Phase I analysis. During this step the outliers are removed until all the profiles are in an in – control situation and the profile parameters are estimated.
- Phase II analysis. In this step, the charting statistics that each researcher will use are calculated (here, the well-known T^2 and MEWMA control charts are applied) as well as the corresponding control limits. Finally, the stability of the model is checked over time in such a way that if the statistics are outside the control limits, then an alarm will be noted for a possible out – of – control situation, while if it is within the limits then the process is in – control and there is not any problem.
- Signal interpretation. As a final step, the researcher should interpret the signal and find related assignable causes.

The conclusions on the three most popular challenges faced by most companies are conducted through a simulation study and are the following:

- For the evaluation of irregular patterns in internet usage, it was observed that, while there is no autocorrelation and equality of variances applies, the assumption of normality is violated. For this reason, the response variables are transformed appropriately. Furthermore, during Phase I analysis, two outliers were found, which were removed from the data, and it took three iterations to bring the process to an in-control state. Finally, for its ability to detect shifts in the profile parameters during Phase II, the T^2 chart performed quite poorly, especially in detecting small changes. In contrast, the MEWMA chart proved significantly superior to the T^2 control chart, demonstrating in enhanced capability to identify even minor shifts.

- To assess the impact of discount policy, where the aim is to find how and when the proposed scheme identifies the increase in hours of internet use when there are discounts for specific hours, it was observed that while equality of variances applies, there is nonnormality and between-profile autocorrelation. Moreover, the T^2 control charts demonstrated superior performance by quickly detecting the out-of-control situation on the first day of the discount, whereas the MEWMA chart required two days to signal. This suggests that a significant shift in profile parameters occurred after the commencement of the discount, with the T^2 control chart, which is more sensitive to early detection, exhibiting earlier detection capability.
- To evaluate general fluctuations in social behavior, which may be viewed as reflective of customer requirements, it was observed that there is no autocorrelated data and it took two iterations to put the process into an in-control condition during Phase I analysis. Finally, for Phase II analysis, both proposed control charts can detect a change soon, but it was observed that the MEWMA chart takes a little longer to return to an in-control situation.
- In general, through this practical application it was realized that, with appropriate configurations, adjustments and using the five steps of the proposed framework, companies can rapidly identify abnormal situations in order to make appropriate solutions.

CHAPTER 6

Nonparametric profiles

Introduction

The nonparametric profile comes into play when the data lacks adherence to a specific assumed parametric structure, when there are inaccuracies in the specification of the parametric model, and when identifying the correct parametric form poses challenges. In such instances, where the underlying data distribution cannot be reliably characterized by a predetermined mathematical model, the nonparametric profile proves instrumental. It serves as an effective approach for situations where the assumptions or specifications of parametric models are either inappropriate or hard to ascertain. Therefore, the nonparametric model is described below.

Considering $\{(x_{ij}, y_{ij})$: i = 1, 2, …, n_j and j = 1, 2, … $\}$ as the j^{th} random sample, where y_{ij} be the measurement of the i^{th} observations in the j^{th} profile and x_{ij} represents the vector of corresponding explanatory variables. When the process is in an in – control situation, the nonparametric model is of the form:

$$y_{ij} = f(x_{ij}) + \varepsilon_{ij}, \quad (6.1)$$

where f represents an in – control regression function and ε_{ij} are the error terms, which are independent and identically distributed with a normal distribution, i.e., $\varepsilon_{ij} \sim N(0, \sigma^2)$ and represents the random noise associated with the process.

In cases where the values of explanatory variables are fixed for different j's and each profile includes the same number of observations, then Eq. (6.1) is transformed as follows:

$$y_{ij} = f(x_i) + \varepsilon_{ij}, \; i = 1, 2, \ldots, n \quad j = 1, 2, \ldots \quad (6.2).$$

Table 6_1 briefly mentions previous research conducted to monitor nonparametric profiles over a decade from 2008 to 2018. More specifically, lists the researchers, whether the expert study concerned Phase I or Phase II of

the profile, and the criterion for measuring the performance of the control charts used.

Research	Phase I	Phase II	Performance criterion
Zou et al. (2009)	-	Yes	ARL & SDRL
Qiu and Zou (2010)	-	Yes	ARL & SDRL
Qiu et al. (2010)	-	Yes	ARL & SDRL
Hung et al. (2012)	Yes	Yes	Type I and II errors
Chuang et al. (2013)	Yes	Yes	ARL, SDRL & ATS
Chen et al. (2015a)	Yes	-	Correct classification, signal probability
Colosimo et al. (2015)	-	Yes	ARL, SDARL, Type II error
Yang et al. (2017)	-	Yes	ARL, SDRL, median, quartiles, False alarm rate

Table 6_1. A brief overview of methods developed to monitor nonparametric profiles from 2008 to 2018. (Adapted from Maleki, M. R., Amiri, A., & Castagliola, P. (2018)).

The continuation of this chapter is intended to bring together some recent developments for monitoring nonparametric profiles. Therefore, since after the remarkable review papers of Woodall (2007) and Maleki et al. (2018) there is no newer paper that includes methods for profile monitoring from 2018 until today, the continuation of the chapter comes to fill this scientific gap regarding nonparametric profiles.

6.1 Change point detection approaches

In this section, two methods will be presented, which refer to the monitoring of nonlinear nonparametric profiles and aim at change point detection. More specifically, in the first place, the study by Li et al. (2019), which focuses on nonparametric profile monitoring using a nonparametric exponentially weighted moving average (EWMA) control chart in order to identify process shifts in Phase II monitoring, specifically designed for nonlinear profile data, will be discussed. Then, this section will close by presenting the study by Iguchi et al. (2021), who suggested a nonparametric approach employing a single index model (SIM).

6.1.1 Advanced nonlinear profiling using support vector regression

In practical scenarios, the functional relationship within profile data seldom arises to a linear form, and real-world data often deviates from a normal distribution. Consequently, to accurately capture the nature of profile data, Li et al. (2019) developed a nonparametric regression model. Furthermore, a nonparametric rank-based exponentially weighted moving average (EWMA) control chart is devised to effectively identify process shifts in Phase II monitoring, particularly tailored for nonlinear profile data.

The initial step involves applying a support vector regression (SVR) model to effectively smooth the nonlinear data, thereby eliminating any noise present in the data set. More specifically, in the SVR method, the explanatory variables, x, undergo a mapping onto a feature space, where a linear model is then constructed. Therefore, the linear model in this feature space is defined as follows:

$$g(x, w) = w' \varphi(x) + b, \tag{6.3}$$

where w represents a normal vector, $\varphi(\cdot)$ is a nonlinear function and b represents the bias term.

Assuming that during Phase I there are (g – 1) in – control profiles, the SVR model turns into a minimization problem as:

$$min \frac{1}{2} \|w\|^2 + C\sum_{i=1}^{n}(\xi_i + \xi_i^*), \; i = 1, 2, \ldots, n \quad j = 1, 2, \ldots, (g-1) \tag{6.4}$$

with $y_{ij} - g(x_i, w) \leq \varepsilon + \xi_i$, $g(x_i, w) - y_{ij} \leq \varepsilon + \xi_i^*$ and $\xi_i, \xi_i^* \geq 0$, where ε ($\varepsilon>0$)

is a threshold, C (C>0) represents a constant to control overfitting and ξ_i, ξ_i^* are the slack variables.

Based on the model of Eq. (6.4) it follows that the reference profile for the i^{th} observation is of the form:

$$\tilde{y}_i = \sum_{j=1}^{g-1} \dot{y}_{iJ} / (g - 1), \quad (6.5)$$

where $\dot{y}_{iJ}$ represents the predicted value for y_{ij}.

Having the above information, the five metrics, introduced by Williams et al. (2007), are derived as follow:

$$M_{j,1}^* = sign(\max_{i=1,\dots,n} \{|\dot{y}_{iJ} - \tilde{y}_i|\}), \ j = 1, 2, \dots, (g - 1) \quad (6.6)$$

$$M_{j,2}^* = \sum_{i=1}^{n} |\dot{y}_{iJ} - \tilde{y}_i|, \ j = 1, 2, \dots, (g - 1) \quad (6.7)$$

$$M_{j,3}^* = (1 / n) \sum_{i=1}^{n} |\dot{y}_{iJ} - \tilde{y}_i|, \ j = 1, 2, \dots, (g - 1) \quad (6.8)$$

$$M_{j,4}^* = |M_{j,1}^*|, \ j = 1, 2, \dots, (g - 1) \quad (6.9)$$

$$M_{j,5}^* = \sum_{i=1}^{n} |\dot{y}_{iJ} - \tilde{y}_i|^2, \ j = 1, 2, \dots, (g - 1) \quad (6.10)$$

where M_1, M_2, M_3, M_4 and M_5 represent the maximum deviation, the sum of absolute deviations, the mean absolute deviation, the absolute value of maximum deviation and the sum of squared differences between the predicted values for the measurement y_{ij} and the corresponding baseline profiles, respectively.

Finally, to monitor the quality characteristic of the nonlinear profile data, a nonparametric rank-based exponentially weighted moving average (EWMA) control chart incorporating these five metrics is employed. Therefore, the proposed nonparametric EWMA charting statistic is defined as follows:

$$EWMA_{j,p} = (1 - \lambda) EWMA_{j-1,p} + \lambda R_{j,p}, \ j = 1, 2, \dots \quad (6.11)$$

where λ ($0 < \lambda < 1$) is the smoothing parameter, $EWMA_{0,p} = 0$ and $R_{j,p}$ represents the standardized rank of the metrics $\{M_{1,p}^*, M_{2,p}^*, \dots, M_{g-1,p}^*\}$ with p = 1, 2, 3, 4, 5.

A simulation study was used to conduct the conclusions, where the in-control nonlinear model used follows an exponential form:

$$y_{ij} = 0.9 \exp(\beta_0 + \beta_1 x_{ij}) + \varepsilon_{ij}, \quad (6.12).$$

Therefore, the results obtained were based on two possible scenarios, a) the error terms follow a standard normal distribution, or b) the error terms follow an exponential distribution with parameter $\theta = 0.5$, and are the following:

- As the smoothing parameter increases, the ARL values become larger, so detecting a change in the profile parameters is slower. In contrast, the proposed nonparametric EWMA control chart is more effective as shift values increase.
- Based on the ARL criterion, the performance of the EWMA chart with metrics M_1 and M_4 is worse than that of metrics M_2, M_3 and M_5, probably because M_1 and M_4 do not use all the information in the data set. Note that the returns of the EWMA control charts with the metrics M_2 and M_3, respectively, they are the same.
- When the error terms follow an exponential distribution, then the EWMA charts with metrics M_2, M_3 and M_5 perform similarly for any size shift in parameters.

6.1.2 Nonlinear profile monitoring through single index models

In a Single Index Model (SIM), the assumption is that the connection between the expected response and a d-dimensional explanatory variable is expressed by a univariate function g, known as the link function. This link function's argument, referred to as the index, is a linear combination of the predictor vector x. Rather than monitoring the function of the fitted response directly, Iguchi et al. (2021) proposed a new method, which monitors a statistic based on the vector of coefficients, known as index parameters. These index parameters are employed to define the index within the SIM. Therefore, in their nonparametric approach using the SIM, the focus is shifted from monitoring the profile itself for a change to monitoring an l_2-based statistic on the coefficients generated by the SIM.

First, based on the nonparametric model of Eq. (6.2), a single index model can be represented in the following form:

$$y_i = g(x_i'\alpha) + \varepsilon_i,\ i = 1, 2, \ldots, n \qquad (6.13)$$

where $g(\cdot)$ is a smooth function, α represents an unknown object for which it is true that $E(y|x) = E(y|\alpha' x)$ and ε_i represent the error terms.

Having briefly mentioned the form of a SIM, the next step is to transform the nonparametric model of Eq. (6.2) into a model with discretely sampled functions, i.e., discretely profiles. Therefore, as the objectives of the research

include determining whether the process is in – control during the time periods t = 1, 2, ..., T, the nonparametric model of Eq. (6.2) is transformed as follows:

$$y_i^t = f^0(x_i^t) + \varphi(x_i^t)\, I(t \geq \tau) + \varepsilon_i^t, \quad (6.14)$$

with $\varepsilon_i^t \sim N(0, \sigma_\varepsilon^2)$, where y_i^t is the vector of a profile at time t, $f^0(x_i^t)$ represents the relationship between the explanatory and response variables when the process is in – control, $\varphi(\cdot)$ represents an unidentified functional change that occurs when the process deviates from its in-control state and $\tau \in \{1, 2, \ldots, T\}$ represents the time of the first out – of – control profile.

Using the above information, Iguchi et al. (2021) defined charting statistic for the change point detection in the following form:

$$\max_{t \in \{k,..,T\}} \left\| a^t - \frac{\overline{\alpha_T^0}}{\left\| \overline{\alpha_T^0} \right\|} \right\|, \quad (6.15)$$

where k (k>0) represents the starting point of the observation period under consideration in such a way that if for some k>0 the condition $\max_{t \in \{k,..,T\}} \left\| a^t - \overline{\alpha_T^0} \right\|$ holds true, then the claim is made hat a change point has occurred by time T, $\| . \|$ represents the l_2 – norm, α^t is the index parameter at time t (t>0) and $\overline{\alpha_T^0}$ represents the bootstrapped index parameter for the in – control profiles at time T.

Of particular interest is the fact that this study compares the performance of the proposed method by Iguchi et al. (2021) with a method, which is similar to the one examined but with the difference that a linear model is used instead of a SIM. Finally, the proposed method is also compared to the method by Li et al. (2019) and, specifically, to M_2, M_3 and M_5 metrics, which described in subsection 6.1.1.

The conclusions on the performance of the methods were made with the help of the average run length (ARL) criterion and are as follows:

- The proposed method consistently exhibits the smaller ARL values across all conditions. Moreover, it generally maintains comparable false alarm rates when compared to the detectors introduced by Li et al. (2019). Therefore, it is observed that the proposed method of Iguchi et al. (2021) shows better results regarding performance and ability to detect a change during Phase II analysis.

- An important piece of information we get from this research is that the detector employing the linear model failed to identify a change point even after observing $T = 10^4$ profiles. Furthermore, for the method of Li et al. (2019) it was observed that the average run time for detecting a change was on the order of 10^{-3} seconds, while the remarkable performance of proposed method is achieved at the expense of increased computation time.
- In general, despite being characterized by its speed, the performance of the Li et al. (2019) detectors demonstrated a relatively consistent pattern across various signal-to-noise conditions. This stability is attributed to the inherent characteristics of their rank-based methodology. On the other hand, the new proposed method preserves information about the difference between an observed profile and the historical profile by avoiding the need for ranking summary statistics for each profile. Therefore, the proposed approach, which gives a non–rank-based monitoring procedure, demonstrates superior performance compared to other change-point detection approaches. Finally, it excels in quickly and uniformly detecting changes from the in – control profile, all the while maintaining a minimal false alarm rate.

6.2 Correlation in profile monitoring methods

In this section we will present two methods, which use correlated data to monitor nonparametric profiles. Initially, we will discuss the study by Zhou and Qiu (2022), who proposed a new mixed – effects model designed to describe serially correlated univariate profile data and then, the study by Ding et al. (2024), who proposed real-time nonparametric monitoring schemes considering covariates to monitor correlated profiles will be discussed.

6.2.1 A study based on serially correlated nonparametric profiles

Addressing serial data correlation among profiles observed at different time points is a notably challenging task in profile monitoring research. This aspect has not been adequately addressed in the statistical process control literature. Serial data correlation is a prevalent occurrence in practical scenarios, and

existing literature highlights that control charts become unreliable when serial data correlation is disregarded. For this reason, Zhou and Qiu (2022) proposed a novel mixed – effects model designed to capture serial correlation in univariate profile data and, building upon this model, they developed a Phase I nonparametric profile monitoring chart. Therefore, below will be given the new mixed – effects model, which describes nonparametric univariate profiles, incorporating both within – profile and between – profile data correlation. Thus, based on the simple nonparametric model of Eq. (6.1), the new model is as follows:

$$y_{ij} = f(x_{ij}) + \xi_j + \gamma(x_{ij}) + \varepsilon_{ij},\ i = 1, 2, \ldots, n_j,\ \ j = 1, 2, \ldots, m \qquad (6.16)$$

where y_{ij} be the measurement of the i^{th} observations in the j^{th} profile, $x_{ij}\epsilon[0, 1]$ represents the vector of corresponding explanatory variables, ξ_j represents a random – effects term to characterize the variation of the j^{th} profile from the population mean profile function f(x) and used to describe within – profile data correlation, $\gamma(x_{ij})$ represents a random – effects term which used to describe between – profile data correlation and ε_{ij} is the error term. Please note that, ξ_j, $\gamma(x_{ij})$ and ε_{ij} are independent of each other and follow a normal distribution, i.e, $\xi_j \sim N(0, \sigma_\xi^2)$, $\gamma(x_{ij}) \sim N(0, \sigma_\gamma^2)$ and $\varepsilon_{ij} \sim N(0, \sigma_\varepsilon^2)$.

In the above model, the design points $\{x_{ij}\}$ are permitted to vary across all m profiles. Consequently, the set of all design points could encompass numerous distinct values. In the extreme scenario where no two of the design points in the set $\{x_{ij},\ i = 1, 2, \ldots, n_j,\ \ j = 1, 2, \ldots, m\}$ are identical, the count of random – effect terms in $\{\gamma(x_{ij})\}$ would be equivalent to the total number of observations. Therefore, the model in Eq. (6.16) is deemed inestimable and so, can be approximated by:

$$y_{ij} = f(x_{ij}) + \xi_j + \eta_q + \varepsilon_{ij},\ q = 1, 2, \ldots, p,\ \ i = 1, 2, \ldots, n_j,\ \ j = 1, 2, \ldots, m \qquad (6.17)$$

with $x_{ij}\epsilon[d_{q-1}, d_q]$, $d_0 = 0$, $d_p = 1$, $d_q = q / p$, where p is the number of subintervals into which the initial interval of x_{ij} was divided, i.e., the interval [0, 1] and η_q represents the random – effect term when $x_{ij}\epsilon[d_{q-1}, d_q]$ and is based only on q. Please note that, ξ_j and η_q are independent, identically distributed and describe the within – profile and between – profile data correlation, respectively.

Finally, the control chart, which was designed to monitor Phase I, was based on the idea that, since the quantities $f(x_{ij})$ and η_q of the model of Eq. (6.17)

both depend on the design points x_{ij}, then it seems logical and appropriate to monitor the j^{th} profile to use the quantity $(1/n_j)\ \sum_{i=1}^{n_j}[y_{ij} - \widehat{f(x_{ij})} - \widehat{\eta_q}]^2$ instead of quantity $(1/n_j)\ \sum_{i=1}^{n_j}[y_{ij} - \widehat{f(x_{ij})}]^2$, where $\widehat{f(x_{ij})}$ and $\widehat{\eta_q}$ represent the estimates of $f(x_{ij})$ and η_q, respectively. The interested readers are referred to the comprehensive article for the detailed calculation of estimated parameters by Zhou and Qiu (2022). Therefore, charting statistic, which is used to quantify the discrepancy between the observed profile and the estimated profile, is called in the literature as TM because it indicates that the model in Eq. (6.17) has two mixed – effects terms and is defined as follows:

$$S_{TM} = \max_{j=1,..,m} (1/n_j) \sum_{i=1}^{n_j}[y_{ij} - \widehat{f(x_{ij})} - \widehat{\eta_q}]^2, \qquad (6.18).$$

Finally, the TM control chart gives a signal for an outlier profile when

$$S_{TM} > CL, \qquad (6.19)$$

where CL (CL>0) represents a control limit, which is specified via a bootstrap procedure.

To conduct the conclusions, Zhou and Qiu (2022) considered the following four cases for specifying the three random terms in model of Eq. (6.17). In the first case, within-profile data correlation is assumed, but there is no between-profile data correlation, in the second case addresses a scenario where within-profile data correlation is absent, but there is between-profile data correlation and, finally, the last two cases explore situations where both within-profile and between-profile data correlation exist, but the random variables have different distributions. Furthermore, for the in – control mean function f(x), they assume the following three situations: a) f(x) represents a linear profile, b) f(x) consists of the linear component as in the first case and a nonlinear component, and c) f(x) adds a quadratic term to the previous profile. Moreover, until now, no existing univariate nonparametric profile monitoring methods have been identified that can handle between-profile data correlation. However, there are already Phase II profile monitoring methods capable of accommodating within-profile data correlation. To compare their proposed method with existing approaches, the following three representative Phase II profile monitoring methods, which consider within-profile data correlation, are adapted for Phase I profile monitoring: a) the proposed method by Jensen et al. (2008), which is based on linear mixed – effects model and is use to monitoring linear profiles

with possible within-profile data correlation, b) the proposed approach by Zhang et al. (2014a), in which the within-profile correlation is addressed using the Gaussian process model and is use to monitoring linear profiles with possible within-profile data correlation, and c) the method by Qiu et al. (2010), which is based on nonparametric mixed – effects model and is use to monitoring nonparametric profiles with possible within-profile data correlation. Finally, the performance of the models used in this simulation study was measured in mean square error (MSE) terms and the in – control performance of the above charts measured with the help of false alarm rate (FAR). In evaluating the out – of – control performance of a Phase I control chart, Zhou and Qiu (2022) employed the following criteria: a) the alarm probability which denotes the percentage of simulations where the chart signals at least one profile as out – of – control, b) the fraction of correctly classified profiles which measures the accuracy in distinguishing between in – control and out – of – control profiles, and c) the false positive rate which quantifies the proportion of identified out – of – control profiles that are actually in – control.

Therefore, the results obtained were as follows:

- MSE values for estimating linear profile models are typically smaller than those for estimating nonlinear profile models. This discrepancy arises because nonlinear profile models are generally more challenging to estimate than their linear counterparts. As a result, the associated MSE values for estimating nonlinear profile models tend to be larger.
- MSE values tend to decrease as the number of profiles (m) increases.
- MSE values generally decrease with an increase in p because the model in Eq (6.34) approximates the model in Eq. (6.33). A larger p leads to a better approximation. However, choosing p to be excessively large can result in extensive computational requirements during the model estimation process.
- In cases where there is no between-profile data correlation, the actual in – control false alarm rate (FAR) values of the methods by Jensen et al. (2008), Zhang et al. (2014a) and Qiu et al. (2010) are reasonably close to the nominal in – control FAR value of $\alpha = 0.05$. However, when a significant between-profile data correlation is present, the actual in – control FAR values of the above methods deviate considerably from $\alpha =$

0.05. On the other hand, the actual in – control FAR values of TM approach are reasonably close to $\alpha = 0.05$ in all considered scenarios. Therefore, the proposed TM method exhibits reliable in – control performance, especially when substantial between-profile data correlation is present, while the three alternative methods may not be as reliable in such cases.

- In scenarios where there is no between-profile data correlation, all the methods perform almost the same. Furthermore, the new proposed TM outperforms the other approaches when there is a substantial between-profile data correlation. Moreover, it is worth noting that, the methods of Jensen et al. (2008), Zhang et al. (2014a) and Qiu et al. (2010) perform similarly for monitoring linear profiles, while for monitoring nonlinear profiles it was observed that the method of Qiu et al. (2010) outperforms the other two.
- In general, the proposed method TM demonstrates superior performance compared to other nonparametric profile monitoring methods, particularly in cases where there is between-profile data correlation.

6.2.2 Enhanced real-time monitoring with Gaussian process incorporating covariate information

In the rapidly development of technology and cyber manufacturing, sensors are increasingly utilized across industries, from manufacturing to services, to collect valuable information. Sensor data support the data collection for quality management and further analysis. The correlation often observed in sensor data at different times gave a concentrated interest in profiles. For this reason, adaptable and precise nonparametric profile models are essential to capture the intricacies of vast, complex, and correlated datasets. Gaussian processes, serving as a nonparametric technique and a machine learning method, have found applications in a wide array of profile monitoring scenarios. Moreover, another challenge is the fact that, many control charts focus only on monitoring quality variables without considering covariate information. Incorporating covariates into the process monitoring framework becomes crucial for enhancing accuracy and effectiveness. In profile monitoring, however, there's a notable dearth of studies that take covariate information into account.

Consequently, Ding et al. (2024) built on the above philosophy and wanted to find a solution to these challenges in the field of profiling. Therefore, they introduced profile monitoring schemes that integrate covariates for real-time process monitoring. Finally, the devised profile model addresses within-profile correlations through Gaussian process and effectively incorporates covariate information to account for its impact on the profile data.

Initially, a Gaussian process can be described as a collection of random variables, where the joint distribution of any finite subset follows a Gaussian distribution. Based on this and considering one covariate, Ding et at. (2022) defined the proposed nonparametric model as follows:

$$y_i = \alpha T_i + \beta + f(x) + \varepsilon, \quad i = 1, 2, \ldots, n \tag{6.20}$$

where $y_i = (y_{1i}, y_{2i}, \ldots, y_{mi})'$ represents the i^{th} profile, which is measured at the location $x = (x_1, x_2, \ldots, x_m)'$, $T_i = (T_1, T_2, \ldots, T_n)$ is the covariate, α, β are parameters of the covariate, ε represents the error term and $f(x)$ is a realization of the Gaussian process. Please note that, the error term is assumed to be independent with $f(x)$ and follows normal distribution, i.e., $\varepsilon \sim N(0, \sigma_\varepsilon^2)$.

Given a specific covariate T_i, the above in – control model predicts an expected profile, which is forecasted by the proposed model utilizing the estimated parameters, that is theoretically in – control. In detail, if an observed profile $y' = (y_1', y_2', \ldots, y_m')$ is associated with a covariate T, which is obtained from the real-time process, then, using the same covariate, the proposed model predicts an expected profile $y^* = (y_1^*, y_2^*, \ldots, y_m^*)$. Moreover, as the model is trained with samples from the in – control process, y^* is theoretically in – control. Therefore, the comparison between the observed profile y' and the expected profile y^* determines whether y' is in an in – control situation. Consequently, if the process goes out – of – control, the observed profile may significantly differ from the theoretically in – control expected profile, making the difference between the two profiles meaningful.

Two control statistics have been developed to measure the difference between observed and expected profiles and are the following:

- The Euclidian distance (ED) statistic measures the distance between the corresponding points of the two profiles, i.e., the observed profile y' and the expected profile y^*, and its formula is given by the following equality:

$$ED = \sqrt{\sum_{j=1}^{m}(y_j^{'} - y_j^{*})^2} \quad (6.21).$$

Note that, if the difference between the two profiles is significant then the value of ED statistic will be large.

- The Area statistic measures the difference between observed and expected profiles more accurately than ED statistic, as it calculates the region enclosed by the two profiles, and the formula can be expressed as follows:

$$Area = \int_{x_1}^{x_2} \left| y^{'} - y^{*} \right| \, dx, \quad (6.22)$$

where x_1 and x_2 are locations in which the two profiles have been measured.

Please note that, the value of the area changes with the difference between the expected and the observed profiles and the greater the difference, the higher the value Area statistic will take.

Ding et al. (2024) formulated the exponentially weighted moving average (EWMA) control charts with both ED and Area statistics. Thus, the standard form of the EWMA control chart for the i^{th} profile could be expressed as:

$$E_i = \lambda s_i + (1 - \lambda)E_{i-1}, \quad i = 1, 2, \ldots, n, \quad (6.23)$$

where λ ($0 < \lambda < 1$) represents the smoothing parameter, s_i is the control statistic (either the ED or the Area statistics) and E_0 is equal to the mean of s_i.

It is worth noting that, for $\lambda = 1$, the above EWMA becomes the Shewhart – type chart. Furthermore, this research compares the two proposed charting statistics with the Hotelling´s T^2 statistic. Therefore, the comparison, which is carried out through simulation studies, includes the three Shewhart – type statistics, i.e., ED, Area and Hotelling´s T^2, and the results, which are obtained with the help of ARL and SDRL performance criteria, are the following:

- For changes in the profile parameters, it was observed that the Area charting statistic performs slightly better than the ED, which in turn shows better results than the T^2 statistic.
- The Area charting statistic provides quicker signals as shifts become larger. This shows its ability to detect larger changes faster.

- In general, the two proposed charting statistics show lower ARL and SDRL values than the Hotelling´s T^2 and, so, they are judged more effective.
- Comparing ED and Area statistics with each other, it was found that the Area has smaller ARL and SDRL values than ED and thus shows better performance and is more efficient at quickly detecting shifts in the profile parameters. Therefore, the Area statistic is superior.
- Constructing the EWMA control chart with the Area statistic it was observed that for smaller values in the smoothing parameter λ the chart has the ability to detect small shifts faster, while for larger λ values it has better efficiency in larger changes. Note that similar conclusions are reached by constructing the EWMA control chart with the ED statistic.
- In general, the EWMA control chart, built with Area statistic, demonstrates greater sensitivity to process shifts. Utilizing the same smoothing parameters (λ), this chart shows smaller ARL and SDRL values than the EWMA control chart built with ED statistics. However, the last control chart is also effective in detecting shifts, and the ED statistic offers the advantage of being simpler and quicker to compute.

6.3 Approaches for monitoring both regression parameters and profile variance

In this section, recent studies will be discussed, which aim to monitor nonparametric profiles taking into account both regression parameters and profile variance. In the first place, we will develop the study by Abbasi et al. (2022), who proposed a new control chart for Phase II analysis, uniquely designed to monitor both regression parameters and profile variance, using an adaptive approach. This section will be closed analyzing the study by Yeganeh et al. (2022), who introduced an innovative ensemble framework designed to monitor shifts in both the regression relationship and variation of profiles for Phase II applications utilizing a pool of artificial neural networks (ANNs) as learners to augment the effectiveness of a base control chart.

6.3.1 An adaptive EWMA control chart

In a comprehensive sense, a control chart is considered adaptive if it involves the change in real time of chart´s parameters such as sample size, control limit coefficient, sample sampling. These adjustments are made based on estimations of the shifts that have occurred in the process. Building on this philosophy, Abbasi et al. (2022) introduced a new adaptive approach for nonparametric profile monitoring, filling a current research gap in adaptive control charts for Phase II statistical process control applications. The proposed approach aims to enhance the detection capability of nonparametric exponentially weighted moving average (NEWMA) chart statistics, as proposed by Zou et al. (2008), particularly in terms of the average run length (ARL) criterion.

First, the charting statistic defined by Zou et al. (2008) will be briefly given below and then, this idea will be used to structure the proposed approach of Abbasi et al. (2022). Therefore, based on the nonparametric model in Eq. (6.2), Zou et al. (2008) calculated the nonparametric EWMA charting statistic as follow:

$$E_j = \lambda U_j + (1 - \lambda)E_{j-1}, \tag{6.24}$$

with $U_j = (Z_j, \widetilde{\sigma}_j)'$, where $Z_j = (Y_j - F) / \sigma$, $Y_j = (y_{1j}, y_{2j}, \ldots, y_{nj})$, $F = (f(x_1), f(x_2), \ldots, f(x_n))$, σ is the standard deviation of ε_{ij}, $\widetilde{\sigma}_j$ represents the transformation of estimated $\widehat{\sigma_j^2}$ to a standard normal random variable, $E_0 = 0$ and λ $(0 < \lambda < 1)$ is the smoothing parameter.

Finally, the final form of NEWMA is given by positive chart statistic:

$$Q_j = E_j' \Sigma E_j, \tag{6.25}$$

where Σ represents the symmetric covariance matrix of U_j.

Note that, the statistic will give an out – of – control signal when

$$Q_j > L\,[\lambda / (2 - \lambda)], \tag{6.26}$$

where L is assigned based on a desired in – control ARL.

Now, the primary concept of Abbasi et al. (2022) involves introducing an adaptive approach that is formulated based on the tendency (relative distance) of obtained statistics to the out – of – control situations. This proposed tendency, or relative distance, is calculated by evaluating the ratio of the statistic's distance from the upper control limit (UCL) to the lower control limit (LCL). Thus, the tendency of the j^{th} sample, denoted as T_j, is defined as follows:

$$T_j = (UCL - Q_j) / (Q_j - LCL), \quad (6.27).$$

In nonparametric EWMA method, LCL is equal to zero. Therefore, the above form transforms to:

$$T_j = (UCL - Q_j) / Q_j, \quad (6.28).$$

It is worth noting that, a higher tendency is associated with lower charting statistics. Naturally, the average of tendencies decreases when an out – of – control situation is observed. It is therefore appropriate to define the average of tendencies and then, mapped to a specific rate for applying in an adaptive approach. Thus, the average of tendencies, denoted as T_j^*, is defined as follows:

$$T_j^* = (T_1 + T_2 + \ldots + T_j) / j, \quad (6.29).$$

Furthermore, the NEWMA statistic (Q_j) is increased when the tendency index (T_j) is decreased, while is decreased when T_j is increased. Thus, based on all the above information, the updating of the NEWMA statistic is done by using the tendency rate as follows:

$$Q_j^* = Q_j \times T_{rj}, \quad (6.30)$$

where T_{rj} represents the tendency rate.

It is worth noting that, to enhance the sensitivity of the control chart to out – of – control shifts, it is anticipated that T_{rj} should be less than 1 when T_j has a large value (indicative of an in – control situation). However, it is worth noting that, T_{rj} can be greater than 1 when T_j has a small value (indicating an out – of – control situation).

Interestingly, the proposed method was compared through simulation studies with other existing control charts. More specifically, these charts were the following: a) the nonparametric EWMA (NEWMA) chart, introduced by Zou et al. (2008) and discussed above, b) the naïve multivariate EWMA (NM) control chart, which treats Z_j as an extended multivariate vector and employs the MEWMA scheme to construct control chart, c) the EWMA_3 chart, which introduced by Zhang et al. (2014b), is a nonparametric extension of the well-known EWMA_3 control chart of Kim et al. (2003) developed in Chapter 1 and aims to address processes with different in – control and out – of – control characteristics, and d) the parametric MEWMA (PM), which was introduced by Zou et al. (2007) and involves obtaining parameter estimates for each profile and subsequently applying the multivariate exponentially weighted moving average (MEWMA) scheme for the transformation of these estimated

parameters. Finally, in these simulations, the robustness of the proposed scheme is demonstrated through the exploration of three different scenarios, each involving polynomial, exponential, and linear models. Therefore, the conclusions obtained through simulation studies, where the results are obtained with the help of average run length (ARL) performance criterion, are the following:

- In the scenario where polynomial profiles were employed, the proposed method proves effective for all shifts. Notably, the performance of the proposed method is roughly better, particularly for significant shifts in the process parameter, showcasing an advantage over competing methods. Furthermore, it was observed that, the NEWMA control chart has a faster ability to detect changes than NM and PM charts. Importantly, the degree of outperformance increases with the complexity of the out – of – control model.
- In the scenario where exponential profiles were employed, the proposed method shows the best performance, except in a few cases, where as the model becomes more complex the NEWMA approach was observed to perform similarly or slightly better.
- In the scenario where linear profiles were employed, where the proposed method compared with the EWMA_3 and NEWMA control charts, it was observed that, the proposed method demonstrated superior performance in detecting small shifts, while the NEWMA method yielded slightly better results for the detection of moderate and large shifts. As the proposed control chart naturally enhances the detection ability of NEWMA, it logically achieves the best overall performance for the detection of all shifts. Finally, the predictability of the superiority of NEWMA over EWMA_3 arises from the linear structure inherent in the EWMA_3 control chart.

6.3.2 An ensemble neural network framework

In practical applications, detecting out – of – control situations is crucial to prevent the production of non-compatible products, while from a theoretical part of view, achieving better performance criteria, such as a lower average run length (ARL_1), can offer valuable contributions. Yeganeh et al. (2022), based

on the above philosophy and, considering both the rapid development of technology and the competition that prevails between different industries and the quality of the products produced, proposed an ensemble framework based on artificial neural networks (ANNs) as a supplementary tool to enhance the sensitivity of a predetermined base control chart. This enhancement aims at improving the detection of out – of – control situations in the monitoring of nonparametric profiles during Phase II, which leads to better performance in industrial processes.

First, it is worth emphasizing that, to the best of the researchers' knowledge, this proposed method is the first attempt to introduce a novel ensemble framework designed for monitoring profiles with different in – control and out – of – control characteristics. Furthermore, the present study is based on the nonparametric model of Eq. (6.2) and uses the nonparametric exponentially weighted moving average (NEWMA) chart, introduced by Zou et al. (2008), described in subsection 6.3.1, the format of its charting statistic (Q_j) was given by Eq. (6.25) and is considered appropriate due to its capability in monitoring different types of shifts. Finally, it is stated that, the general idea of a neural network ensemble is to employs learning techniques, which involve combining the predictions of the multiple models to produce more accurate and precise results than what individual models can achieve. Therefore, utilizing the above information, below is briefly given the structure of the proposed ensemble-based ANN control chart, which is denoted by ensemble ANN with NEWMA (EANNN).

For the j^{th} profile, the first step involves calculating the statistic of the NEWMA chart (Q_j) and comparing it with its control limit, which is denoted by base control chart limit (BL). Thus, if $Q_j > BL$, the control chart triggers an out – of – control signal, while if $Q_j < BL$, indicating the in – control region, the EANNN is utilized to determine the process condition. Please note that, BL is always greater than $L[\lambda / (2 - \lambda)]$, which is the control limit of the NEWMA method, due to the incorporation of EANNN as a supplementary tool. Moreover, the next step is to divide the in – control area of the NEWMA chart, denoted as [0, BL], into k_t ($t = 1, 2, \ldots, N$) regions and then, the number of points in each is counted in the j^{th} profile. Determining an optimal number of regions is a challenging task, prompting the use of a neural network ensemble

to address this issue. This approach involves training N ANNs with varying input layer sizes based on different numbers of regions in the in – control region. An additional ANN, known as the incorporator, acts as a reasoning scheme to combine the predictions of the N trained ANNs and produce the outcome. In summary, the EANNN structure consists of N + 1 (N > 1) ANNs, with N ANNs incorporating specific features from the base control chart and the $(N + 1)^{th}$ ANN integrating the outputs of the N ANNs. Therefore, to simplify the design process and eliminate arbitrary decisions, the following formula is proposed to determine the size of the input layer for the learners:

$$k_t = 2t + 1, \text{ with } t = 1, 2, \ldots, N, \quad (6.31).$$

Finally, the output of the incorporator identifies the final process condition, i.e., if the output of the incorporator is greater than a predefined control limit, which is called cutting value (CV), then the proposed approach triggers an out – of – control signal, while if the output of the incorporator is smaller than CV, then the process is in an in – control situation.

Interestingly, the proposed EANNN chart was compared through simulation studies with other existing control charts. More specifically, these charts were the following: a) the nonparametric EWMA (NEWMA) chart, b) the naïve multivariate EWMA (NM) control chart, c) the parametric MEWMA (PM) chart and d) the nonparametric EWMA_3 control chart. Finally, in these simulations, the robustness of the proposed scheme is demonstrated through the exploration of three different scenarios, each involving polynomial, exponential, and linear models. Therefore, the conclusions obtained through Monte Carlo simulation studies, where the results are obtained with the help of average run length (ARL) performance criterion, are the following:

- In the scenario where polynomial profiles were employed, the EANNN control chart consistently outperforms the other methods, demonstrating notably superior performance for large shifts in the process parameter. For smaller shifts, EANNN yields comparable results to the NEWMA, NM and PM control charts. Furthermore, it was observed that, the NEWMA control chart has a faster ability to detect changes than NM and PM charts.
- In the scenario where exponential profiles were employed, the proposed method exhibits the smallest ARL values, which indicates its excellent

performance for any size of shift in the profile parameters. It was observed that the EANNN method performs better than the NEWMA approach, which in turn shows better ARL values than the NM method.

- In the scenario where linear profiles were employed, where the proposed method compared with the EWMA_3 and NEWMA control charts, it was observed that, the proposed method demonstrated superior performance in detecting changes in the profile parameters. Moreover, the expected superiority of NEWMA over EWMA_3 arises from the linear structure inherent in the EWMA_3 control chart. Therefore, as the proposed EANNN control chart naturally enhances the detection ability of NEWMA, it logically achieves the best overall performance for the detection of all shifts.
- Interested are the results obtained from the scenario where polynomial profiles were employed and PM was used as the base control chart instead of NEWMA. Through the simulation study, it was observed that the proposed ensemble framework could improve the performance of the NP chart in all shifts. Moreover, the model created using the NP as the base control chart can detect the negative shifts in variance, which the NP chart alone could not do. Based on this observation, it is concluded that, integrating the suggested ensemble framework with other base control charts has the potential to mitigate their inherent weaknesses. Despite this, EANNN still shows the best performance due to the superior performance of NEWMA compared to NM across all shifts.

6.4 Other techniques for monitoring nonparametric profiles

In this section we will talk about two different approaches, where the monitoring of nonparametric profiles occurs under a specific framework. In more detail, initially, we will refer to the study of Varbanov et al. (2019), who proposed a Bayesian method based on wavelets, utilizing inference derived from the posterior distribution of the change point and this approach avoids imposing restrictive assumptions on the profile´s form. Then, we will discuss the nonparametric nonlinear profile monitoring approach of Deng et al. (2022),

which has been adapted for machine condition monitoring (MCM) and aims at surveillance of the health condition of rotating machines.

6.4.1 Bayesian sequential monitoring of nonlinear profiles with wavelets

Nonparametric methods typically depend on the use of smoothing and dimension reduction tools. These tools play a crucial role in distinguishing signal from noise, allowing the computation of metrics that precisely measure the disparity between observed profiles and an in-control pattern. Therefore, the study by Varbanov et al. (2019) focuses on nonlinear profile monitoring during Phase II and identifying changes in the profile parameters in the presence of Gaussian white noise, using a wavelet-based Bayesian (WBB) method.

Initially, as the objectives of the research include determining whether the process is in-control during the time periods t = 1, 2, ..., T, the nonparametric model of Eq. (6.2) is transformed as follows:

$$y^t = f^0(x) + g(x)\, I(t \geq \tau) + \varepsilon^t, \tag{6.32}$$

with $\varepsilon^t \sim N(0, \sigma_\varepsilon^2)$, where y^t is the vector of a profile at time t, $f^0(x)$ represents the relationship between the explanatory and response variables when the process is in – control, $g(\cdot)$ represents an unidentified functional change that occurs when the process deviates from its controlled state and $\tau \in \{1, 2, \ldots, T\}$ represents the time of the first out – of – control profile.

Then, when examining the observed data, each y^t profile is transformed into a vector of coefficients in the wavelet using the discrete wavelet transform. Therefore, denoting the resulting vector as d^t, which encompasses all empirical wavelet coefficients of the profile y^t, we distinguish the following two cases:

- When the process is in – control and $t < \tau$, then the vector d^t is given by:

  $$d^t = W\, \varepsilon^t = \varepsilon^{t'}, \tag{6.33}$$

  where W represents an orthogonal matrix and $\varepsilon^{t'}$ is the Gaussian white noise.
- When the process is out – of – control and $t \geq \tau$, then the vector d^t is defined as:

$$d^t = W\, g(x) + W\, \varepsilon^t = \theta + \varepsilon^{t'}, \quad (6.34)$$

where θ represents the wavelet coefficients of g(x), i.e., the noise – contaminated observations, and $\varepsilon^{t'}$ is the Gaussian white noise.

Once a process is identified as out – of – control, the precise change point can be estimated by selecting:

$$\hat{\tau} = arg \max_{1 \le t \le \tau} \pi(\tau = t \mid D), \quad (6.35)$$

where $D = \{d^1, d^2, \ldots, d^T\}$ is the empirical wavelet coefficients and $\pi(\tau = t \mid D)$ represents the marginal posterior distribution of τ.

To derive an expression for the posterior distribution of the change point given the available data, it is necessary to assign prior distributions to the unknown parameters in our model. Thus, the prior distribution for the parameter τ is as follows:

$$\pi_\tau(\tau = t) = (1 - p)^{t-1}\, p, \quad t = 1, 2, \ldots \quad (6.36)$$

where p represents the probability of being out – of – control at the next time.

Furthermore, for the vector θ, which can be written in the form:

$$\theta = (\xi_{j01}, \xi_{j02}, \ldots, \xi_{j02^{j_0}}, \theta_{j01}, \theta_{j02}, \ldots, \theta_{J-1,2^{J-1}}), \quad (6.37)$$

where ξ_{jok} represent the smooth coefficients and θ_{jk} are the detail coefficients, the prior distribution is given by:

$$\pi_{\theta jk}(\theta_{jk}) = (1 - \omega)\, \delta_0(\theta_{jk}) + \omega\, \gamma_s(\theta_{jk}), \quad j = j_0, \ldots, J\text{-}1 \quad k = 1, \ldots, 2^j \quad (6.38)$$

where ω and s are hyperparameters of θ, representing sparsity and the scale of the detail coefficients, respectively, δ_0 is the Dirac delta function at zero and γ_s represents a symmetric density. For γ_s consider either normal or Laplace density.

Moreover, setting ω = 1 in the Eq. (6.38), the prior distribution for smooth coefficients of θ is of the form:

$$\pi_{\xi j0k}(\xi_{j0k}) = \gamma_s(\xi_{j0k}), \quad k = 1, \ldots, 2^{j0} \quad (6.39).$$

It is worth noting that, by choosing the above approach, we expect nonzero values for all smooth coefficients in the model, aligning their scale with nonzero detail coefficients. The focus is on detecting subtle changes, prioritizing cases where the magnitude of these changes is relatively small. The orthogonality of the wavelet representation allows for the independent modeling of each coefficient in the prior, a common assumption in Bayesian

wavelet estimation. Based on the above information, the posterior distribution of τ is defined as follows:

$$f(D|\tau) = \int f(D|\theta,\tau)\,\pi_\theta(\theta)\,d\theta$$

$$= [\prod_{t=1}^{\tau-1}\prod_{i=1}^{n}\varphi\,(d_i^t \mid 0,1)]\,[\prod_{i=1}^{n}u(d_i^{t\geq\tau})\,v(\overline{d_i^{t\geq\tau}})], \quad (6.40)$$

where $\pi_\theta(\theta)$ is the prior distribution of θ, φ(·) represents a normal density function, $d_i^{t\geq\tau}$ is the empirical coefficient in position i from out – of – control profiles, $\overline{d_i^{t\geq\tau}}$ is the mean of $d_i^{t\geq\tau}$ and u, v are functions, resulting from factorization of the density of $d_i^{t\geq\tau}$.

Finally, before proceeding to the conclusions of this study, it is noted that, we have outlined all the necessary components for deriving the posterior of τ. To operationalize the process monitoring method, the next step involves selecting hyperparameters for the prior distributions of τ and θ. Therefore, Varbanov et al. (2019) utilized the median of the posterior distribution as the estimated coefficient. Consequently, the posterior median and the relationship between the hyperparameters and posterior median threshold are given in the following forms:

$$median(\theta_i \mid d_i) = max(0, h(d_i, \omega, s)), \quad (6.41)$$

$$\lambda_{median} = min\{d: d \geq 0, h(d, \omega, s) > 0\}, \quad (6.42)$$

where h(d, ω, s) is the posterior median threshold.

Finaly, during the calibration of the method to achieve a desired in-control average run length, the user has two options: a) adjust p for a fixed upper control limit or b) adjust the upper control limit for a fixed p. Due to the intractability of the distribution of in-control run length, the calibration of either p or the upper control limit to achieve a specific in-control ARL can be conducted using a Monte Carlo simulation study. Thus, below are presented the results from the research of Varbanov et al. (2019), who compare the conclusions with those of the probability ratio test (LRT) method, which introduced by Chicken et al. (2009) and used to monitor nonlinear profiles using wavelets. The results, which are based on the ARL and SDRL criteria, are as follows:

- Although both WBB and LRT methods are adjusted to achieve the same in – control average run length (in – control ARL value equal to 200), WBB approach achieves this average with significantly lower

variability. On the other hand, LRT method exhibits a much higher SDRL values and includes extreme run length values that surpass those seen in any WBB setting. Due to the occurrence of these extreme values in the run length distribution, the LRT method tends to produce a higher proportion of early false alarms to align with the desired in-control ARL.

- Either in the case where $\tau = 1$, i.e., the process is never in an in – control situation, or in the case where $\tau = 20$, it was observed that, for large changes, both examined methods show similar results. In contrast, for the ability to detect small shifts, the proposed WBB method significantly outperform LRT approach was observed. This can be elucidated by the WBB method's capability to integrate frequency and location information across profiles.
- Measuring the efficacy of change-point estimation, LRT method encounters difficulties perceiving not obvious changes, hampering its precision in pinpointing their location. On the other hand, the proposed WBB approach presents more favorable outcomes, showcasing an adept ability to precisely identify the location of the change.

6.4.2 A study for machine condition monitoring

Machine Condition Monitoring (MCM) seeks to assess the health of machines through statistical analysis of machine condition data, aiming to enhance machine reliability. Key aspects of MCM involve detecting incipient failures and evaluating degradation trends. Incipient fault detection involves using health indicators (HIs) to identify the onset of failure as an alarm for machine health conditions, while the degradation trends of health indicators serve as valuable predictors for estimating the remaining useful life of machines. Consequently, the construction of suitable and effective HIs holds significant importance in the field of MCM. For this reason, Deng et al. (2022) proposed a method, which attempts to characterize nonparametric nonlinear profiles through B-spline fitting and constructs a Hotelling T^2 health indicator (HTHI) using coefficients that encapsulate the profile model. Below is briefly given the form of the B-spline model, as well as the Hotelling T^2 health indicator. Therefore, the B-spline model is defined as:

$$SES(t) = f(t) + \varepsilon(t) = \sum_{i=0}^{p} B_{i,k}(t)\, P_i + \varepsilon(t), \quad (6.43)$$

with $B_{i,0}(t) = \begin{cases} 1, & t \epsilon [t_i,\ t_{i+1}] \\ 0, & otherwise \end{cases}$

and $B_{i,k}(t) = [(t - t_i)B_{i,k-1}(t) / (t_{i+1} - t_i)] + [(t_{i+k+1} - t_i)B_{i+1,k-1}(t) / (t_{i+k+1} - t_{i+1})]$ for k>0, where f(t) represents a B-spline curve at time point t, P_i is the i^{th} control points, p represents the dimension of control points and ε(t) represents the error between the square envelope spectra (SES) and B-spline model at time point t. It is worth noting that, if a sample set SES conforms to the B-spline curve, the following equation should hold:

$$SES(t) = \sum_{i=0}^{p} B_{i,k}(t)\, \widehat{P}_i, \quad (6.44).$$

But Eq. (6.44) can be written equivalently in a matrix form as follows:

$$SES = B\widehat{P}, \quad (6.45).$$

Therefore, the estimated control points can be calculated from the following relationship:

$$\widehat{P} = (B'\, B)^{-1}\, B'\, SES, \quad (6.46).$$

Based on the above information, it is emphasized that, the number of control points is determined manually. Specifically, various quantities of control points are selected to visualize B-spline curves, and the smallest number is chosen that can precisely fit a given data curve. Ultimately, the B-spline fitting curves can be derived through this process. Furthermore, the above control points can be employed to formulate a health indicator using Hotelling T^2. However, the dimensionality of control points becomes excessively large due to the complex shape of SES, leading to a dimensionality problem. To address this issue, a proposed solution involves segmenting the B-spline fitting curves. The average deviations of a testing profile piece and the average profile piece can then be calculated by:

$$D_{i,j} = \sum_{k=1}^{q} \left\| x_{ijk} - \overline{x_{ijk}} \right\| / q, \quad i = 1, 2, \ldots, N, \quad j = 1, 2, \ldots, c, \quad (6.47)$$

where q represents the number of control points for each piece, c is the number of pieces of the profile curve, $\|\cdot\|$ represents the Euclidian distance, x_{ijk} represents the k^{th} control point of the i^{th} profile in the j^{th} piece and $\overline{x_{ijk}}$ is the mean of x_{ijk}.

Therefore, HTHI for the i^{th} profile is defined as follows:

$$HTHI_i = (Z_i - \bar{Z})' S' (Z_i - \bar{Z}), \quad (6.48)$$

where $Z_i = (D_{i1}, D_{i2}, \ldots, D_{ic})'$, $\bar{Z}$ represents the mean vector of Z_i and S is the covariance matrix of standard profiles, i.e., in a normal condition.

Two health indicator metrics, namely monotonicity and trendability, were used to conduct the conclusions of this research, and were employed to quantitatively evaluate the degradation trends of four commonly used HIs, i.e., the negative entropy, kurtosis, smoothness index, and Gini index, and the proposed Hotelling T^2 health indicator. The results were as follows:

- The values of the two health indicator metrics of the proposed HTHI, i.e., monotonicity and trendability, are higher than the other examined HIs. Specifically, the sum of monotonicity and trendability of the HTHI was observed to be greater than that of the Gini index, which in turn presents a larger sum value than the negative entropy. Finally, the smallest values are presented in the smoothness index and the kurtosis.
- In general, the proposed Hotelling T^2 health indicator demonstrates a superior monotonic degradation tendency compared to four commonly used health indicators and can effectively detect an early fault.

CHAPTER 7

Multivariate profiles

Introduction

The popularity of monitoring multiple linear profiles has increased in recent times due to its effectiveness in various fields. This approach is widely adopted because it provides a comprehensive view of interconnected linear relationships, allowing for a more careful understanding of complex systems. More specifically, a multiple linear profile, which is a category of linear profiles, applies in cases where a regression profile has a multiple form with p predictor variables, (x_1, x_2, …, x_p) and the model formula is given below.

For the j^{th} sample profile, where j = 1, 2, ... is the number of sample profiles, which is denoted by {(x_{ik}, y_{ij}), i = 1, 2, ..., n, k = 1, 2, …, p}, where n denotes the number of observations in each profile and p represents the number of predictor variables, we get the following model:

$$y_{ij} = \beta_0 + \beta_1 x_{i1} + \beta_2 x_{i2} + \ldots + \beta_p x_{ip} + \varepsilon_{ij}, \quad (7.1)$$

where β_0, β_1, …, β_p are the regression coefficients and ε_{ij} represent the error terms between profiles, which are independent and identically distributed with a normal distribution, i.e., $\varepsilon_{ij} \sim N(0, \sigma_\varepsilon^2)$.

Please note that, if p = 1, then the above model reduces to a simple linear profile, discussed in Chapter 3.

In certain applications, it is essential to assess the stability of multiple correlated profiles simultaneously over time. Employing separate control charts for each profile may yield misleading outcomes if the inherent correlation structure between the response variables is ignored. A multivariate multiple linear profile, as a general multivariate regression model, is characterized by p response variables and q explanatory variables and is formulated as follows:

$$Y_j = X_j B + E_j, \quad j = 1, 2, \ldots \quad (7.2)$$

where Y_j is the n×p matrix of responses variables, X_j is the n×q+1 matrix of

explanatory variables, B represents a (q+1)×p matrix of regression coefficients and E_j is the n×p matrix of error terms.

Please note that, if q = 1, then the above model is converted to multivariate simple linear model. Furthermore, if p = 1, then the model in Eq. (7.2) becomes equal to multiple linear profile described in Eq. (7.1) and, finally, if p = q = 1, then the model reduces to a simple linear profile.

Table 7_1 briefly mentions previous research conducted to monitor multiple linear and multivariate multiple linear profiles over a decade from 2008 to 2018. More specifically, lists the researchers, whether the expert study concerned Phase I or Phase II of the profile, and the criterion for measuring the performance of the control charts used.

Research	Phase I	Phase II	Performance criterion
Mahmoud (2008)	Yes	-	Signal probability
Noorossana et al. (2010a) (*)	Yes	-	Signal probability
Noorossana et al. (2011b)	-	Yes	ARL
Amiri et al. (2012)	-	Yes	ARL
Xu et al. (2012)	-	Yes	ATS & $\hat{\tau}$
Zi et al. (2012)	-	Yes	ARL & SDRL
Zou et al. (2012) (*)	-	Yes	ARL & SDRL
Adibi et al. (2014a)	-	Yes	ARL
			(continued)

Amiri et al. (2014a) (*)	-	Yes	Accuracy percent
Ayoubi et al. (2014) (*)	-	Yes	$\bar{\hat{\tau}}$ & precision
Huwang et al. (2014a)	-	Yes	ARL
Huwang et al. (2014b)	-	Yes	ARL, SDRL, $\bar{\hat{\tau}}$, SD($\hat{\tau}$), precision & accuracy percent
Kazemzadeh et al. (2015) (*)	-	Yes	$\bar{\hat{\tau}}$ & precision
Mahmoud et al. (2015)	-	Yes	ARL
Xu et al. (2015)	-	Yes	SSATS & $\bar{\hat{\tau}}$
Ayoubi et al. (2016) (*)	-	Yes	$\bar{\hat{\tau}}$ & precision
Khedmati and Niaki (2016c)	-	Yes	ARL
Ghashghaei and Amiri (2017a) (*)	-	Yes	ARL, SDRL & accuracy percent
Ghashghaei and Amiri (2017b) (*)	-	Yes	ARL & accuracy percentage
Ghashghaei et al. (2018) (*)	-	Yes	ARL
Motasemi et al. (2017)	Yes	Yes	ARL & Signal probability
Xia and Tsung (2017)	Yes	Yes	ARL & diagnosis percentage
Cheng and Yang (2018)	-	Yes	ARL & accuracy detection

Table 7_1. A brief overview of methods developed to monitor multiple linear profiles from 2008 to 2018. (Adapted from Maleki, M. R., Amiri, A., & Castagliola, P. (2018)). Please note that, (*) represents the multivariate multiple linear profiles.

The subsequent sections of this chapter are intended to bring together some recent developments for monitoring multivariate profiles. Therefore, since after the remarkable review papers of Woodall (2007) and Maleki et al. (2018) there is no newer paper that includes methods for profile monitoring from 2018 until today, the continuation of the chapter comes to fill this scientific gap regarding multivariate profiles.

7.1 Multivariate principal component analysis methods

In this section, recent studies will be discussed, which aim to monitor multivariate multiple linear profiles with the use of principal component analysis (PCA). In the first place, we will develop the study by Wang et al. (2018), who proposed a new thresholded multivariate principal component analysis (PCA) approach to reduce the dimension of a multivariate profile and then monitor it in Phase I. Moreover, we will discuss the study by Ren et al. (2019), who introduced the exponentially weighted moving average (EWMA) scheme with multichannel functional principal component analysis (MFPCA) for monitoring multichannel profiles in Phase II. Finally, this section will discuss the study by Herzer et al. (2023), who proposed an approach for the product life cycle to monitor time-series behavior patterns.

7.1.1 Thresholded principal component analysis for Phase I

In today's manufacturing systems, the widespread use of multiple sensors capable of simultaneous data collection introduces the challenge of monitoring multichannel or multivariate profiles. This issue holds significant implications for enhancing manufacturing systems. Wang et al. (2018), taking into account the above philosophy stemming from the high needs of industries, the rapid development of technology, the increasing competition for the best quality of products among businesses and the high expectations of consumers, proposed a Phase I method for multivariate profile data, particularly in scenarios where multiple sensors measure similar process variables or quality characteristics. The historical data used for this method includes both in – control and out – of – control observations. Furthermore, this approach not only has the capability to identify and eliminate out – of – control observations but also allows for the

estimation of baseline model parameters, i.e., mean and variance functions, based on in – control data. These estimated parameters are subsequently utilized for Phase II monitoring. In detail, this proposed methodology involves the incorporation of multivariate functional principal component analysis (PCA), shrinkage, and change-point detection approaches for the analysis of Phase I data contaminated with out – of – control observations. In this framework, PCA and shrinkage techniques are employed for dimensionality reduction, focusing on extracting monitoring features that exhibit the highest sensitivity to process changes as reflected in out – of – control data. The change-point detection method then combines these features to identify the time of the change in the system. The idea of Wang et al. (2018) will be given in more detail below. Suppose a random sample of m multichannel profiles, each comprising p channels, collected from a production process. Each observation in the set of m multichannel profiles is represented as a p-dimensional curve, i.e., $X_j(t) = (X_j^{(1)}(t), X_j^{(2)}(t), \ldots, X_j^{(p)}(t))'$, for j = 1, 2, …, m and t ϵ [0, 1]. Based on the multivariate model of Eq. (7.2), we assume that initially the process is in an in-control state and the $X_j(t)$ have a mean equal to $\mu_1(t)$. However, the process at an unknown time gets out – of – control and so the mean of the $X_j(t)'$s changes and becomes equal to $\mu_2(t)$. Therefore, the above procedure can be modeled as follows:

$$X_j(t) = \begin{cases} \mu_1(t) + Y_j(t), \ j = 1, \ldots, \tau \\ \mu_2(t) + Y_j(t), \ j = \tau + 1, \ldots, m \end{cases}, \text{ for t } \epsilon \text{ [0, 1]}, \tag{7.3}$$

where $\mu_1(t)$ and $\mu_2(t)$ are the two unknown mean functions of $X_j(t)$. The purpose of this research is to examine whether a change will occur at some unknown time t. Therefore, using the observed $X_j(t)$ variables, the following hypothesis test is tested:

$$\begin{cases} H_0 : \mu_1(t) = \mu_2(t) \quad (no\ change) \\ H_1 : \mu_1(t) \neq \mu_2(t) \ (a\ change\ occurs) \end{cases}', \tag{7.4}.$$

Moreover, must be enforced the classical Type I error probability constraint:

$$P_{H_0}(reject\ H_0 : \mu_1(t) = \mu_2(t)) \leq \alpha, \tag{7.5}$$

for a specific constant α.

Based on the above information, Wang et al. (2018) proposed the following statistic for hypothesis test in Eq. (7.4):

$$\Delta_l(t) = \sqrt{\frac{l\,(m-l)}{m}}\left\{\frac{1}{l}\sum_{j=1}^{l} X_j\,(t) \;-\; \frac{1}{m-l}\sum_{j=l+1}^{m} X_j(t)\right\}, \tag{7.6}$$

where l (l = 1, 2, …, m – 1) represents a potential change-point at which the first l observations have mean μ_1 and the remaining (m – l) observations have mean equal to μ_2.

Now, the objective is to introduce an effective method to assess whether $\Delta_l(t)$ is a zero function, i.e., there is no change in the process, by integrating shrinkage with PCA. Therefore, below are the basic steps to implement the proposed method.

Initially, to simplify the hypothesis testing problem, this study employs the multivariate functional PCA method, which translates the testing from the functional space to the space of PCA coefficients. This method involves estimating both the basis and covariance matrices. More specifically, as mentioned above, the study by Wang et al. (2018) was based on scenario where multiple sensors measure similar process variables or quality characteristics. Therefore, assuming that, all the components of the p – dimensional functions $Y_j(t)'s$ exhibit similar covariance structures over time and can be decomposed into the same real-valued basis functions $u_k(t)'s$, the study focuses on examining the inner-channel covariance structure over time through the following total covariance function:

$$c(t, s) = E[\langle Y_j(t)', Y_j(s)\rangle] = \sum_{i=1}^{p} E[(Y_j^{(i)}(t))\; Y_j^{(i)}(s)], \;\; 0 \leq t, s \leq 1, \tag{7.7}$$

Thus, the $u_k(t)'s$ are calculated as the eigenfunctions of c(t, s). Moreover, the projection of the p – dimensional function $Y_j(t)$ on the k^{th} principal component has the following form:

$$\xi_{jk} = \int_0^1 [\, Y_j(t)\; u_k(t)]\; dt, \tag{7.8}$$

with j = 1, 2, …, m, k = 1, 2, …, d, where d is the number which represents the first d eigenfunctions $u_k(t)'s$, i.e., d is the number of principal components. Please note that, the vectors $\xi_{jk}'s$ are considered to be independent multivariate

normal distributions across various bases (k's) and observations (j's), each having distinct p×p covariance matrices for different principal components. In the scenario where the $Y_j(t)'s$ are observable, the covariance matric is defined by the following relationship:

$$\Sigma_k = E(\xi_{jk}\, \xi_{jk}') = E\left\{\int_0^1 Y_j(t)u_k(t)\, dt \int_0^1 Y_j'(t)u_k(t)\, dt\right\}, \quad (7.9).$$

In the scenario where the $Y_j(t)'s$ are unobservable, then the total covariance function in Eq. (7.7) can be approximated by:

$$\hat{c}(t,s) = \frac{1}{2(m-1)} \sum_{j=1}^{m-1} (X_{j+1}(t) - X_j(t))' (X_{j+1}(t) - X_j(t)), \quad (7.10)$$

where the differences $Y_{j+1}(t) - Y_j(t) = X_{j+1}(t) - X_j(t)$ are observable for all j except for $j = \tau$, if the change-point τ occurs.

Then, the $\widehat{u_k}(t)'s$ are calculated as the eigenfunctions of $\hat{c}(t, s)$ and the covariance matrix in Eq. (7.9) approximate by:

$$\widehat{\Sigma_k} = \frac{1}{2(m-1)} \sum_{j=1}^{m-1} \int_0^1 \{X_{j+1}(t) - X_j(t)\}\, \widehat{u_k}(t)\, dt \times \int_0^1 \{X_{j+1}(t) - X_j(t)\}'\, \widehat{u_k}(t)\, dt \quad (7.11).$$

The next step is to define a statistic on the basis of which we can decide whether or not the null hypothesis $H_0 : \mu_1(t) = \mu_2(t)$ is true. Thus, the proposed statistic was defined in this study as follows:

$$Q_m = \max_{1 \le l < m} \sum_{k=1}^{d} max\,(U_{l,k} - c,\ 0), \quad (7.12)$$

with $U_{l,k} = \eta_{lk}'\, \widehat{\Sigma_k}^{-1}\, \eta_{lk}$, where $\widehat{\Sigma_k}$ is the covariance matric defined in Eq. (7.11), $\eta_{kl} = \int_0^1 \Delta_l(t)\, \widehat{u_k}(t)\, dt$, the $\widehat{u_k}(t)'s$ are computed as the eigenfunctions of $\hat{c}(t, s)$ and $c \geq 0$ represents a prespecified "soft-thresholding" parameter. Furthermore, we reject the null hypothesis H_0 if and only if,

$$Q_m > L, \quad (7.13)$$

where L represents a prespecified control limit.

Please note that, when Eq. (7.13) holds, then the estimated change-point is given by the following formula:

$$\hat{\tau} = arg \max_{1 \le l < m} \sum_{k=1}^{d} (U_{l,k} - c)^+, \quad (7.14).$$

The interested readers are referred to the comprehensive article for the detailed

guidance on selecting appropriate tuning parameters, i.e., d, c, L, with the above method for multichannel process monitoring by Wang et al. (2018). Remarkably, the proposed new method developed here is compared to the method of Paynabar et al. (2016), in which null hypothesis $H_0 : \mu_1(t) = \mu_2(t)$ rejected if and only if $\max_{1\le l<m} \sum_{k=1}^{d}(U_{l,k}) > L$, where L is a prespecified control limit. Thus, it is understood that the method of Paynabar et al. (2016) is a special case of the proposed method of Wang et al. (2018) when the soft-thresholding parameter is equal to zero, i.e., c = 0. In addition to this, it is emphasized that, Paynabar et al. (2016) made an assumption that all principal components are affected by the change simultaneously, while Wang et al. (2018) assumed that only some principal components are significantly affected, particularly when the number d of principal components is large. Therefore, the comparison is made by putting three different values in the parameter c, i.e., $c_0 = 0$, $c_1 = 7$, $c_3 = 11.6$, and the following three scenarios are used: a) a local change occurs for $30 \le j \le 37$, b) a local change occurs for $16 \le j \le 29$, and c) a global change occurs for all $1 \le j \le 66$. Note that, with the same magnitude of the change, detecting the local change in the first scenario, where the peak of the profile occurs, is the most challenging, while detecting the global change in the last scenario is the easiest. Finally, the results refer to the case where all the p channels (here, p = 4) are affected by the change simultaneously, were derived through Monte Carlo simulation studies and were the following:

- In the first scenario, where a local change affects the rise, peak, and fall segments of the profiles, all three methods exhibit comparable detection powers, although the method by Paynabar et al. (2016), i.e., $c_0 = 0$ is slightly worse.
- In the second scenario, when the shift is small then both c_1 and c_2 significantly enhance the detection power compared to the method by Paynabar et al. (2016). However, for large change magnitudes, all three approaches demonstrate detection powers close to 1, indicating that they are capable of detecting large changes effectively.
- In the third scenario, where a global change occurs, it was observed that, in the presence of a small shift, both c_1 and c_2 exhibit a higher detection power than $c_0 = 0$. This outcome might be not logical, as one would

expect that thresholding would not significantly help in detecting a global change.

- In the special case where only the first two channels are affected by the change, while the last two maintain the in – control mean μ_1, it was observed that, the c_1 and c_2 values significantly outperform the c_0 value for almost all shifts in the first and second scenarios. In the case of global change, the improvement in detection power is particularly significant for c_2 compared to the method by Paynabar et al. (2016). This improvement may be attributed to the new spatial sparsity, where only the profile means of two channels have shifted.
- In general, the proposed method of Wang et al. (2018) has the ability to detect the true change-point more accurately and effectively than the method of Paynabar et al. (2016).

7.1.2 Multichannel functional principal component analysis in Phase II

The advent of advanced sensing technologies in complex manufacturing systems has ushered in an era of plentiful and real-time data. While this presents unprecedented opportunities for monitoring and enhancing product quality and process efficiency, it also poses substantial challenges to traditional statistical process control methods. Ren et al. (2019), wanting to provide a solution to the above challenge, proposed a Phase II monitoring approach tailored for multichannel profiles. This innovative method leverages functional principal components to extract features, effectively characterizing process variations. These extracted features are then utilized to construct an exponentially weighted moving average (EWMA) chart. Therefore, they developed the exponentially weighted moving average (EWMA) scheme with multichannel functional principal component analysis (MFPCA), which is specifically designed to reduce dimensionality and extract a limited number of major and representative features essential for process monitoring. Below is briefly given the structure of the method proposed by Ren et al. (2019). Initially, in Phase II monitoring for multichannel profiles, Ren et al. (2019), based on the multivariate linear profile of Eq. (7.2), consider sequential collection of profile observations according to the following model:

$$X_j(t) = \begin{cases} \mu(t) + Y_j(t), & j = 1, \ldots, \tau \\ \mu(t) + \delta(t) + Y_j(t), & j = \tau + 1, \ldots, \end{cases}, \text{ for } t \in [0, 1], \quad (7.15)$$

where μ(t) represents the in – control mean function of profiles, δ(t) is the change in the mean function at time point τ, i.e., τ represents the change-point. Using MFPCA for online-collected observations $X_j(t)$, j = 1, 2, …, we can reduce their dimensions and extract crucial information by projecting them onto the principal functions. The projections, known as PC-scores, corresponding to the largest d eigenvalues are obtained by:

$$\xi_{jk} = \int_0^1 X_j(t)\, u_k(t)\, dt, \quad k = 1, \ldots, d, \quad (7.16)$$

where $u_k(t)'$s are the known eigenfunctions of c(t, s) from Phase I analysis, which is calculated in Eq. (7.7) of the previous section and d is the number of principal components.

Based on the ξ_{jk}, the EWMA charting statistic is defined as follows:

$$\eta_{jk} = (1 - w)\, \eta_{j-1,k} + w\, \xi_{jk}, \quad k = 1, \ldots, d, \quad (7.17)$$

where w ($0 < w < 1$) represents the smoothing parameter and $\eta_{0k} = 0$ in the p – dimension space. Please note that, a smaller w leads to a quicker detection of smaller shifts. Therefore, Ren et al. (2019) chose $w \in [0.05, 0.2]$.

The proposed control chart, which is denoted as Q_j and is referred to as the principal components based EWMA (PCEWMA) chart, triggers a signal if,

$$Q_j = \left[\frac{2 - w}{w} \sum_{k=1}^{d} \eta_{jk}' \, \Sigma_k^{-1} \, \eta_{jk} \right] > L, \quad (7.18)$$

where L > 0 is a specified control limit based on the in – control ARL value chosen by each researcher and Σ_k represents the covariance matrix of ξ_k set during Phase I analysis.

A particularly interesting part of this study is the fact that researchers explored a potential extension of the PCEWMA chart to illustrate its adaptability. In practical scenarios, shifts in the mean function can impact the correlation among channels, even if Σ_k remains at its in – control value. To detect changes in the covariance matrix, monitoring the principal component scores ξ_{jk} can be effective for constructing the control chart. When the process is in – control, the ξ_{jk}'s are random vectors with a mean equal to zero and a covariance matrix

Σ_k. Thus, they follow a multivariate normal distribution when $X_j(t)$ follows a Gaussian process. Therefore, an EWMA sequence based on ξ_{jk} can take the following form:

$$S_{jk} = (1 - w)\, S_{j-1,k} + w\, \xi_{jk}\, \xi_{jk}', \quad k = 1, \ldots, d, \tag{7.19}$$

with $S_{0k} = 0$. It is worth noting that, when the process is an in – control state then $E(S_{jk}) = \Sigma_k$.

Then, the proposed control chart for the covariance matrix, which is denoted by T_j, triggers a signal if,

$$T_j = \sum_{k=1}^{d} \{tr(S_{jk}) - log|S_{jk}| - p\} > CL, \tag{7.20}$$

where CL is a specified control limit.

Because monitoring changes in both location and scatter concurrently is a good approach, Ren et al. (2019) proposed implementing the EWMA scheme for the covariance matrix alongside a PCEWMA to effectively identify shifts in multichannel profiles. Finally, to assess the effectiveness of the proposed PCEWMA, they employ three distinct approaches for comparative analysis. More specifically, the initial approach for monitoring multichannel profiles involves stacking profiles from each channel and converting them into a high-dimensional vector. Subsequently, PCA is applied to the resulting vector to extract features for constructing an EWMA control chart. This method is denoted as vectorized-PCA EWMA (VPEWMA) and breaks the correlation structure in the original data, potentially losing valuable representations available in the original form. Moreover, the second method, which is referred to as sIPEWMA, involves applying standard functional principal component analysis to each individual channel to construct EWMA statistics. The monitoring statistics are then obtained by summing up these individual statistics. However, this approach neglects the correlation among the multichannel profiles. The last method is the approach of Zou et al. (2008), which proposes the nonparametric EWMA (NEWMA) control chart for single-channel functional profiles and has been discussed in Chapter 6. To adapt it to multichannel profile data, one could apply NEWMA to each channel's profile and then sum up their statistics. This method is referred to as mNEWMA and it

does not consider the correlation among profile channels. The comparison between the above control charts was made with the help of the ARL and SDRL performance criteria and the results were as follows:

- In general, the PCEWMA chart with a larger value of smoothing parameter w is superior in detecting large shifts, while the PCEWMA with a smaller w is better at detecting small shifts.
- Based on the ARL values with high-level and low-level correlation in the covariance matrix Σ_k, respectively, it was observed that, the proposed PCEWMA control chart demonstrates superior efficiency for both strong and weak between-profile correlations. Furthermore, as the degree of correlation increases, both mNEWMA and sIPEWMA exhibit slower detection of shifts.
- In general, PCEWMA exhibits improved performance with higher level of correlation, as the model by Ren et al. (2019) effectively incorporates and leverages the correlation information among channels.
- In general, the PCEWMA chart consistently exhibits superior efficiency in most cases, and its advantage becomes more pronounced, particularly in detecting larger shifts. Therefore, the proposed PCEWMA chart significantly outperforms the other control charts in terms of efficiency and sensitivity, particularly for large shifts.
- Both VPEWMA and sIPEWMA outperform the mNEWMA chart, as these PCA-based methods capture significant information from multichannel profiles. In contrast, the mNEWMA chart is inefficient in detecting shifts. This inefficiency arises from its failure to consider the correlation among channels and its assumption that the stochastic noise at each observation point is independent.

7.1.3 A recent study in product portfolio management

To address the limitations of existing product portfolio management methods, Herzer et al. (2023) proposed a novel approach that integrates financial information with economic performance, product competitiveness, and macroeconomic data. Specifically, the aim was to create a robust profile

monitoring scheme that can effectively identify patterns and changes in the product lifecycle. By continuously monitoring key indicators, their method seeks to provide timely insights for editing the product portfolio when necessary. Furthermore, this approach addresses the challenges posed by the unique and dynamic nature of each project, making it a valuable tool for corporate management in navigating the complexities of product portfolio management. Below are briefly given the steps of the methodology followed by Herzer et al. (2023) for this new approach to product portfolio management. Therefore, the steps are as follows:

- Variable selection. The initial step is to select variables, which will be used appropriately for the specific study. Thus, Herzer et al. (2023) categorizes variables into dependent (Y) and independent (X) ones, where Y variables represent product factors and X variables encompass macroeconomic data related to the business.
- Principal Component Analysis (PCA). While there is no strict limit on the number of selected variables, PCA is applied to simplify the model significantly. Specifically, PCA is employed in the proposed method to reduce dimensionality, a statistical technique that retains essential information in the first components, resulting in a more manageable dataset for analysis. The proposal suggests applying PCA to both dependent and independent variables to derive model residuals. This process aids in capturing key information and reducing the complexity of the model.
- Multivariate linear regression model. The next step is to define the model to be used and connect the dependent variables with a set of variables describing the system (explanatory variables). For this reason, the multivariate multiple linear model defined in Eq. (7.2) is used. Based on this model, the estimate of the regression coefficient matrix, B, is given by the following relationship:

  $\hat{B} = (X' X)^{-1} (X' Y)$, (7.21).

  To compute the inverse of (X'X), it is crucial to address issues related to high collinearity among independent variables. Thus, to remove the multicollinearity, PCA methods are applied. Once the components are

derived, a cause-effect model is constructed using this information. The residuals obtained from this model serve as the basis for monitoring the product portfolio through a multivariate control chart.

- Hotelling control chart. As a last step, it is recommended to control the process and identify any assignable causes that lead the process to out – of – control situations. In this study, Hotelling´s T^2 control chart is used in order to controls the residuals obtained from the multivariate regression model and its statistic is given by:

  $$T^2 = (X - \bar{X})' S^{-1} (X - \bar{X}), \quad (7.22)$$

  where S represents the covariance matrix of X and $\bar{X}$ is the average vector of X.

Please note that, generating control charts for each component (X and Y) becomes crucial when an out – of – control data point is detected in the residual control chart. This approach is vital for identifying the source of change in the regression model pattern. If the change is attributed to the X component, it signifies a shift in the macroeconomic scenario, requiring a review of the strategic business plan. However, if the change is associated with the Y component, intervention in the company's product portfolio becomes necessary. This method enables a targeted response to changes in both macroeconomic conditions and product performance. Finally, the new proposed method is compared to that of Villalobos et al. (2005), where the researcher examined the case in which a shift occurred in just one variable. The results were conducted through simulation studies and were the following:

- In this study, a shift in a single variable and later in the entire set of Y variables was tested using the proposed control procedure. On average, one false alarm was detected every 209/210 months, similar to Villalobos et al. (2005).
- When a shift occurred in one variable, the average time to signal (ATS) metric rapidly declined. Introducing a constant change in all components led to an expected acceleration in the decline, showing faster results compared to Villalobos et al. (2005).
- In general, the proposed method demonstrates a quicker identification of changes in the model patterns compared to usual multivariate

monitoring procedure. This enhanced speed in model responsiveness translates to faster availability of information for effective decision-making.

7.2 Correlation in profile monitoring methods

In this section we will present two methods, which use correlated data to monitor multivariate profiles. Initially, we will discuss the study by Khalili and Noorossana (2021), who proposed a multivariate linear mixed model (MLMM) scheme in order to account for autocorrelation within profiles and then, the study by Rodrigues et al. (2021), who introduced a statistical process monitoring procedure designed for flexible environments characterized by a finite production horizon and p correlated observed variables will be discussed.

7.2.1 Auto-correlated profiles: A multivariate MLMM approach

The majority of studies in profile monitoring often assume the absence of correlation structure among observations within profiles. However, this assumption is unrealistic, especially in cases where data is collected over time or space, leading to the presence of serial or spatial correlation. When observations are collected in short time intervals or close spatial distances, within-profile correlation becomes noticeable. This correlation challenges the independence assumption underlying traditional control charts and significantly influences the performance of existing methods. Khalili and Noorossana (2021), wanting to provide a solution to the above challenge and focusing on autocorrelation within multivariate multiple linear profiles (MMLP) in Phase II, proposed a multivariate linear mixed model (MLMM) in order to account for autocorrelation within profiles. Furthermore, based on the proposed model, they proceeded to develop two control charts for monitoring the shifts in the mean vector and covariance matrix. Below are briefly given the steps of their method.

Khalili and Noorossana (2021), based on the multivariate multiple linear models of Eq. (7.2), defined the MLMM for the j^{th} autocorrelated profile as follows:

$$Y_j = X_j B + Z_j b_j + E_j, \quad j = 1, 2, \ldots, m, \tag{7.23}$$

where Y_j is the n×p matrix of responses variables, X_j is the n×q matrix related to explanatory variables of fixed effects, B represents a (q+1)×p matrix for regression coefficients of fixed effects, Z_j is the n×r matrix related to explanatory variables of random effects, b_j represents a r×p matrix for regression coefficients of random effects and E_j is the n×p matrix of error terms.

The Eq. (7.23) can be transformed in the following model:

$$vec(Yj') = (X_j \otimes I_p)\, vec(B') + (Z_j \otimes I_p)\, vec(b_j') + vec(E_j'), \quad j = 1, 2, \ldots \tag{7.24}$$

with $vec(b_j) \sim N_{rp}(0, \Psi)$, where vec represents the vectorization operator, the symbol $\otimes$ represents the Kronecker product, I_p is an identity matrix of size p, Ψ is an $rp \times rp$ block diagonal covariance matrix equals to $\varphi \otimes I_p$ and φ represents the autocorrelation coefficient.

Proceeding to the definition of the proposed control charts, we first assume that the in – control profile parameters are known or have been accurately estimated through Phase I analysis. Therefore, the two proposed control charts are the following:

- The multivariate exponentially weighted moving average (MEWMA) control chart is used to monitor the fixed effects in Phase II and its charting statistic for the j^{th} profile is defined as follows:

  $$T_{Zj}^2 = Z_j' \Sigma_Z^{-1} Z_j, \tag{7.25}$$

  with $Z_j = \lambda\, (vec(\widehat{B}_j) - \beta) + (1 - \lambda)\, Z_{j-1}$, where λ $(0 < \lambda < 1)$ is the smoothing parameter, $\widehat{B}_j$ is the j^{th} estimation of the fixed effect coefficients, β represents the mean of $vec(\widehat{B})$, Z_0 is a vector with zero entries, $\Sigma_Z = [\, \lambda / (2 - \lambda)] \, \Sigma_{vec(\widehat{B}_j)}$, and $\Sigma_{vec(\widehat{B}_j)}$ represents the covariance matrix of $vec(\widehat{B})$.

- The multivariate exponentially weighted moving covariance (MEWMC) control chart is utilized to identify both increases and decreases in the marginal variability of a multivariate normal process, i.e., to monitor the covariance matric in Phase II, and its charting statistic for the j^{th} profile is defined as follows:

  $$C_j = tr(S_j) - log|S_j| - p, \quad (7.26)$$

  with $S_j = \lambda\ vec(U_j)\ [vec(U_j')]' + (1 - \lambda)\ S_{j-1}$, where λ $(0 < \lambda < 1)$ is the smoothing parameter, tr represents the trace, S_0 is equal to the identity matrix I_{np} of size np, $U_j = A\ (vec(Y_j) - vec(\mu_0))$, $vec(\mu_0)$ is in – control values of mean matrix, matrix A is defined as inverse Cholesky root matrix of V_0 and V_0 represents the variance – covariance matrix of Y for the j = 0 profile.

Note that, in order to monitor process stability when both fixed effects and covariance matrix change simultaneously, a combination of MEWMA and MEWMC charting statistics can be employed.

Finally, the results on the performance of the proposed control charts, which were examined through simulation studies and with the help of the ARL criterion, were the following:

- In scenario where shifts occur in the profile intercept, it was observed that, under a constant correlation coefficient between responses, both the two proposed control charts exhibit better performance when the autocorrelation (φ) is strong compared to the case when autocorrelation is weak.
- In scenario where shifts occur in the profile intercept, it was observed that, when both between-responses and within-profile correlations (φ) are weak, then the MEWMA control chart performs better than MEWMC for $\lambda < 1.6$. However, for strong correlation levels, MEWMC is superior to MEWMA for $\lambda > 0.6$. Moreover, the combined method is faster than the other two methods in moderate to large shifts.
- In scenario where shifts occur in the profile slope, it was observed that, the MEWMA control chart performs better than MEWMC chart for small shifts.

- In general, the two proposed charts exhibit better performance for slope shifts than for intercept changes.
- In scenario where shifts occur in standard deviation, it was observed that, MEWMA and MEWMC control charts have superior performance under strong correlation among responses and weak autocorrelation coefficient. However, MEWMC chart has the ability to more quickly detect an out – of – control situation when a shift takes place in the covariance matrix.
- In general, the MEWMC exhibits superiority to the MEWMA and shows better results in all correlation and shift levels.

7.2.2 A study for flexible production environments

Traditional control chart methods, particularly univariate charts, face challenges in modern production environments characterized by small series and production lots. Short production runs do not yield sufficient data for accurate estimation of process parameters like mean, standard deviation, and control limits. Moreover, the assumption of independence in univariate charts is often violated, as the quality of an item is influenced by correlated variables. In processes with a limited production horizon and correlated variables, designing effective control charts becomes a challenge for researchers. Rodrigues et al. (2021), wanting to give a modern answer to the above challenge, proposed a statistical process monitoring procedure designed for flexible environments characterized by a finite production horizon and p correlated observed variables. Therefore, based on the multivariate multiple linear profile in Eq. (7.2), they made a preprocessing of the multivariate Hotelling´s T^2 control chart, including the standardization of each variable observed in each product. Subsequently, modifications for bootstrapping and monitoring multiple products with varying dimensions are implemented. Thus, the format of the recommended control chart is as follows:

$$T_j^2 = Z_{ij}' \, \hat{\Sigma}_i^{-1} \, Z_{ij}, \quad i = 1, 2, \ldots, m, \quad j = 1, 2, \ldots, p, \tag{7.27}$$

where $Z_i = (\varepsilon_{ij} / \widehat{\sigma_{ij}})$ be the vector of the standardized observed variables of the quality characteristics p, $\widehat{\sigma_{ij}}^2 = \sum_{i=1}^{n} \varepsilon_{ij}^2 / (n_i - 1)$, ε_{ij} represents the observed

difference of the quality characteristic j of product i from the value specified in design, n_i represents the number of samples observed for product i in Phase I analysis and $\widehat{\Sigma}_i$ is the covariance matrix of Z_i.

The control limits vary depending on Phase I or Phase II that we will apply the proposed control chart. Therefore, we have the following control limits:

- In Phase I analysis, the control limit of the proposed chart follows a Beta distribution and is defined as follows:

$$L_1 = \frac{(n_i - 1)^2}{n_i} B_{1-\alpha/2;\, p/2;\, (n_i - p - 1)/2}, \quad (7.28)$$

  where $B_{1-\alpha/2;\, p/2;\, (n_i - p - 1)/2}$ is the percentile of Beta distribution with parameters p/2 and $(n_i - p - 1)/2$.

- In Phase II analysis, the control limit of the proposed chart follows a F distribution and is defined as follows:

$$L_2 = \frac{(m+1)(m-1)p}{m(m-p)} F_{(p,\, m-p)}, \quad (7.29)$$

  where F represents the quantile of the cumulative distribution F.

The control chart in this study was validated through Monte Carlo simulation, replicating the variability in product characteristics randomly based on the actual historical data set. A flexible process was simulated with four product families: A, B, C, and D. These families had 2, 3, 4, and 5 critical quality characteristics that required monitoring. The results obtained were as follows:

- The ARL chart indicates that a false alarm is generated for every 96 observations. In the case of a shift in the process, such as an upward shift in the average due to equipment variation, the chart takes an average of 42 observations to detect this shift. When there is a change of two standard deviations, the chart only needs one observation to trigger an alarm. The decreasing curve in the ARL graph demonstrates the expected performance, highlighting the graph's utility in detecting changes in process parameters.

7.3 Other techniques for monitoring multivariate profiles

In this section we will talk about three different approaches, where the monitoring of multivariate profiles occurs under a specific framework. In more detail, initially, we will refer to the study by Ahmadi Yazdi et al. (2019), which aims to assess the impact of parameter estimation on the performance of three Phase II approaches for monitoring multivariate simple linear profiles. Furthermore, we will mention the study of Ghashghaei et al. (2019), who used the exponentially weighted moving average semicircle (EWMA-SC) and generally weighted moving average semicircle (GWMA-SC) control charts to simultaneously monitor the mean vector and covariance matrix of multivariate multiple linear regression profiles in Phase II analysis. Finally, this module will develop the study by Park and Lee (2022), who monitored profiles in multistage processes using the multivariate multiple regression model.

7.3.1 The effect of parameter estimation on the performance of control charts in Phase II analysis

In certain statistical process monitoring applications, there is a common assumption that the process parameters are known during Phase II analysis. However, this assumption is often unrealistic, as in many practical situations, these parameters are unknown and need to be estimated using historical data in Phase I. More specifically, in the context of Phase II profile monitoring, it is frequently assumed that in – control parameters are known. The values of profile parameters are seldom known in practical environments and should be estimated during Phase I. Then, this assumption can impact the performance of control charts due to the additional variability introduced by parameter estimation. Ahmadi Yazdi et al. (2019) explores the impact of parameter estimation on three methods for monitoring multivariate simple linear profile data. The investigated approaches include the following control charts: a) the multivariate exponentially weighted moving average (MEWMA) control chart for monitoring profile parameters, b) a combination of a MEWMA control chart based on the vector of residual means and a chi-square (χ^2) chart for monitoring

process variability (MEWMA/χ^2), and c) a combination of three separate MEWMA control charts (MEWMA_3) for monitoring the vector of intercepts, the vector of slopes, and the process variability. Before we move on to the definition of the statistics of the above charts, we will define the model that will guide us through the rest of this study. Therefore, the multivariate simple linear regression model can be represented as:

$$Y_j = X\,B + E_j, \quad j = 1, 2, \ldots, \tag{7.30}$$

where Y_j is the n×p matrix of responses variables, X = [1 x] is a n×2 matrix of explanatory variables, x = (x_1, x_2, …, x_n), B = (β_{0j}, β_{1j})′ represents a 2×p matrix of regression coefficients and E_j is the n×p matrix of error terms. Here, it is assumed that the matrix B is unknown and should be estimated through in – control Phase I samples. Therefore, an estimation of B is given by:

$$\widehat{B_J} = (X'\,X)^{-1}\,X'\,Y_j = (\widehat{\beta_{0J}},\ \widehat{\beta_{1J}})', \quad j = 1, 2, \ldots, \tag{7.31}.$$

Please note that, the question is whether the estimation of parameter B has an impact on the efficacy of MEWMA, MEWMA_3, and MEWMA/χ^2 methods, initially designed under the assumption of known parameters. Thus, the aim is to identify which method exhibits greater resilience to the effects of parameter estimation.

The charting statistics of the above control charts are the following:

- For the statistic of the MEWMA control chart, we rewrite the B_j by a 1×2p vector as follows:

  $$\beta_j' = (\beta_{01j},\ \beta_{02j},\ \ldots,\ \beta_{0pj},\ \beta_{11j},\ \beta_{12j},\ \ldots,\ \beta_{1pj}), \tag{7.32}.$$

  So, the statistic for the MEWMA control chart is given by:

  $$T_{zj}^2 = Z_j\,\Sigma_{zj}^{-1}\,Z_j', \quad j = 1, 2, \ldots, \tag{7.33}$$

  with $Z_j = \lambda\,(\widehat{\beta_J} - \beta)' + (1 - \lambda)\,Z_{j-1}$, where λ is the smoothing parameter, Z_0 is a vector with zero entries, $\widehat{\beta_J}$ represents the estimation of β_j', β is the mean vector of β_j', $\Sigma_{zj} = [\,\lambda / (2 - \lambda)]\,\Sigma_{\hat{\beta}}$, and $\Sigma_{\hat{\beta}}$ is the covariance matrix of $\hat{\beta}$.
- The statistic for the MEWMA/χ^2 control chart is given by:

  $$T_{zj,e}^2 = Z_{j,e}\,\Sigma_{zj,e}^{-1}\,Z_{j,e}', \quad j = 1, 2, \ldots, \tag{7.34}$$

  with $Z_{j,e} = \lambda\,\overline{e_J} + (1 - \lambda)\,Z_{j-1,e}$, where $\overline{e_J}$ is the vector of the average error

for the j^{th} profile, $\Sigma_{zj,e} = [\ \lambda / n(2 - \lambda)]\ \Sigma$, and Σ represents the covariance matrix of E_j.

Please note that, $\chi_{ij}^2 = e_{ij}\ \Sigma^{-1}\ e_{ij}'$, i.e., χ_{ij}^2 statistic follows a Chi – square distribution.

- When $\bar{X} = 0$, the covariance between the estimated slope and intercept of the profile becomes zero as well. Consequently, the monitoring of regression parameters, along with process variability, can be effectively performed using three distinct control charts. In this scenario, the relationship between the explanatory and response variables for the i^{th} observation is expressed as:

$$y_{ij} = \beta_0^* + x_i^*\ \beta_1^* + \varepsilon_{ij},\ \ i = 1, 2, \ldots, n, \tag{7.35}$$

where $x_i^* = (x_i - \bar{x})$, $\beta_0^* = \beta_0$, $\beta_1^* = \beta_1 + \bar{x}\ J$, and J is a $1 \times p$ vector of 1´s.

The MEWMA_3 statistic for monitoring the intercept is given by:

$$T_{Ij}^2 = Z_{Ij}\ \Sigma_{ZI}^{-1}\ Z_{Ij}', \tag{7.36}$$

with $Z_{Ij} = \lambda\ (\widehat{\beta_{0J}}^* - \beta_0^*)' + (1 - \lambda)\ Z_{I(j-1)}$, where $\widehat{\beta_{0J}}^*$ represents the estimation of intercepts and $\Sigma_{ZI} = [\ \lambda / n(2 - \lambda)]\ \Sigma$.

The MEWMA_3 statistic for monitoring the profile slope is given by:

$$T_{Sj}^2 = Z_{Sj}\ \Sigma_{ZS}^{-1}\ Z_{Sj}', \tag{7.37}$$

with $Z_{Sj} = \lambda\ (\widehat{\beta_{1J}}^* - \beta_1^*)' + (1 - \lambda)\ Z_{S(j-1)}$, where $\widehat{\beta_{1J}}^*$ represents the estimation of intercepts, $\Sigma_{ZS} = [\ \lambda / S_{xx}\ (2 - \lambda)]\ \Sigma$ and $S_{xx} = \sum_{i=1}^{n}(x_i - \bar{x})^2$.

The MEWMA_3 statistic for monitoring the process variability is:

$$Z_{Ej} = max\{\lambda\ ln(\chi_j^2) + (1 - \lambda)\ Z_{E(j-1)},\ np\}, \tag{7.38}$$

with $\chi_j^2 = \sum_{i=1}^{n} e_{ij}\ \Sigma^{-1}\ e_{ij}'$.

Given that the ARL is no longer a fixed parameter under the assumption of estimated process parameters, three metrics, the average of ARL (AARL), the standard deviation of ARL (SDARL) and the coefficient of the variation of ARL (CVARL), are employed. The objective is to compare the methods and determine the most robust one in the face of the effects of parameter estimation. The results were obtained through simulation studies and were the following:

- Under in – control conditions, when more samples of Phase I are used to estimate the unknown parameter then the estimation leads to be better.

- Based on the AARL metric, the MEWMA/χ^2 performs better in most cases, as it exhibits higher AARL values. Moreover, the MEWMA_3 control chart in most cases it has higher AARL values compared to MEWMA and thus has greater efficiency.
- In general, it was observed that the AARL value increases when the value of the smoothing parameter increases.
- Selecting the superior method based on the SDARL metric is not straightforward in this case. However, it was observed that, the MEWMA_3 chart outperforms the other competing control charts in terms of the SDARL metric when $\lambda = 0.2$. Furthermore, for small values of samples, i.e., m = 10 and m = 70, the MEWMA/χ^2 chart has lower SDARL values, which signals greater effectiveness of this method.
- Utilizing the CVARL metric enables the consideration of both AARL and SDARL simultaneously in determining the superior method. While both the MEWMA_3 and MEWMA/χ^2 control charts outperform the MWEMA, the MEWMA_3 consistently exhibits superior performance compared to other competing charts. Additionally, the performance of the MEWMA_3 improves with an increase in the value of samples.
- When a shift in the intercept of the first profile (β_{01}) occurs, then the AARL measurement indicates that the performance of the MEWMA and MEWMA/χ^2 control charts consistently outperforms that of the MEWMA_3 across all values of m. It is worth noting that, the MEWMA/χ^2 chart exhibits superior performance to the MEWMA for small shifts, while their performances are comparable for large changes.
- When a shift in the intercept of the first profile (β_{01}) occurs, then the MWEMA chart shows the best performance in terms of the SDARL, as it has the smallest SDARL values. Moreover, similar results to MEWMA have the MEWMA/χ^2 control chart, which has greater efficiency than MEWMA_3.
- When a shift in the intercept of the first profile (β_{01}) occurs, then the MEWMA method performs better than the other competing methods in terms of the CVARL. However, it is worth noting that previous research by Noorossana et al. (2010) indicated that the MEWMA/χ^2 method

outperforms other methods in terms of ARL when parameters are known. Therefore, based on this observation we see that the performance of control charts changes, depending on whether the parameters of the model are known or estimated.

- When a shift in the slope of the first profile (β_{11}) occurs, then the evaluation of all three metrics, i.e., AARL, SDARL, CVARL, suggests that the MEWMA method outperforms the other competing methods. However, it's noteworthy that the MEWMA⁄χ^2 chart exhibits better performance in detecting very small shifts, particularly in terms of the CVARL metric. Please note that, both in case the parameters are known and, in the case, where the parameters are unknown and need to be estimated, the MEWMA control chart shows the greatest effectiveness.
- In general, the performance of the control chart approaches is significantly influenced by parameter estimation. Finally, the use of estimated parameters in calculating the control chart statistic requires a larger number of Phase I samples to achieve the same in-control performance as when parameters are known. However, obtaining more Phase I samples for parameter estimation improves detection performance.

7.3.2 Simultaneous monitoring of the mean vector and covariance matrix

Simultaneously monitoring the mean vector and covariance matrix in multivariate processes enables researchers to avoid the inflated false alarm rate associated with using two independent control charts. Ghashghaei et al. (2019), based on this philosophy, used the exponentially weighted moving average semicircle (EWMA-SC) and generally weighted moving average semicircle (GWMA-SC) control charts to simultaneously monitor the mean vector and covariance matrix of multivariate multiple linear regression profiles in Phase II. Then, the above control charts have only one statistic with one control limit to simultaneously monitor all the profile parameters. First, before proceeding to define the control charts used in this study, we will define the model on

which Ghashghaei et al. (2019) were based. Therefore, the multivariate multiple linear model is given as follows:

$$Y_j = X B + E_j, \quad j = 1, 2, \ldots \tag{7.39}$$

where Y_j is the n×p matrix of responses variables, X is the n×q+1 matrix of explanatory variables, B represents a (q+1)×p matrix of regression coefficients and E_j is the n×p matrix of error terms.

Note that, for the j^{th} sample, the least square estimator of matrix B is given by:

$$\widehat{B_J} = (X_j' X_j)^{-1} X_j' Y_j, \tag{7.40}.$$

Moreover, the matrix $\widehat{B_j}$ could be rewritten as a 1×(q+1)p random vector $\widehat{\beta_j}$, where $\widehat{\beta_j} = (\hat{\beta}_{01j}, \hat{\beta}_{11j}, \ldots, \hat{\beta}_{q1j}, \hat{\beta}_{02j}, \hat{\beta}_{12j}, \ldots, \hat{\beta}_{q2j}, \ldots, \hat{\beta}_{0pj}, \hat{\beta}_{1pj}, \ldots, \hat{\beta}_{qpj})$.

Based on the above model, the charting statistics of the proposed control charts are defined as follows:

- The exponentially weighted moving average semicircle (EWMA-SC) was originally developed by Chen et al. (2004) to monitor mean and variance of a univariate quality characteristic. Ghashghaei et al. (2019) extended the original idea of Chen et al. (2004) with the goal of simultaneously monitoring mean vector and covariance matrix of multivariate multiple linear regression profiles in Phase II analysis. Therefore, the proposed charting statistic is defined as follows:

  $$U_j = \lambda T_j + (1 - \lambda) U_{j-1}, \quad j = 1, 2, \ldots, \tag{7.41}$$

  with $T_j = Z_j + W_j$, where $\lambda \in (0, 1]$ represents the smoothing parameter, $U_0 = p(n + q + 1)$, $Z_j = (\widehat{\beta_j} - \beta)' \Sigma_{\widehat{\beta_j}}^{-1} (\widehat{\beta_j} - \beta)$, β is the expected value of $\widehat{\beta_j}$, $\Sigma_{\widehat{\beta_j}}$ is the covariance matrix of $\widehat{\beta_j}$, $W_j = \sum_{i=1}^{n} (y_{ij} - x_i B) \Sigma^{-1} (y_{ij} - x_i B)'$ and Σ represents the covariance matrix of E_j.

  Furthermore, the upper control limit of this chart is given as follows:

  $$UCL = p(n + q + 1) + L \sqrt{\frac{2p\lambda [1 - (1 - \lambda)^{2j}]}{(2 - \lambda)} (n + q + 1)}, \tag{7.42}$$

  where the value of L is determined by the value of the in – control ARL given by each researcher.

- The generally weighted moving average semicircle (GWMA-SC) control chart originally developed by Sheu et al. (2009) in order to monitor mean

and variance in the situation where an individual observation is taken over time. Ghashghaei et al. (2019) extended the original concept of Sheu et al. (2009) for the purpose of simultaneous monitoring of mean vector and covariance matrix of multivariate multiple linear regression profiles in Phase II analysis. Therefore, the proposed charting statistic is given by:

$$V_j = \sum_{t=1}^{j}(\theta^{(t-1)^\alpha} - \theta^{t^\alpha})\, T_{j-t+1} + \theta^{j^\alpha} V_0,\ \mathrm{j} = 1, 2, \ldots, \qquad (7.43)$$

where $T_j = Z_j + W_j$ as previous, $V_0 = p\,(n + q + 1)$, θ $(0 < \theta < 1)$ is the design parameter which is constant and $\alpha \in (0, 1]$ represents the adjustment parameter determined by the researcher.

Furthermore, the upper control limit of this chart is given as follows:

$$UCL = p\,(n + q + 1) + L^* \sqrt{2p\,(n + q + 1)\,Q}\,, \qquad (7.44)$$

where the value of $L^* > 0$ is determined by the value that each researcher will give to the in – control ARL and $Q = \lim_{j \to \infty}\{\sum_{t=1}^{j}(\theta^{(t-1)^\alpha} - \theta^{t^\alpha})^2\}$.

Of particular interest is the comparison made between the two proposed control charts developed above with three other existing EWMA-based charts. More specifically, EWMA-SC and GWMA-SC are compared with the following control charts: a) the EWMA-based generalized likelihood ratio (ELR) control chart proposed by Eyvazian et al. (2011), who developed four methods to monitor multivariate multiple linear regression profiles in Phase II analysis, b) the sum of squares EWMA-based (SS-EWMA) control chart proposed by Ghashghaei and Amiri (2017b) in order to identify the out-of-control parameter responsible for a shift in the process, and c) the maximum multivariate exponentially weighted moving average (Max-MEWMA) control chart proposed by Ghashghaei and Amiri (2017a) to monitor mean vector and covariance matrix simultaneously. The comparison between the above control charts was made with the help of the ARL performance criterion and the results were as follows:

- When a shift in the intercept of the first profile occurs, then the GWMA-SC chart shows enhanced performance as parameter θ increases, although the influence of α is not consistently ordered.

Furthermore, the EWMA-SC control chart performs better with $\lambda = 0.2$ compared to other λ values. It is worth noting that, the GWMA-SC control chart outperforms the EWMA-SC chart only for $\theta = 0.8$ and 0.9.

- When a shift in the standard deviation of the first profile occurs, the two proposed charts show better results than the three existing control charts. In particular, the GWMA-SC chart shows slightly better efficiency than the EWMA-SC for small and moderate shifts, while for large changes the two control charts perform similarly. Moreover, while it is accurate to state that the performance of all control charts improves when the level of correlation parameter increases, the proposed control charts consistently demonstrate superior performance.
- When a shift in the intercept of the first profile occurs, for large changes the two proposed charts are more effective than the ELR, SS-EWMA and Max-MEWMA control charts. Moreover, similar results arise for moderate shifts if the level of the correlation parameter is equal to 0.5. However, for small changes in the intercept the SS-EWMA is the one that has the greatest efficiency and performance. Please note that, similar results are obtained in case which a change occurs in the slope of the first profile.
- When simultaneous changes occur in the intercept and standard deviation of the first profile, then both EWMA-SC and GWMA-SC charts perform better than the other three control charts, for any size of change and for any degree of correlation.
- When a shift in the intercept of the second profile occurs, then the proposed control charts show better results for large shifts than the rest of the charts, with GWMA-SC being a bit better than EMWA-SC in most cases. Moreover, when the value of correlation parameter is equal to 0.9 (strong correlation) then the proposed charts perform better than the other three control charts for moderate shifts, since they have smaller ARL values. Finally, for small changes the SS-EWMA control chart was observed to perform best in most cases and thus is able to detect a small change faster.

7.3.3 Monitoring profiles in multistage processes

In modern production processes, the quality of final products is often influenced by multiple stages, emphasizing the importance of effective profile monitoring across these stages. To achieve this, a multistage process is dissected into individual single-stage processes, each treated as a profile structure. In each stage, Park and Lee (2022) implemented the multivariate multiple linear regression model using orthogonal design coding. The utilization of orthogonal design coding ensures independence among the row vectors of the coefficient estimator matrix, allowing for the independent monitoring of the process. This independence is crucial for effectively assessing each stage of the multistage process, contributing to enhanced control and quality assurance. Below will be briefly given the model that will be used in this study as well as the idea of constructing the proposed control chart for monitoring such multistage processes.

For a specific stage of the multistage process, sequential samples are collected for monitoring. In this context, P input variables are represented as $\{x_1, x_2, \ldots, x_P\}$ and K output quality variables are denoted as $\{y_1, y_2, \ldots, y_K\}$. Assuming that the conditional distribution of output quality variables given input variables follows a multivariate normal distribution with a mean vector $\mu = (\mu_1, \mu_2, \ldots, \mu_K)'$ and a covariance matrix Σ, the observed output quality vectors are $\{y_k = (y_{1k}, y_{2k}, \ldots, y_{nk})', k = 1, 2, \ldots, K\}$ and the observed input vectors are $\{x_p = (x_{1p}, x_{2p}, \ldots, x_{np})', p = 1, 2, \ldots, P\}$. For an in – control process sample of size n, the sample in – control process model for a given stage is expressed as a multivariate multiple linear regression model:

$$Y = X\beta + \varepsilon, \tag{7.45}$$

where $Y = (y_1, y_2, \ldots, y_K)$, $X = (1, x_1, x_2, \ldots, x_P)$, $\beta = (\beta_1, \beta_2, \ldots, \beta_K)'$ represents the coefficient matrix and ε is the error matrix.

The fitted model for Eq. (7.45) could be written as follows:

$$\hat{Y} = XB, \tag{7.46}$$

where $\hat{Y} = (\hat{y}_1, \hat{y}_2, \ldots, \hat{y}_K)$ and $B = (b_1, b_2, \ldots, b_K)'$ represents the coefficient least square estimator matrix.

Moreover, the least squares estimators for the k^{th} column of B are given by:

$$b_k = (X' X)^{-1} X' y_K, \quad (7.47).$$

Please note that, the design matrix X is properly formed to become orthogonal, or near orthogonal, and then, the independence of row vectors in matrix B enables the monitoring of a given stage using (P+1) independent multivariate control charts with K variables.

Based on the above model, the proposed charting statistic has the following form:

$$T_{pt}^2 = (b_{pt} - \bar{b}_p)\, S_p^{-1}\, (b_{pt} - \bar{b}_p)', \; p = 0, 1, \ldots, P, \; t = 1, 2, \ldots, \quad (7.48)$$

where b_{pt} represents the coefficient estimator vector for the p^{th} coefficient at sample t, $\bar{b}_p$ is the mean vector of the b_{pt} and S_p represents the covariance matrix for the p^{th} regression coefficient.

It is worth noting that, the control limits vary depending on Phase I or Phase II that we will apply the proposed control chart. Therefore, in Phase I analysis the control limit for the proposed chart follows a Beta distribution, while in Phase II follows a F distribution. Finally, the efficiency of the proposed control chart was examined through a simulation study, the results of which were as follows:

- Based on the ARL metric, when a large change occurs in only one of the regression coefficients then the proposed T^2 chart has the ability to detect it quickly and efficiently, while for small and moderate shifts it is considered ineffective.
- Similar results are obtained in the case of shifts occurring in two regression coefficients, with the T^2 control chart being sensitive to large shifts, while for smaller changes its performance is not good.
- Comparing the performance of the proposed chart in cases where changes occur in only one of the regression coefficients and in two regression coefficients, respectively, it was observed that in the latter case the T^2 chart shows better results, as it can detect shifts faster and more correctly.

CHAPTER 8

Conclusions and further research

Profile monitoring is a statistical technique employed to assess the stability of functional relationships between response and explanatory variables over time. Specifically, through statistical analysis, profile monitoring helps identify any deviations or changes in the relationships, enabling timely interventions and maintaining process stability. Since this technique is a relatively new area in statistical process control, Woodall's review paper (2007) is an important contribution and paved the way for the publication of an increasing number of papers in this area. This growing trend was framed in the detailed review paper of Maleki et al. (2018), almost a decade later than Woodall's remarkable paper, which presents a classification scheme and classify the papers in this area since 2008 up to 2018. However, after these two review papers, there is no document summarizing recent research in profiling. Therefore, the purpose of this thesis was to fill this scientific gap by gathering and discussing recent studies and trends around profile monitoring, especially in the period after 2018. Finally, the discussion takes place around the main types of profiles, i.e., simple linear, generalized linear, generalized linear mixed, geometric, polynomial, nonlinear, nonparametric and multiple profiles, respectively, the conclusions of which are presented below.

Initially, this thesis presented recent studies, research and developments for monitoring simple linear profiles, the most popular type of profile. In the first place, two methods aimed at simultaneous shifts in the profile parameters were examined. These approaches were by Saeed et al. (2018), who used a memory type chart based on progressive mean, and Yeganeh et al. (2021), who constructed a MEWMA control chart with a set of new run-rules. It was observed that the two new proposed control charts perform more effectively in monitoring simple linear profiles than existing charts, for example the EWMA_3 and the Hotelling´s T^2 chart. Interestingly, the comparison made

between these two recent methods, where the approach by Yeganeh et al. (2021) was judged better at detecting changes. Of course, the study by Saeed et al. (2018) shows quite good performance, which gives rise to interest in extending it to other types of profiles, such as nonlinear profiles. Furthermore, useful conclusions were also obtained from the studies of Hassanvand et al. (2019), Salmasnia et al. (2019) and Moheghi et al. (2020), which use robust estimators to estimate regression parameters. Through these studies, the performance of ordinary least squares estimators is compared with robust estimation methods, assuming the existence of outliers, showing the superiority of robust estimators in detecting different types of shifts. Further research that could expand the study by Hassanvand et al. (2019), who examined monitoring simple linear profiles for multistage processes, is the profiling study for multivariate or multiple linear profiles using robust estimation methods. Another interesting extension would be to compare the above profiles between the performances of robust approaches and extensions of ordinary least square method. This chapter closed by discussing the studies of Aytaçoğlu, B., and Bayrak, Ö. T. (2019), Abbas et al. (2019) and Yeganeh et al. (2023), which concerned the effect of both estimation and violation of normality assumption, the monitoring of simple linear models with one random explanatory variable in the Bayesian framework, where it was observed that the Bayesian EWMA chart is capable of detecting small shifts in the process parameters more quickly, and the proposal of a new scheme to financial market monitoring, respectively. Further research that could extend the study of Abbas et al. (2019) is the profiling study for generalized multivariate setups, where the model would consist of multiple response and random independent variables and would be examined under Bayesian framework. Finally, the study by Yeganeh et al. (2023) based on the CCPM method could be studied and researched to extend and draw interesting conclusions regarding parameter shifts with profile diagnosis techniques. Moving on to the next chapter, interest turned to generalized linear and generalized linear mixed profiles. In the framework of robust estimators, the study by Moheghi et al. (2021) was initially presented, focusing on logistic and Poisson profile monitoring aiming at reducing the presence of outliers and estimating regression parameters. Making a comparison with maximum likelihood estimators (MLEs), it was observed that robust estimators are more

accurate and effective, do not show sensitivity to the presence of outliers in Phase I and detect shifts in Phase II analysis faster. Significant results were conducted from the studies of Nassar and Abdel-Salam (2022) and Bandara et al. (2020), where the former monitored linear mixed models using the semiparametric MRR2 technique while the latter examined the monitoring of generalized linear mixed profiles with a semiparametric method using binomial distribution for the response variables and the T^2 charting statistic. These semiparametric methods were compared with their nonparametric and parametric counterparts, concluding that the proposed semiparametric methods were more sensitive to detecting changes and provided better and more accurate estimates of profile parameters. It is worth noting that, further research that could expand the study of Bandara et al. (2020) is the profile monitoring study for generalized linear mixed models where the distribution of the response variable will be different from the binomial, but will belong to the family of exponential distribution, say Poisson or gamma distributions. Furthermore, through the study of Mohamed et al. (2022), who monitored profiles under gamma regression models, it was observed that the EWMA control chart based on deviance residuals was judged more effective, with better performance and more accurate results than the EWMA chart based on Pearson residuals. Moreover, the study by Mohammadzadeh et al. (2021), which concerned the monitoring of logistic profiles using variable sample interval approach, proved that the use of sample intervals as variables improves the performance of control charts as mainly small and moderate shifts are detected faster than if sampling intervals are considered fixed. The use of other approaches such as variable sample size, i.e., the sample size to behave as variable rather than fixed, to evaluate the performance of appropriate control charts in Phase II analysis and comparison with methods using constant sample sizes are suggested for the future research. Finally, Liu et al. (2018) developed a new scheme for surgical outcomes based on EWMA control charts, which was compared to the RA-CUSUM chart. The above control charts were used to detect upward and downward shifts simultaneously, with the proposed EWMA chart performing better for monitoring random effects belonging within the same group.

Moving on to the fifth chapter, interest turned to geometric and polynomial profiles. Zhao et al. (2020) examined circular and cylindrical profiles, respectively, using T^2 and Shewhart control charts for monitor the variance of error term under spatial correlations. The proposed methods, one for each type of the above geometric profiles, were compared with the already existing OOR, LOC, SARX and PCA approaches. The results highlighted the new proposed methods and the SARX approach as the most effective, while the OOR method was considered less efficient. An important conclusion was that methods using spatial correlations perform better, more efficiently and show greater accuracy to detect changes in the profile parameters. Of course, the proposed method for cylindrical profile was observed to show better results than the method for circular profile, as the detection rate was higher. It is worth mentioning that, in the future, the above methods could be generalized for other geometric specifications or even used to monitor nonparametric profiles. Also, an interesting suggestion for future study would be to use other control charts, say EWMA and CUSUM, instead of T^2 and residual charts and compare their results. Through the study by Song et al. (2023), who monitored polynomial profiles in the presence of attribute responses and between-profile correlation, it was observed that the proposed dEWMA chart with dynamic control limits and not constant performs better than GLR and iEWMA charts. It is concluded that the dynamic nature in the dEWMA achieves accuracy and efficiency by reducing the frequency of false alarms. Effectively monitoring profiles with attribute responses, considering both within – and between – profile correlations, remains a challenging yet valuable research area. Exploring the monitoring of autocorrelated nonparametric profiles with attribute responses deserves further investigation. Further studies are also needed for Phase I analysis of profiles with attribute responses in the presence of between-profile correlation. Furthermore, studies by Yao et al. (2020) and Atashgar and Abbassi (2021), which concerned monitoring polynomial profiles for simultaneous shifts in the regression parameters, proposed WLRT and MGWMA-PF methods, respectively, and compared them with already existing control charts, was discussed. Yao et al. (2020) proved that the WLRT and Ortho control charts performed the best, while the T^2 chart proved to be the least effective. Moreover, in the research of Atashgar and Abbassi (2021) the proposed

MGWMA-PF chart was capable of detecting very small shift types effectively and was the most effective, compared to other existing methods of the literature. It is worth noting that, MGWMA-PF performs better when shifts occur in the profile intercept than the WLRT approach. Moving on to examine the impact of Phase II control chart performance from various factors, the study by Ghasemi Eshkaftaki et al. (2021) emphasizes that the accuracy of Phase II monitoring directly depends on the parameter estimation that will be made during the Phase I analysis. It was observed that when estimated parameters are used, then the performance and effectiveness of both Phase I and Phase II analysis is significantly better compared to when known parameters are used. Furthermore, the F method was considered more effective for parameter estimation than the T^2 approach because the former has the ability to improve the performance of control charts in Phase II. Also noteworthy was the research of Liu et al. (2023), who showed that the effect of ignoring measurement errors significantly affects the ability to detect changes in control charts. In an effort to mitigate this effect, they reconstructed the charts they used in their study, i.e., the dMEWMA, MCUSUM, MEWMA and T^2 charts, using consistent MALS and ALS estimators. It turned out that the MALS-based charts perform better than the ALS-based control charts. However, ignorance of measurement errors still has a significant impact on the performance of Phase II analysis. Thus, two remedial approaches were proposed to reduce the impact of measurement errors, which proved to be extremely important. Closing this chapter, the study by Netshiozwi et al. (2023) concludes that if every business follows the five proposed steps, i.e., model estimation, model verification, Phase I analysis, Phase II analysis, signal interpretation, then it will be able to recognize abnormal situations correctly and accurately.

The next chapter aimed to examine and conduct results on monitoring nonparametric profiles. Initially, in the context of change point detection methods, the study of Li et al. (2019) was presented, who proposed a rank-based EWMA control chart using SVR model. It turned out that the proposed chart in combination with the M_2, M_3 and M_5 metrics, respectively, performs better than the M_1 and M_4 metrics. Almost two years later, Iguchi et al. (2021) developed a l_2-based statistic of SIM coefficients and compared the results with

those of Li et al. (2019). Simulation studies have shown that the non-rank-based monitoring procedure of Iguchi et al. (2021) shows superior performance, better results and a lower false alarm rate compared to the method of Li et al. (2019), which despite its excellent speed to detect a change is considered a little less effective. Furthermore, excellent results and basis for future research were provided by the studies of Zhou and Qiu (2022) and Ding et al. (2024), respectively, which included correlation in profile monitoring. Specifically, the study by Zhou and Qiu (2022) centers on Phase I monitoring of univariate profile data under serially correlation. The research showed that the proposed method performs better than existing nonparametric approaches, mainly under between-profile correlation. There is a potential avenue for further research, exploring the generalization of the proposed method for Phase II monitoring, encompassing both univariate and multivariate profiles, particularly in situations where both between-profile and within-profile data correlation are present. The very recent study by Ding et al. (2024) examines the results of the EWMA control chart constructed with ED, Area and T^2 statistics, respectively. The Area statistic could detect larger changes more quickly and has generally been shown to perform better than ED statistic, which in turn shows better results than T^2. Moreover, the EWMA control chart built with Area statistic was judged to be slightly more efficient and more sensitive to process shifts compared to the EWMA chart with ED statistic. Notably, the results were based on only one covariate. Thus, further work could include more covariates in the proposed model. Furthermore, the Gaussian process-based profiling model proposed in this study effectively addresses within-profile correlation. One suggestion for further research is to explore advanced machine learning approaches for modeling between-profile correlation. Moving on to studies looking at monitoring both regression parameters and profile variance, Abbasi et al. (2022) and Yeganeh et al. (2022) proposed an adaptive NEWMA control chart based on relative distance and a NEWMA control chart based on ANNs, respectively. Both proposed charts improve the performance and ability to detect changes of the original NEWMA chart and were judged to be more effective than NEWMA, which in turn appeared to perform better than PM, NM and EWMA_3 control charts. Furthermore, another interesting study was that of Varbanov et al. (2019), who compared their proposed method, the WBB, with

the LRT approach. The results showed that the WBB approach has a lower false alarm rate, lower variability, accurately detects the location of the change and, in general, has superior performance compared to the LRT method, mainly for smaller shifts. Finally, this chapter closed with the study by Deng et al. (2022), who investigated the monitoring of the health condition of rotating machines, proposing the T^2 indicator. The results of the survey highlighted the new health indicator as the most effective for detecting an early fault in relation to negative entropy, kurtosis, Gini index and smoothness index indicators, respectively. Reaching the final chapter of this thesis, the focus turned around monitoring multivariate profiles. Under the PCA framework, Wang et al. (2018) examined multichannel profile monitoring during Phase I analysis and demonstrated that their proposed PCA method exhibits superior performance than the method of Paynabar et al. (2016), which is a special case of the new approach. The above efficiency is because the new method has the ability to detect the true change point with greater accuracy and efficiency compared to the specific method of Paynabar et al. (2016). A topic for future research is to extend the new method for profile monitoring during Phase II analysis. Furthermore, the study by Ren et al. (2019) proposed a new EWMA scheme based on MFPCA, which was shown to show better results than other existing methods for monitoring multivariate profiles in Phase II analysis. In fact, the new PCEWMA control chart, as it was called, was observed to perform equally well for either weak or strong between-profile correlation. Of particular interest was the study by Herzer et al. (2023), who focused on an application in product portfolio management proposing four steps for the benefit of companies. The new multivariate profile monitoring process using the four proposed steps has been shown to be able to recognize changes faster compared to standard multivariate monitoring procedures, as it has greater speed and, thus, occupies faster the available information for making effective decisions. A general conclusion that emerged from the above studies was that PCA-based approaches capture significant information from multichannel profiles and, therefore, are extremely useful and effective. Moreover, moving on to research investigating correlation in profile monitoring, the study by Khalili and Noorossana (2021) was first discussed. They tested the multivariate linear mixed model by constructing the MEWMA chart to identify shifts in the fixed effects, while the

MEWMC control chart was constructed to monitor the covariance matrix. The results showed that for shifts in the profile intercept and slope, the above recommended charts perform better mainly for strong between-responses and within-profile correlations, while for changes in the standard deviation it was observed that these control charts provide better results for strong correlation between responses and weak autocorrelation coefficient. Furthermore, in most cases the MEWMC performed superior to the MEWMA control chart. It is worth noting that, the motivation behind the development of the combined method of Khalili and Noorossana (2021) was to monitor the process mean vector and covariance matrix simultaneously. However, diagnosing out – of – control parameters need further investigation and could be a subject of future studies. Moreover, Rodrigues et al. (2021) presented a statistical procedure for process monitoring in flexible environments based on the T^2 control chart. The results showed that the new proposed scheme is capable of detecting changes in the process parameters correctly and effectively. Moving towards the end of this chapter, the study by Ghashghaei et al. (2019), who proposed EWMA-SC and GWMA-SC control charts for simultaneous monitoring of the mean vector and covariance matrix, was discussed. In these recommended charts all of the profile parameters are monitored by only one statistic. Simulation studies have shown that for shifts in the standard deviation, new control charts are more efficient than existing EWMA-based charts, while in cases where changes are made in the profile intercept and slope, the proposed control charts were superior for large shifts. Moreover, Park and Lee (2022) proposed a T^2 charting statistic for examining multi-stage processes using orthogonal design coding, which proved more effective in detecting larger changes in the profile parameters. Finally, Ahmadi Yazdi et al. (2019) studied the effect on parameter estimation, an issue of major importance in profiling. For this reason, this effect was examined in MEWMA, MEWMA\$\chi^2$ and MEWMA_3 control charts and their performances were evaluated in terms of AARL, SDARL and CVARL metrics. These performance criteria were used instead of the well-known ARL metric, as the latter ceases to behave as a parameter due to the estimated parameters. Under in-control conditions, the performance of control charts varied depending on the evaluation criterion. More specifically, based on AARL metric it was observed that the MEWMA\$\chi^2$ chart showed the best results

compared to the other two control charts. On the other hand, the choice for superior performance is not so clear in terms of SDARL metric. However, the results of simulation studies showed that when the smoothing parameter λ is equal to 0.2 then the MEWMA_3 chart is judged to be the most effective, while for small values of samples better results are presented by the MEWMA\χ^2 control chart. Moreover, research showed that, using the CVARL metric, the MEWMA_3 chart uniformly performs better than the other control charts. Finally, by evaluating the performance of the above charts under out – of – control conditions, the study proved that the MEWMA control chart is the one that has the most effectiveness and performs better compared to the rest of the charts for all possible scenarios. Of course, a topic for future research is to propose new performance criteria to better measure the effect of parameter estimation, which is extremely useful for evaluating the performance of control charts and the appropriate selection of superior methods.

References

Abbas, T., Abbasi, S. A., Riaz, M., & Qian, Z. (2019). Phase II monitoring of linear profiles with random explanatory variable under Bayesian framework. *Computers & Industrial Engineering*, *127*, 1115-1129.

Abbasi, S. A., Yeganeh, A., & Shongwe, S. C. (2022). Monitoring non-parametric profiles using adaptive EWMA control chart. *Scientific Reports*, *12*(1), 14336.

Ahmadi Yazdi, A., Hamadani, A. Z., & Amiri, A. (2019). Phase II monitoring of multivariate simple linear profiles with estimated parameters. *Journal of Industrial Engineering International*, *15*, 557-570.

Alkahtani, S., & Schaffer, J. (2012). A double multivariate exponentially weighted moving average (dMEWMA) control chart for a process location monitoring. *Communications in Statistics-Simulation and Computation*, *41*(2), 238-252.

Atashgar, K., & Abbassi, L. (2021). A new model to monitor very small effects of a polynomial profile. *International Journal of Quality & Reliability Management*, *38*(4), 1023-1043.

Aytaçoğlu, B., & BAYRAK, Ö. T. (2019). Effect of Estimation on Simple Linear Profile Monitoring under Non-normality. *Süleyman Demirel Üniversitesi Fen Bilimleri Enstitüsü Dergisi*, *23*(1), 251-262.

Bandara, K., Abdel-Salam, A. S. G., & Birch, J. B. (2020). Model robust profile monitoring for the generalized linear mixed model for Phase I analysis. *Applied Stochastic Models in Business and Industry*, *36*(6), 1037-1059.

Boonpakdee, D., Yévenes, C. F. G., & Surareungchai, W. (2018). Exploring non-linearities of carbon-based microsupercapacitors from an equivalent circuit perspective. *Journal of Materials Chemistry A*, *6*(16), 7162-7167.

Bramwell, S. T., Holdsworth, P. C. W., & Pinton, J. F. (1998). Universality of rare fluctuations in turbulence and critical phenomena. *Nature*, *396*(6711), 552-554.

Cantoni, E., & Ronchetti, E. (2001). Robust inference for generalized linear models. *Journal of the American Statistical Association*, *96*(455), 1022-1030.

Chakraborti, S., Human, S. W., & Graham, M. A. (2008). Phase I statistical process control charts: an overview and some results. *Quality Engineering*, *21*(1), 52-62.

Chen, G., Cheng, S. W., & Xie, H. (2004). A new EWMA control chart for monitoring both location and dispersion. *Quality Technology & Quantitative Management*, *1*(2), 217-231.

Chen, C., Zong, S., Liu, Y., Wang, Z., Zhang, Y., Chen, B., & Cui, Y. (2019). Profiling of exosomal biomarkers for accurate cancer identification: Combining DNA-PAINT with machine-learning-based classification. *Small*, *15*(43), 1901014.

Cheng, C. L., & Schneeweiss, H. (1998). Polynomial regression with errors in the variables. *Journal of the Royal Statistical Society: Series B (Statistical Methodology)*, *60*(1), 189-199.

Cheng, C. L., Schneeweiss, H., & Thamerus, M. (2000). A small sample estimator for a polynomial regression with errors in the variables. *Journal of the Royal Statistical Society Series B: Statistical Methodology*, *62*(4), 699-709.

Chicken, E., Pignatiello Jr, J. J., & Simpson, J. R. (2009). Statistical process monitoring of nonlinear profiles using wavelets. *Journal of Quality Technology*, *41*(2), 198-212.

Crosier, R. B. (1988). Multivariate generalizations of cumulative sum quality-control schemes. *Technometrics*, *30*(3), 291-303.

Delcanale, P., Miret-Ontiveros, B., Arista-Romero, M., Pujals, S., & Albertazzi, L. (2018). Nanoscale mapping functional sites on nanoparticles by points accumulation for imaging in nanoscale topography (PAINT). *ACS nano*, *12*(8), 7629-7637.

Deng, Y., Hou, B., Chen, Y., & Wang, D. (2022, November). Nonparametric nonlinear profile monitoring method for machine condition monitoring. In *Journal of Physics: Conference Series* (Vol. 2369, No. 1, p. 012096). IOP Publishing.

Ding, N., He, Z., He, S., & Song, L. (2024). Real-time profile monitoring schemes considering covariates using Gaussian process via sensor data. *Quality Technology & Quantitative Management*, *21*(1), 35-53.

Elfadaly, F. G., & Garthwaite, P. H. (2015). Eliciting prior distributions for extra parameters in some generalized linear models. *Statistical Modelling*, *15*(4), 345-365.

Eyvazian, M., Noorossana, R., Saghaei, A., & Amiri, A. (2011). Phase II monitoring of multivariate multiple linear regression profiles. *Quality and Reliability Engineering International*, *27*(3), 281-296.

Garthwaite, P. H., Al-Awadhi, S. A., Elfadaly, F. G., & Jenkinson, D. J. (2013). Prior distribution elicitation for generalized linear and piecewise-linear models. *Journal of Applied Statistics*, *40*(1), 59-75.

Ghasemi Eshkaftaki, Z., Zeinal Hamadani, A., & Ahmadi Yazdi, A. (2021). Evaluating Parameter Estimation Effect on the Polynomial Profile Monitoring Methods' Phase II Performance. *Advances in Industrial Engineering*, *55*(2), 133-150.

Ghashghaei, R., & Amiri, A. (2017a). Maximum multivariate exponentially weighted moving average and maximum multivariate cumulative sum control charts for simultaneous monitoring of mean and variability of multivariate multiple linear regression profiles. *Scientia Iranica*, *24*(5), 2605-2622.

Ghashghaei, R., & Amiri, A. (2017b). Sum of squares control charts for monitoring of multivariate multiple linear regression profiles in phase II. *Quality and Reliability Engineering International*, *33*(4), 767-784.

Ghashghaei, R., Amiri, A., & Khosravi, P. (2019). New control charts for simultaneous monitoring of the mean vector and covariance matrix of

multivariate multiple linear profiles. *Communications in Statistics-Simulation and Computation*, *48*(5), 1382-1405.

Hassanvand, F., Samimi, Y., & Shahriari, H. (2019). A robust control chart for simple linear profiles in two-stage processes. *Quality and Reliability Engineering International*, *35*(8), 2749-2773.

Herzer, R., Korzenowski, A. L., Richter, C., de Medeiros, J. F., Goecks, L. S., & Mareth, T. (2023). Multivariate Profile Monitoring Method: An Application in Product Portfolio Management. *Periodica Polytechnica Social and Management Sciences*, *31*(1), 52-62.

Hosseinifard, S. Z., Abdollahian, M., & Zeephongsekul, P. (2011). Application of artificial neural networks in linear profile monitoring. Expert Systems with Applications, 38(5), 4920–4928.

Huang, G., Lin, G., Zhu, Y., Duan, W., & Jin, D. (2020). Emerging technologies for profiling extracellular vesicle heterogeneity. *Lab on a Chip*, *20*(14), 2423-2437.

Huwang, L., Wang, Y.-H.-T., Xue, S., & Zou, C. (2014). Monitoring general linear profiles using simultaneous confidence sets schemes. Computers & Industrial Engineering, 68, 1–12.

Iguchi, T., Barrientos, A. F., Chicken, E., & Sinha, D. (2021). Nonlinear profile monitoring with single index models. *Quality and Reliability Engineering International*, *37*(7), 3004-3017.

Jain, K., Singh, S., & Sharma, S. (2011). Restricted estimation in multivariate measurement error regression model. *Journal of multivariate analysis*, *102*(2), 264-280.

Jensen, W. A., Birch, J. B., & Woodall, W. H. (2008). Monitoring correlation within linear profiles using mixed models. *Journal of Quality Technology*, *40*(2), 167-183.

Kang, L., & Albin, S. L. (2000). On-line monitoring when the process yields a linear profile. Journal of Quality Technology, 32(4), 418–426.

Kazemzadeh, R. B., Noorossana, R., & Amiri, A. (2008). Phase I monitoring of polynomial profiles. *Communications in Statistics—Theory and Methods*, *37*(10), 1671-1686.

Kazemzadeh, R. B., Noorossana, R., & Amiri, A. (2009). Monitoring polynomial profiles in quality control applications. *The International Journal of Advanced Manufacturing Technology*, *42*, 703-712.

Khalili, S., & Noorossana, R. (2021). Phase II monitoring of auto-correlated linear profiles using multivariate linear mixed model. *International Journal of Industrial Engineering*, *32*(1), 1-11.

Kim, K., Mahmoud, M. A., & Woodall, W. H. (2003). On the monitoring of linear profiles. Journal of Quality Technology, *35*(3), 317–328.

Li, C. I., Pan, J. N., & Liao, C. H. (2019). Monitoring nonlinear profile data using support vector regression method. *Quality and Reliability Engineering International*, *35*(1), 127-135.

Liu, L., Lai, X., Zhang, J., & Tsung, F. (2018). Online profile monitoring for surgical outcomes using a weighted score test. *Journal of Quality Technology*, *50*(1), 88-97.

Liu, W., Li, Z., & Wang, Z. (2023). Remedial approaches to decrease the effect of measurement errors on polynomial profile monitoring. *Communications in Statistics-Simulation and Computation*, 1-15.

Lowry, C. A., Woodall, W. H., Champ, C. W., & Rigdon, S. E. (1992). A multivariate exponentially weighted moving average control chart. *Technometrics*, *34*(1), 46-53.

Mahmoud, M. A., Parker, P. A., Woodall, W. H., & Hawkins, D. M. (2007). A change point method for linear profile data. *Quality and Reliability Engineering International*, *23*(2), 247-268.

Maleki, M. R., Amiri, A., & Castagliola, P. (2018). An overview on recent profile monitoring papers (2008–2018) based on conceptual classification scheme. *Computers & Industrial Engineering*, *126*, 705-728.

Mathis, T. S., Kurra, N., Wang, X., Pinto, D., Simon, P., & Gogotsi, Y. (2019). Energy storage data reporting in perspective—guidelines for interpreting the performance of electrochemical energy storage systems. *Advanced Energy Materials*, *9*(39), 1902007.

Mays, J. E., Birch, J. B., & Einsporn, R. L. (2000). An overview of model-robust regression. *Journal of statistical computation and simulation*, *66*(1), 79-100.

Mohamed, S. M., Abozaid, E. S., & Latif, S. H. A. (2022). Profile Monitoring of Residuals Control Charts Under Gamma Regression Model. *Eastern-European Journal of Enterprise Technologies*, *6*(4), 120.

Mohammadzadeh, M., Yeganeh, A., & Shadman, A. (2021). Monitoring logistic profiles using variable sample interval approach. *Computers & Industrial Engineering*, *158*, 107438.

Moheghi, H. R., Noorossana, R., & Ahmadi, O. (2021). GLM profile monitoring using robust estimators. *Quality and Reliability Engineering International*, *37*(2), 664-680.

Moheghi, H. R., Noorossana, R., & Ahmadi, O. (2022). Phase I and phase II analysis of linear profile monitoring using robust estimators. *Communications in Statistics-Theory and Methods*, *51*(5), 1252-1269.

Montgomery, D. C. (2007). *Introduction To Statistical Quality Control*. John Wiley & Sons.

Motasemi, A., Alaeddini, A., & Zou, C. (2017). An area-based methodology for the monitoring of general linear profiles. Quality and Reliability Engineering International, *33*(1), 159–181.

Nassar, S. H., & Abdel-Salam, A. S. G. (2022). Robust profile monitoring for phase II analysis via residuals. *Quality and Reliability Engineering International*, *38*(1), 432-446.

Netshiozwi, U., Yeganeh, A., Shongwe, S. C., & Hakimi, A. (2023). Data-Driven Surveillance of Internet Usage Using a Polynomial Profile Monitoring Scheme. *Mathematics*, *11*(17), 3650.

Noorossana, R., Amiri, A., & Soleimani, P. (2008). On the monitoring of autocorrelated linear profiles. *Communications in Statistics—Theory and Methods*, *37*(3), 425-442.

Noorossana, R., Eyvazian, M., & Vaghefi, A. (2010). Phase II monitoring of multivariate simple linear profiles. *Computers & Industrial Engineering*, *58*(4), 563-570.

Noorossana, R., & Soleimani, P. (2007). Effect of within profile autocorrelation on the performance of linear profiles. In *Proceedings of the 5th International Industrial Engineering Conference, Tehran, Iran (in Farsi)*.

Noorossana, R., Vaghefi, A., & Dorri, M. (2011). Effect of non-normality on the monitoring of simple linear profiles. *Quality and Reliability Engineering International*, *27*(4), 425-436.

Park, C., & Lee, J. (2022). Monitoring profiles in multistage processes using the multivariate multiple regression model. *Quality and Reliability Engineering International*, *38*(7), 3437-3450.

Paynabar, K., Zou, C., & Qiu, P. (2016). A change-point approach for phase-I analysis in multivariate profile monitoring and diagnosis. *Technometrics*, *58*(2), 191-204.

Qiu, P., Zou, C., & Wang, Z. (2010). Nonparametric profile monitoring by mixed effects modeling. *Technometrics*, 265-277.

Ren, H., Chen, N., & Wang, Z. (2019). Phase-II monitoring in multichannel profile observations. *Journal of Quality Technology*, *51*(4), 338-352.

Rodrigues, D. C., Goecks, L. S., Mareth, T., & Korzenowski, A. L. (2021). Multivariate control chart with variable dimensions for flexible production environments. International Journal for Quality Research, *15*(3), 701.

Saeed, U., Mahmood, T., Riaz, M., & Abbas, N. (2018). Simultaneous monitoring of linear profile parameters under progressive setup. *Computers & Industrial Engineering*, *125*, 434-450.

Saghaei, A., Mehrjoo, M., & Amiri, A. (2009). A CUSUM-based method for monitoring simple linear profiles. The International Journal of Advanced Manufacturing Technology, *45*(11), 1252–1260.

Saghaei, A., Noorossana, R., & Amiri, A. (2013). *Statistical analysis of profile monitoring*. Wiley..

Salmasnia, A., Tavakoli, A., Noroozi, M., & Abdzadeh, B. (2019). Robust economic-statistical design of the EWMA-R control charts for phase II linear profile monitoring. *Journal of Industrial Engineering and Management Studies*, *6*(1), 46-67.

Shamma, S. E., Amin, R. W., & Shamma, A. K. (1991). A double exponentially weigiited moving average control procedure with variable sampling intervals. *Communications in Statistics-simulation and Computation*, *20*(2-3), 511-528.

Sheu, S. H., Tai, S. H., Hsieh, Y. T., & Lin, T. C. (2009). Monitoring process mean and variability with generally weighted moving average control charts. *Computers & Industrial Engineering*, *57*(1), 401-407.

Song, L., He, S., Wang, Z., & He, Z. (2023). Dynamic monitoring of polynomial profiles with attribute responses and between-profile correlation. *IISE Transactions*, 1-16.

Steiner, S. H., Cook, R. J., Farewell, V. T., & Treasure, T. (2000). Monitoring surgical performance using risk-adjusted cumulative sum charts. *Biostatistics*, *1*(4), 441-452.

Stover, F. S., & Brill, R. V. (1998). Statistical quality control applied to ion chromatography calibrations. *Journal of Chromatography A*, *804*(1-2), 37-43.

Varbanov, R., Chicken, E., Linero, A., & Yang, Y. (2019). A Bayesian approach to sequential monitoring of nonlinear profiles using wavelets. *Quality and Reliability Engineering International*, *35*(3), 761-775.

Villalobos, J. R., Muñoz, L., & Gutierrez, M. A. (2005). Using fixed and adaptive multivariate SPC charts for online SMD assembly monitoring. *International Journal of Production Economics*, *95*(1), 109-121.

Wang, Y., Mei, Y., & Paynabar, K. (2018). Thresholded multivariate principal component analysis for phase I multichannel profile monitoring. *Technometrics*, *60*(3), 360-372.

Williams, J. D., Woodall, W. H., & Birch, J. B. (2007). Statistical monitoring of nonlinear product and process quality profiles. *Quality and Reliability Engineering International*, *23*(8), 925-941.

Wolfinger, R., & O'connell, M. (1993). Generalized linear mixed models a pseudo-likelihood approach. *Journal of statistical Computation and Simulation*, *48*(3-4), 233-243.

Woodall, W. H. (2007). Current research on profile monitoring. *Production*, *17*, 420-425.

Wu, L., Zeng, T., Zinellu, A., Rubino, S., Kelvin, D. J., & Carru, C. (2019). A cross-sectional study of compositional and functional profiles of gut microbiota in Sardinian centenarians. *Msystems*, *4*(4), 10-1128.

Xu, L., Wang, S., Peng, Y., Morgan, J. P., Reynolds Jr, M. R., & Woodall, W. H. (2012). The monitoring of linear profiles with a GLR control chart. *Journal of Quality Technology*, *44*(4), 348-362.

Yao, C., Li, Z., He, C., & Zhang, J. (2020). A Phase II control chart based on the weighted likelihood ratio test for monitoring polynomial profiles. *Journal of Statistical Computation and Simulation*, *90*(4), 676-698.

Yeganeh, A., Abbasi, S. A., Pourpanah, F., Shadman, A., Johannssen, A., & Chukhrova, N. (2022). An ensemble neural network framework for improving the detection ability of a base control chart in non-parametric profile monitoring. *Expert Systems with Applications*, *204*, 117572.

Yeganeh, A., Shadman, A., & Amiri, A. (2021). A novel run rules based MEWMA scheme for monitoring general linear profiles. *Computers & Industrial Engineering*, *152*, 107031.

Yeganeh, A., & Shongwe, S. C. (2023). A novel application of statistical process control charts in financial market surveillance with the idea of profile monitoring. *PloS one*, *18*(7), e0288627.

Zhang, J., Li, Z., & Wang, Z. (2009). Control chart based on likelihood ratio for monitoring linear profiles. Computational Statistics & Data Analysis, 53(4), 1440–1448.

Zhang, Y., He, Z., Shan, L., & Zhang, M. (2014b). Directed control charts for detecting the shape changes from linear profiles to quadratic profiles. *International Journal of Production Research*, *52*(11), 3417-3430.

Zhang, Y., He, Z., Zhang, C., & Woodall, W. H. (2014a). Control charts for monitoring linear profiles with within-profile correlation using Gaussian process models. *Quality and Reliability Engineering International*, *30*(4), 487-501.

Zhao, C., Du, S., Deng, Y., Li, G., & Huang, D. (2020). Circular and cylindrical profile monitoring considering spatial correlations. *Journal of Manufacturing Systems*, *54*, 35-49.

Zhou, Q., & Qiu, P. (2022). Phase I monitoring of serially correlated nonparametric profiles by mixed-effects modeling. *Quality and Reliability Engineering International*, *38*(1), 134-152.

Zhu, J., & Lin, D. K. (2009). Monitoring the slopes of linear profiles. *Quality Engineering*, *22*(1), 1-12.

Zou, C., Tsung, F., & Wang, Z. (2007). Monitoring general linear profiles using multivariate exponentially weighted moving average schemes. *Technometrics*, *49*(4), 395-408.

Zou, C., Tsung, F., & Wang, Z. (2008). Monitoring profiles based on nonparametric regression methods. *Technometrics*, 512-526.

Zou, C., Zhang, Y., & Wang, Z. (2006). A control chart based on a change-point model for monitoring linear profiles. *IIE transactions*, *38*(12), 1093-1103.